Università per Stranieri di Perugia

United Nations Educational, Scientific and Cultural Organization · World Water Assessment Programme

CiNiD CONSORZIO INTERUNIVERSITARIO PER L'IDROLOGIA

DRONES IN HYDROLOGY

Prof. Salvatore Manfreda

Associate Professor of Water Management and Ecohydrology - http://www2.unibas.it/manfreda

Chair of the COST Action Harmonious - http://www.costharmonious.eu

cost EUROPEAN COOPERATION IN SCIENCE & TECHNOLOGY

Funded by the Horizon 2020 Framework Programme of the European Union

UNIVERSITA' DEGLI STUDI DELLA BASILICATA

Unmanned Arial Systems (UAS) in Hydrology

Scope: state of the vegetation, streamflow (speed and water level), extension of the flooded areas and morphology.

Objective: To define integrated procedures to improve hydrological/hydraulic monitoring capacity using UAS.

Scale: from plot-scale to the river basin scale providing operational monitoring tools.

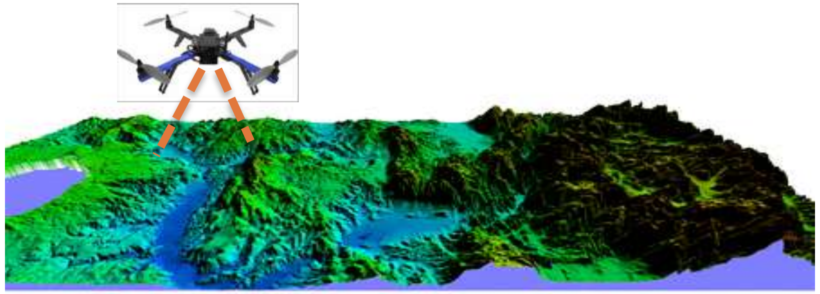

COST
EUROPEAN COOPERATION IN SCIENCE & TECHNOLOGY

TOP APPLICATIONS

Environmental monitoring: ecological state of ecosystems, plant stress, water pollution, soil contamination, water contamination, monitoring of water systems (rivers, lakes, dams etc.).

Precision agriculture: management of crops to guarantee efficiency of inputs like water and fertilizer *and* maximize productivity, quality, and yield. It also involves the minimization of pests, unwanted flooding, and disease.

Energy, mining, and utilities: resources management and research requires monitoring over large territories, often in inaccessible areas.

Real estate, construction, and land development: need managing and mapping large portion of land or collections of buildings.

cost
EUROPEAN COOPERATION IN SCIENCE & TECHNOLOGY

Environmental Monitoring

Global	Few hectars	Few m^2
		
Up to 30cm	Up to 1cm	Up to 1cm

Comparable Scales

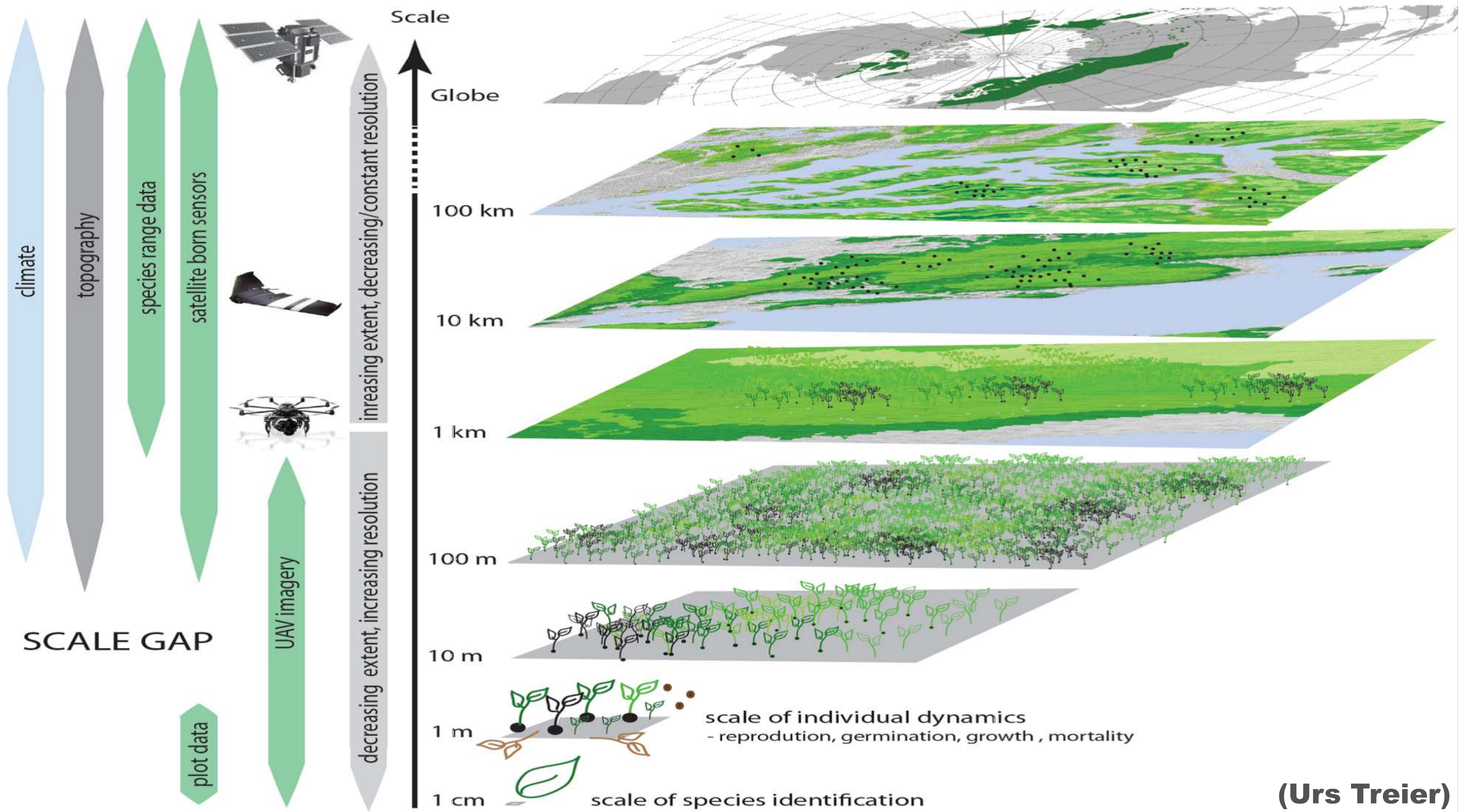

climate
topography
species range data
satellite born sensors
SCALE GAP
plot data
UAV imagery
inreasing extent, decreasing/constant resolution
decreasing extent, increasing resolution
Scale
Globe
100 km
10 km
1 km
100 m
10 m
1 m
1 cm
scale of individual dynamics
- reprodution, germination, growth , mortality
scale of species identification

(Urs Treier)

UAS vs Satellite

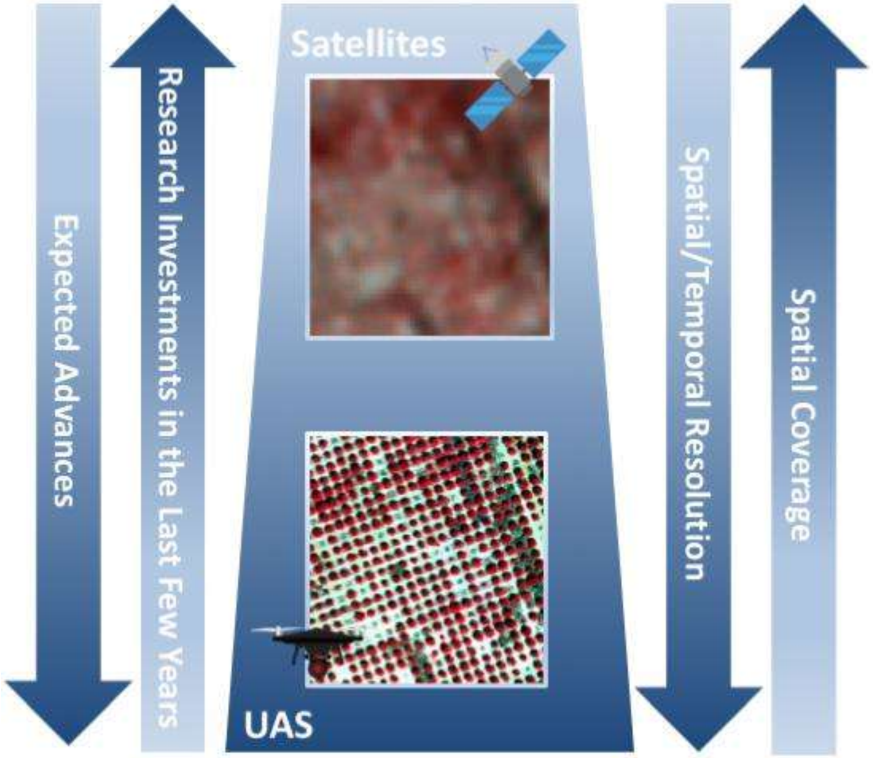

Manfreda et al. (Remote Sensing, 2018)

Number of articles extracted from the database ISI web of knowledge

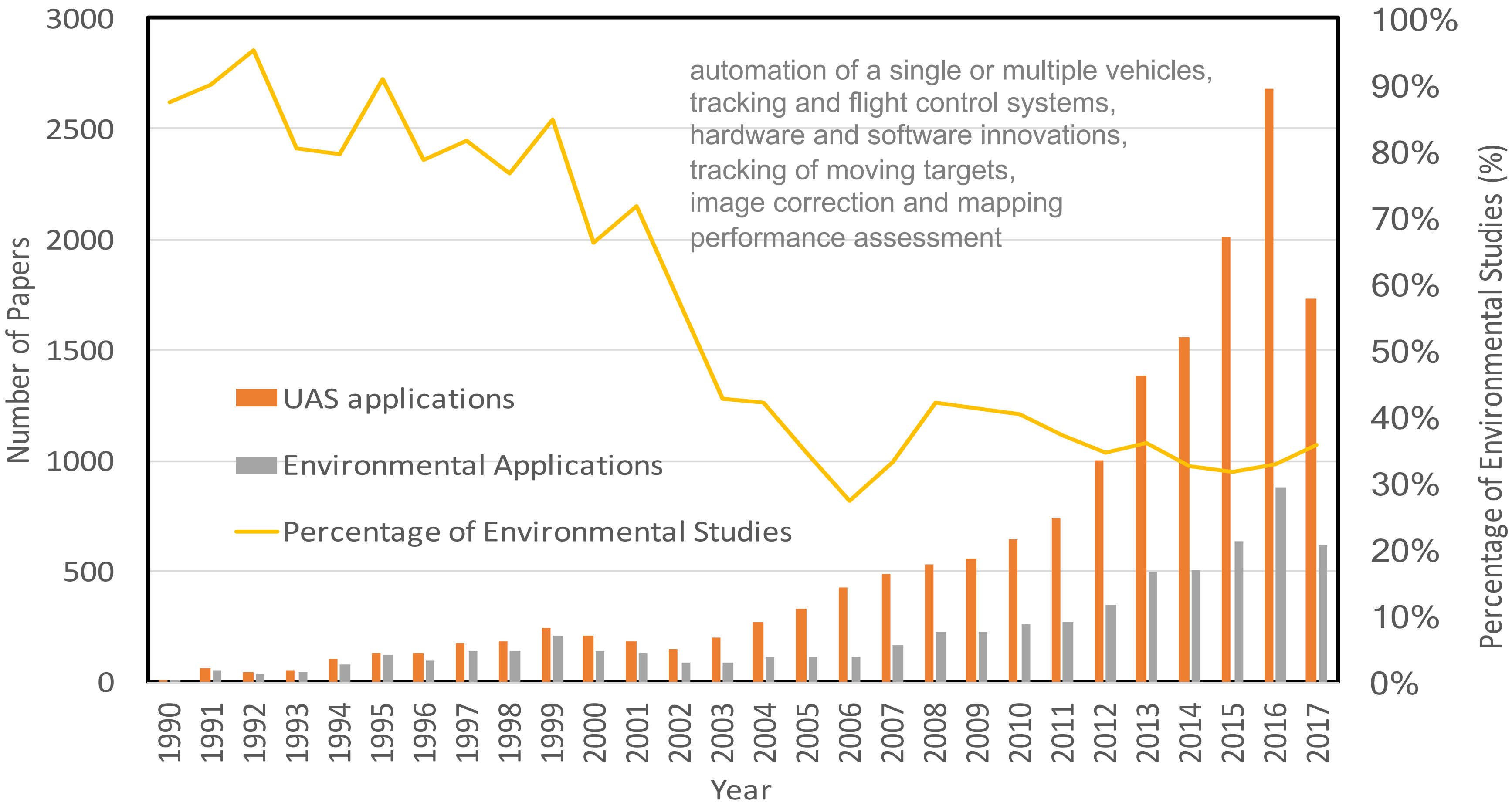

from 1990 up to 2017 (last access 15/01/2018)

DRONES

Large

Medium

Small

Micro

Characteristics	Payload size	Operational constraints	Example platforms
Large operating range (~500 km); long flight time (up to 2 days); medium to high altitude (3–20 km)	~200 kg internally and ~900 kg in under-wing pods	High set-up and running costs; requires ground-station support, full aviation clearance, long runway for takeoff and landing, hangar for storage; altitude ceiling above commercial air traffic	NASA *Ikhana* 
Large operating range (~500 km); medium flight time (~10 hours); medium altitude (< 4 km)	~50 kg	Similar requirements to large UAVs but with reduced overall costs, reduced requirements for takeoff and landing, and easier control	NASA SIERRA 
Small operating range (< 10 km); low endurance (< 2 hours); low altitude (<1 km)	Less than 30 kg (small); up to 5 kg (mini)	Line-of-sight flight only; largely fixed wing; simple launch gear and minimal landing/takeoff requirements; flown by flight planning software or by direct radio control	Quest UAV 
Small operating range (<10 km); very short flight time (<1 hour); very low altitude (< 250 m)	Less than 5 kg	Hand-launched; line-of-sight flight only; soft landing place required; usually copter-type UAVs with rotor blade control; flown by flight planning software or by direct radio control	AR-Drone Parrot 

(Anderson & Gaston, 2013)

cost EUROPEAN COOPERATION IN SCIENCE & TECHNOLOGY

Example: multi-copter 6 engines equipped with a thermal camera

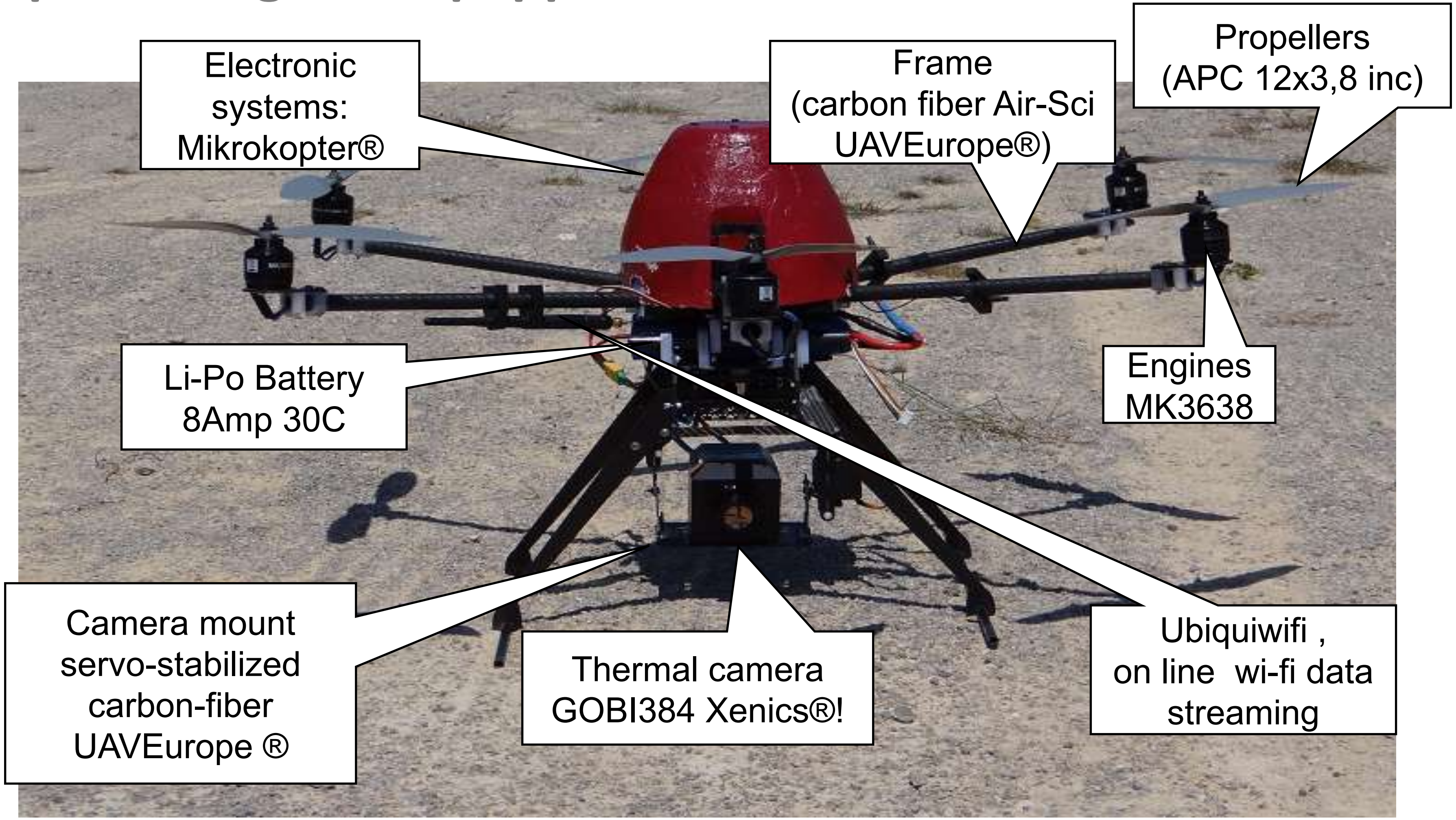

HydroLAB

HydroLAB Equipment

- Phantom 3 and 4 pro;
- Single wing skywalker;
- Portable radar;
- FLIR FLEA USB3;
- Uncooled LWIR Thermal;
- ADC Snap Camera.


Skywalker


Training UAS


FLIR FLEA USB3


Portable Radar


Phantom 3 and 4 pro

Uncooled LWIR Thermal

ADC Snap Camera


3DR

Evolution of a fungal pathogen

14 May 2014

(from Lyndon Estes, 2015)

Evolution of a fungal pathogen

25 July 2014

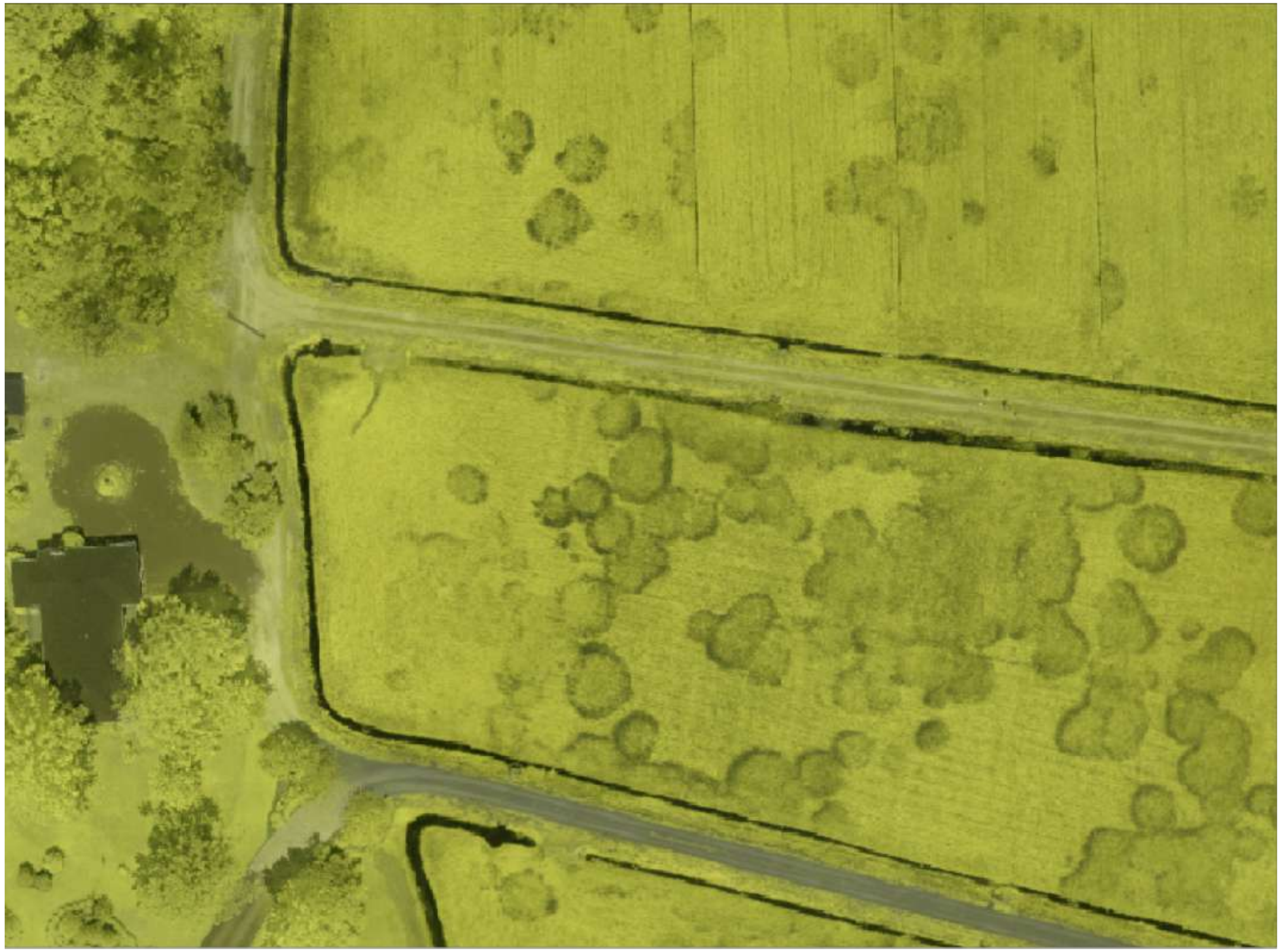

(from Lyndon Estes, 2015)

Related Publications

- Manfreda and McCabe (2019). ***Emerging earth observing platforms offer new insights into hydrological processes***, Hydrolink.
- Perks, Hortobágyi, Le Coz, Maddock, Pearce, Tauro, Dal Sasso, Grimaldi, Manfreda (2019) **Towards harmonization of image velocimetry techniques for determining open-channel flow**, Earth system science data (in preparation).
- Manfreda, Dvorak, Mullerova, Herban, Vuono, Arranz Justel, Perks (2019) ***Assessing the Accuracy of Digital Surface Models Derived from Optical Imagery Acquired with Unmanned Aerial Systems***, Drones.
- Manfreda, ***On the derivation of flow rating-curves in data-scarce environments***, Journal of Hydrology, 2018.
- Dal Sasso, Pizarro, Samela, Mita, and Manfreda (2018) ***Exploring the optimal experimental setup for surface flow velocity measurements using PTV***, Environmental Monitoring and Assessment.
- Manfreda, McCabe, Miller, Lucas, Pajuelo Madrigal, Mallinis, Ben-Dor, Helman, Estes, Ciraolo, Müllerová, Tauro, De Lima, De Lima, Frances, Caylor, Kohv, Maltese (2018), ***On the Use of Unmanned Aerial Systems for Environmental Monitoring***, Remote Sensing.
- Baldwin, Manfreda, Keller, and Smithwick, Predicting root zone soil moisture with soil properties and satellite near-surface moisture data at locations across the United States, Journal of Hydrology, 2017.
- Manfreda, Brocca, T. Moramarco, F. Melone, and J. Sheffield, ***A physically based approach for the estimation of root-zone soil moisture from surface measurements***, Hydrology and Earth System Sciences, 18, 1199-1212, 2014.
- Manfreda, Lacava, Onorati, Pergola, Di Leo, Margiotta, and Tramutoli, ***On the use of AMSU-based products for the description of soil water content at basin scale***, Hydrology and Earth System Sciences, 15, 2839-2852, 2011.


HydroLAB

Summer School on Monitoring and Modeling Surface Hydrological Processes, Parco Appennino Lucano, Marsico, 2011.


Summer School on Applied Course on UAVs for Environmental Monitoring,
UniBas, Matera, 2015.

Summer School on UASs for environmental monitoring, UniBas, Matera, 2016

TRAINING COURSE

Harmonized UAS techniques: Introduction to data acquisition and preprocessing, Reykjavik, Iceland 02-08 September 2018

Università per Stranieri di Perugia

Growing **ideas** through **networks**

DRONES IN HYDROLOGY: HARMONIOUS

uas for environmental monitoring

Prof. Salvatore Manfreda

Associate Professor of Water Management and Ecohydrology - http://www2.unibas.it/manfreda

Chair of the COST Action Harmonious - http://www.costharmonious.eu

cost EUROPEAN COOPERATION IN SCIENCE & TECHNOLOGY

Funded by the Horizon 2020 Framework Programme of the European Union

UNIVERSITA' DEGLI STUDI DELLA BASILICATA

COST Action HARMONIOUS

A network of scientists is currently cooperating within the framework of a COST (European Cooperation in Science and Technology) Action named “Harmonious”.

The intention of “Harmonious” is to promote monitoring strategies, establish harmonized monitoring practices, and transfer most recent advances on UAS methodologies to others within a global network.

COST is supported by the EU Framework Programme Horizon 2020

HARMONIOUS Network

HARMONIOUS Action

Action Chair Salvatore Manfreda
Vice Chair Brigitta Toth
Science Communications Manager: Guiomar Ruiz Perez
STSM coordinator: Isabel De Lima
Training School Coordinator: Giuseppe Ciraolo

WG1: UAS data processing
Leader Pauline Miller
Vice leader Victor Pajuelo Madrigal

- Geometric Correction and image calibration
- Contrast Enhancement

WG2 Vegetation Status
Leader Antonino Maltese
Vice leader Felix Frances

WG3 Soil Moisture Content
Leader Zhongbo Su
Vice leader David Helman

WG4
Leader Matthew Perks
Vice leader Marko Kohv

- River morphology
- Stream flow

WG5: Harmonization of methods and results
Leader Eyal Ben Dor
Vice leader Flavia Tauro

Harmonization of different procedures and algorithms in different environments

WG1: Data Collection, Processing and Limitations

WG2: Vegetation Monitoring

WG3: Soil Moisture Monitoring

WG4: River and Streamflow monitoring

WG5: Harmonization of different procedures and algorithms in different environments

a) Peculiarities and specificity of each topic

b) Identification of the shared problems

c) Identification of possible common strategies for the four WGs

d) Definition of the correct protocol fro UAS Environmental Monitoring

The Home Page - https://www.costharmonious.eu

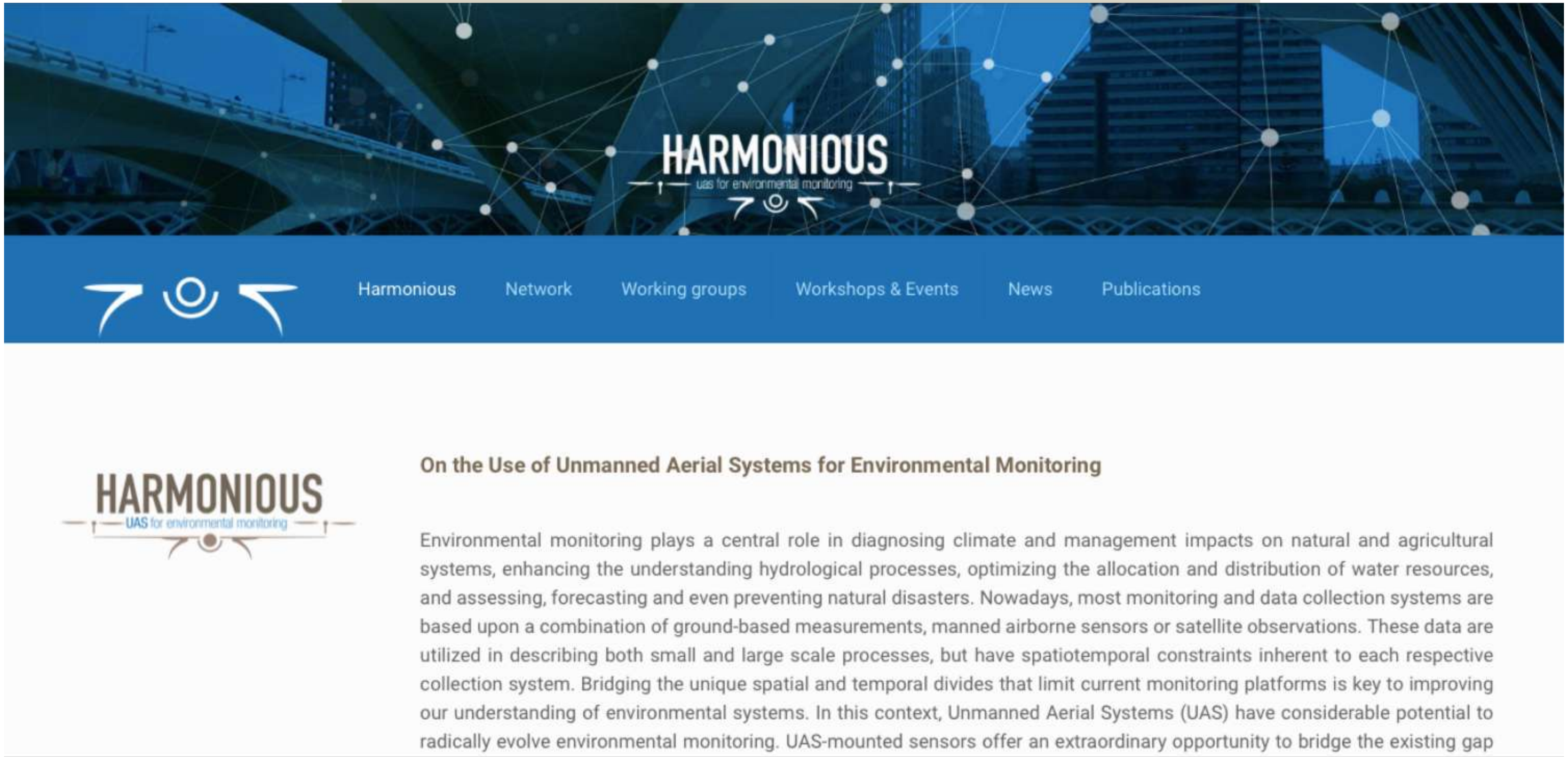

Twitter

HARMONIOUS
Tweet 24
Following 30
Follower 33
Mi piace 31
Liste 0
Momenti 0
Modifica profilo
HARMONIOUS
@COST_HARMONIOUS
The COST Action named Harmonious promotes monitoring strategies, establish harmonized monitoring practices, and transfer recent advances on UASs methodologies.
Matera, Basilicata
costharmonious.eu
Iscrizione a dicembre 2017
Tweet
Tweet e risposte
Contenuti
HARMONIOUS @COST_HARMONIOUS · 27 giu
We are selecting 16 talented trainees (Ph.D. Students, Post-Doc, and young researchers) from COST Full Member and COST Cooperating Member for the Training Course on the Harmonized use of UAS techniques. Check on costharmonious.eu
@COSTprogramme #UAS #UAV
Traduci il Tweet
6
9
HARMONIOUS @COST_HARMONIOUS · 27 giu
Chi seguire · Aggiorna · Visualizza tutto
Leila.Saberi @LeilaSaberi
Segui
Alessio Domeneghetti @...
Segui
Clare Stephens @ClareS...
Segui

Facebook Harmonious-European-COST-Action

352 followers on facebook

https://www.facebook.com/Harmonious-European-COST-Action-485412205186817/

Examples of Common image artifacts

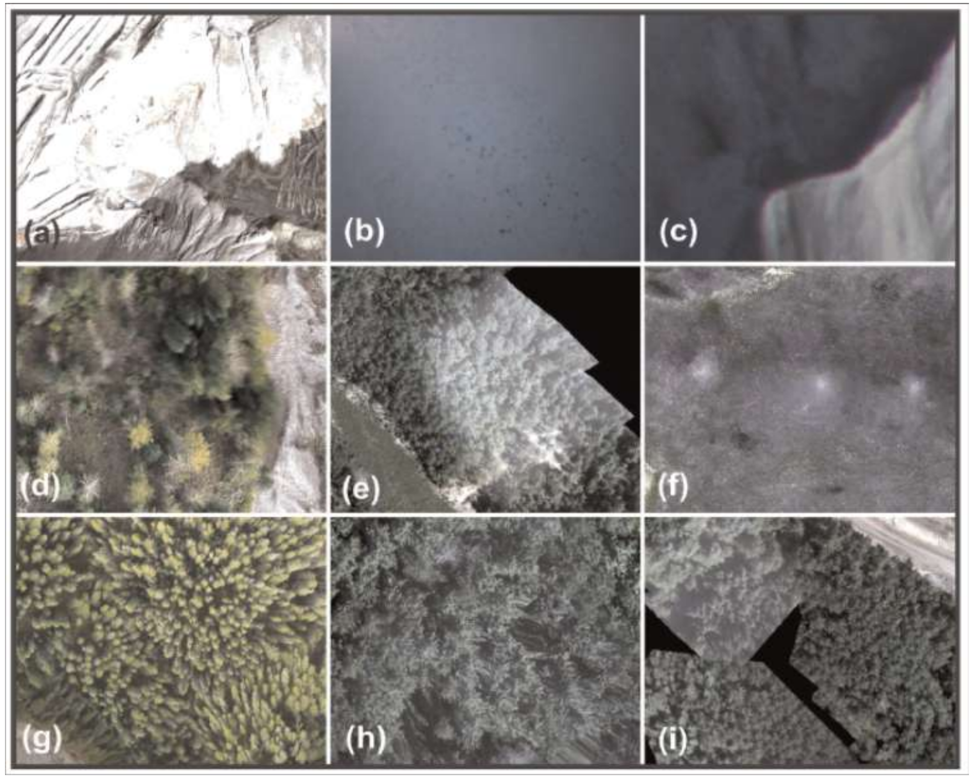

a) saturated image;
b) vignetting;
c) chromatic aberration;
d) mosaic blurring in overlap area;
e) incorrect colour balancing;
f) hotspots on mosaic due to bidirectional reflectance effects;
g) relief displacement (tree lean) effects in final image mosaic;
h) Image distortion due to DSM errors;
i) mosaic gaps caused by incorrect orthorectification or missing images.

(Whitehead and Hugenholtz, 2014)

Comparison between a CubeSat and UAS NDVI map

Multi-spectral false colour (near infrared, red, green) imagery collected over the RoBo Alsahba date palm farm near Al Kharj, Saudi Arabia. Imagery (from L-R) shows the resolution differences between: (A) UAV mounted Parrot Sequoia sensor at 50 m height (0.05 m); (B) a WorldView-3 image (1.24 m); and (C) Planet CubeSat data (approx. 3 m), collected on the 13th, 29° and 27th March 2018, respectively

UAS thermal survey over an Aglianico vineyard in the Basilicata region (southern Italy)

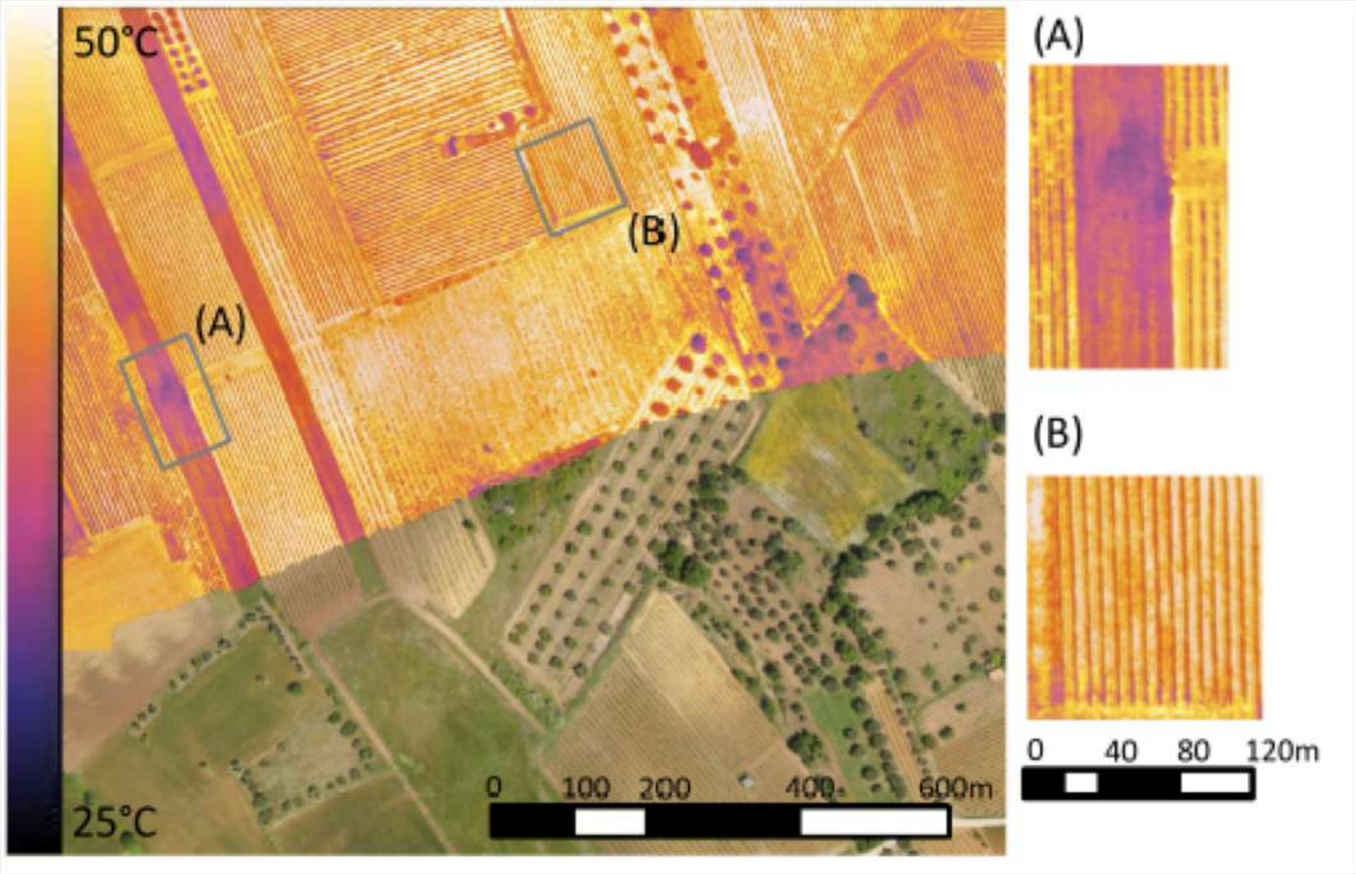

(Manfreda et al., R.S. 2018a)

How to detect water stress from an UAV?

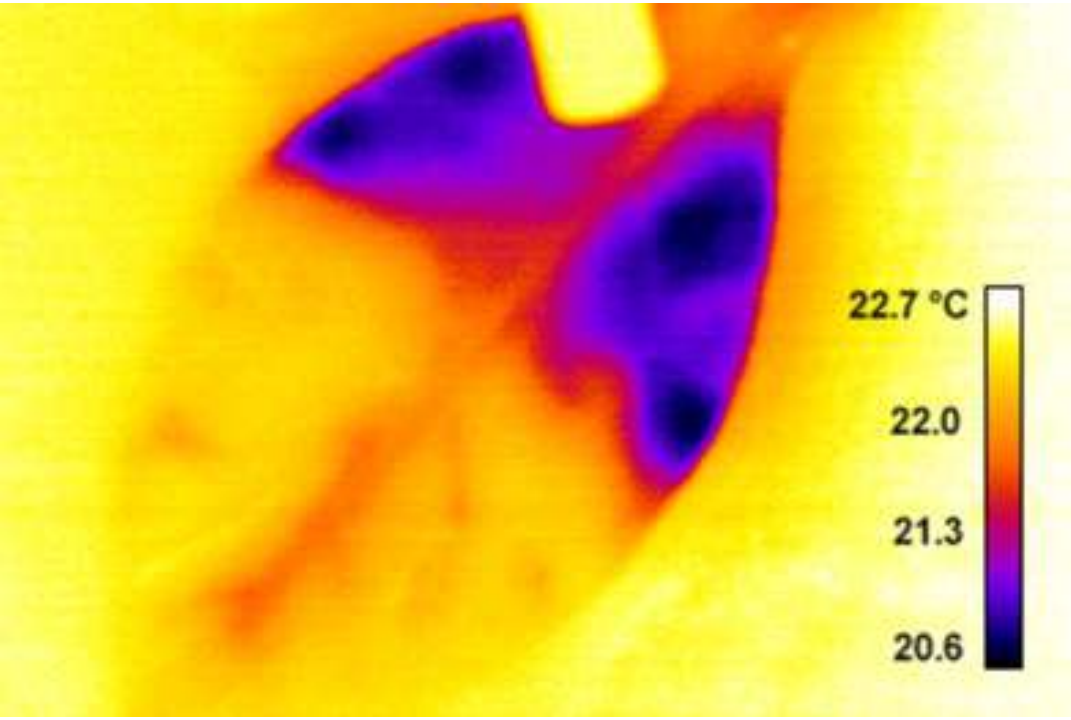

COST
EUROPEAN COOPERATION IN SCIENCE & TECHNOLOGY

From Xurxo Gago

Aerial thermography for water stress detection

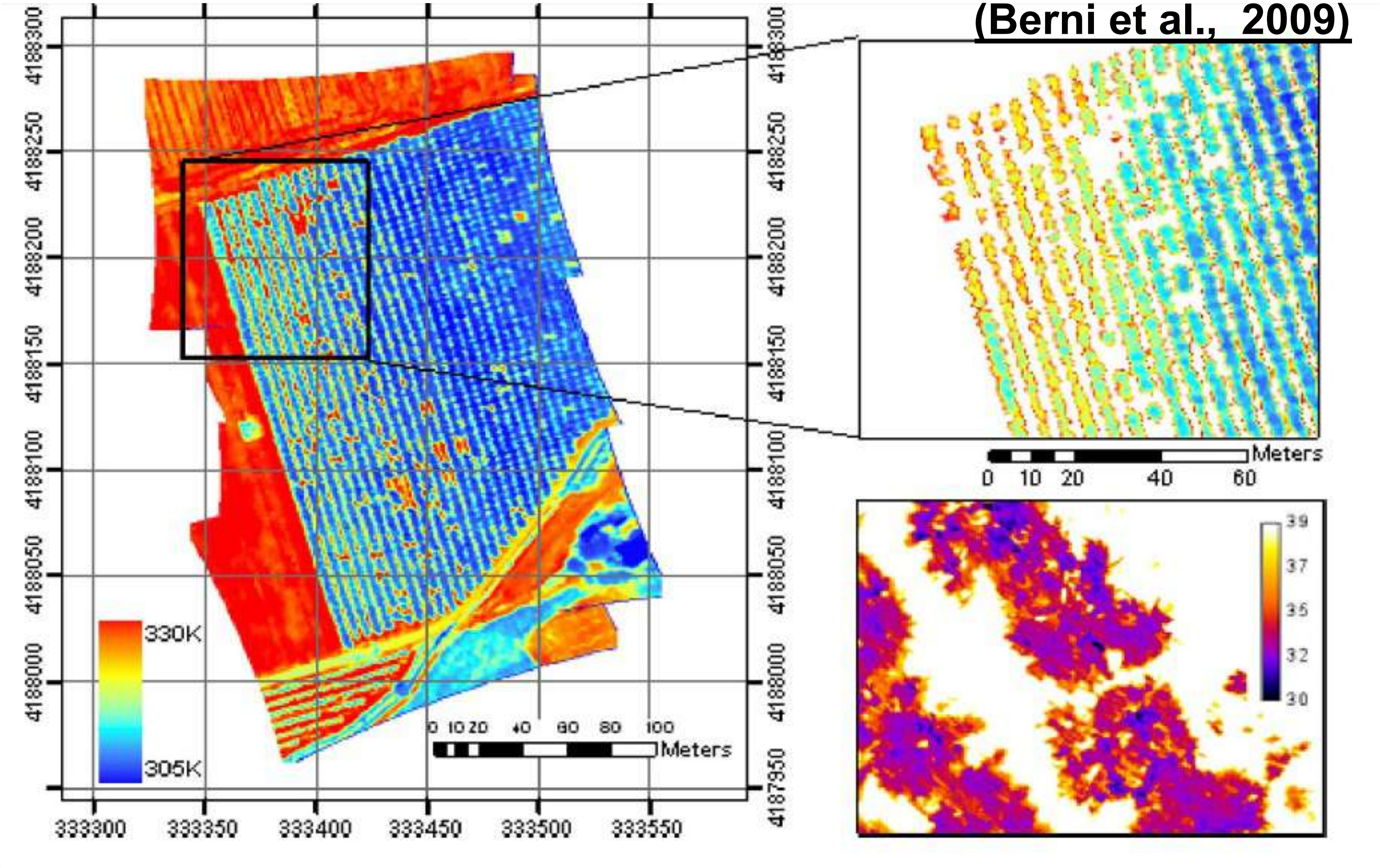

Aerial thermography for water stress detection

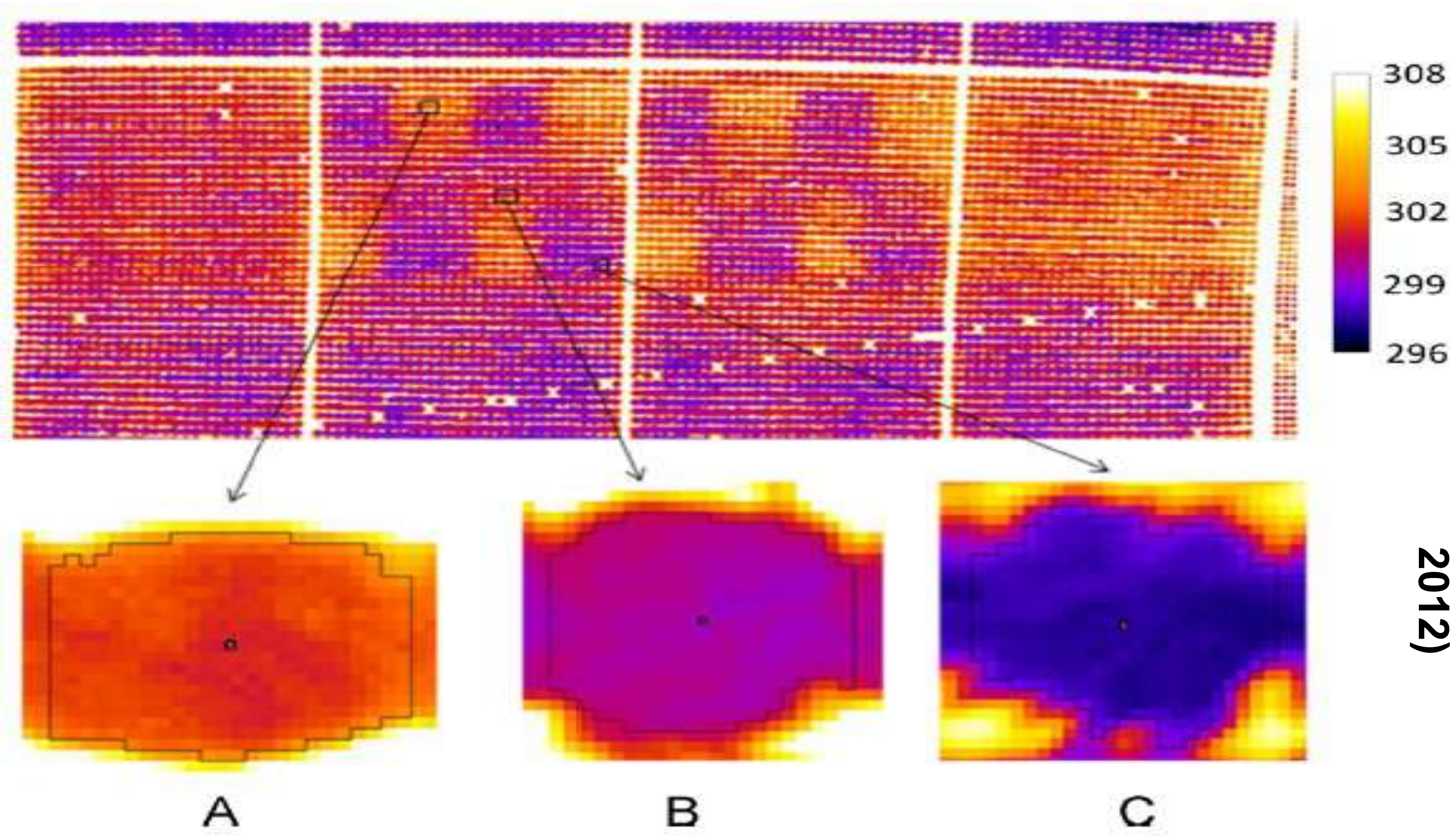

(González-Dugo et al., 2012)

How to detect the drought from an UAV?

Thermal indexes… an attempt to normalize the environment (Idso et al., 1980; Jones, 1999)

- CWSI = T canopy – Twet / Tdry – Twet
- IG = T dry – Tcanopy / Tcanopy – Twet
- I3= T canopy – Twet / Tdry – Tcanopy
- And the leaf energy balance:

$$T_l - T_a = \frac{[r_{HR}(r_{aw} + r_s)\gamma R_{ni} - pc_p r_{HR} D]}{pc_p[\gamma(r_{aw} + r_s) + s r_{HR}]}$$

$$r_s = \frac{-pc_p r_{HR}[s(T_l - T_a) + D]}{\gamma\,[(T_l - T_a)pc_p - r_{HR} R_{ni}]} - r_{aw}$$

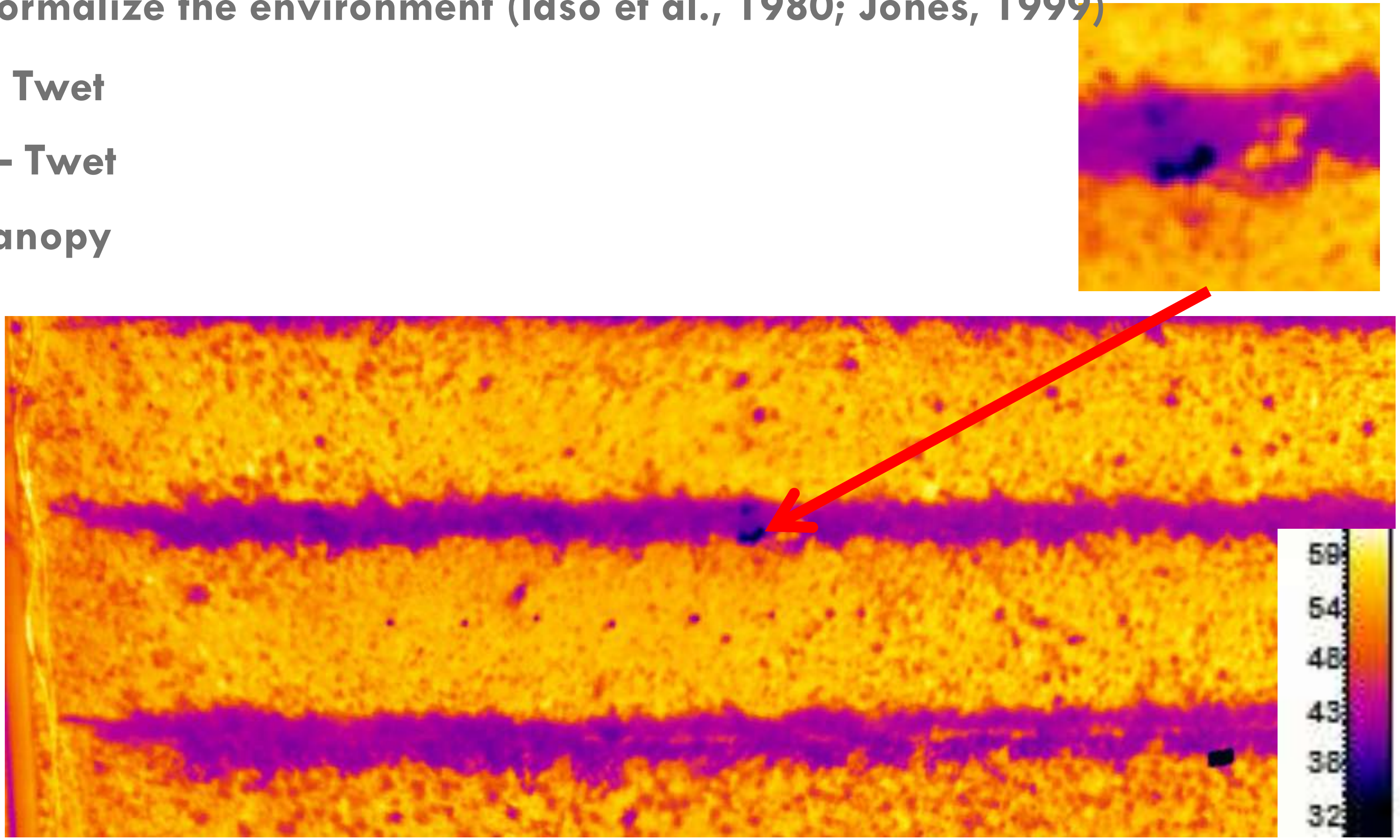

Soil Moisture Monitoring

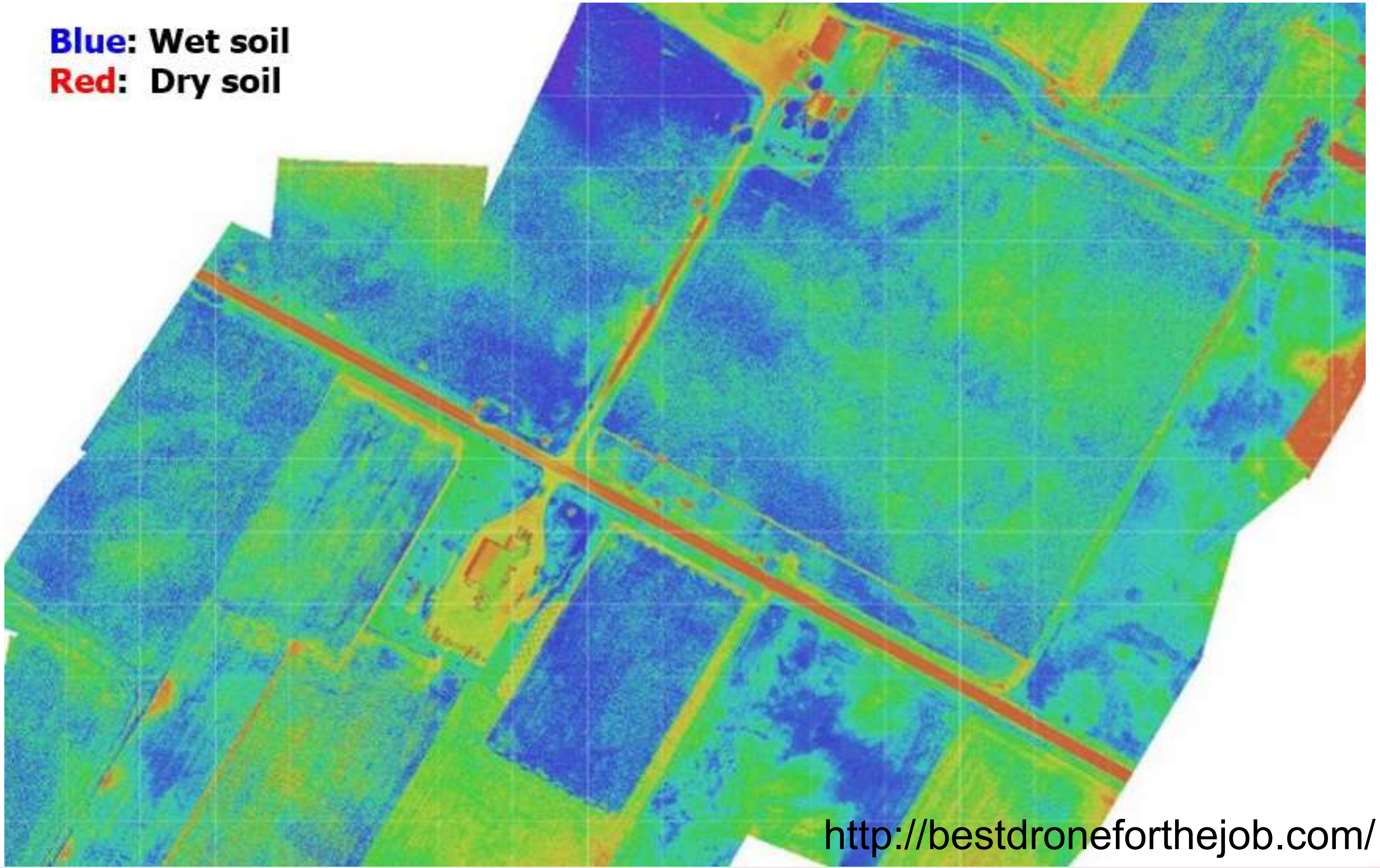

http://bestdroneforthejob.com/

Relationship existing between surface and root-zone soil moisture

Developing a relationship between the relative soil moisture at the surface to that in deeper layers of soil would be very useful for remote sensing applications.

<u>This implies that prediction of soil moisture in the deep layer given the superficial soil moisture, has an uncertainty that increases with a reduced near surface estimate.</u>

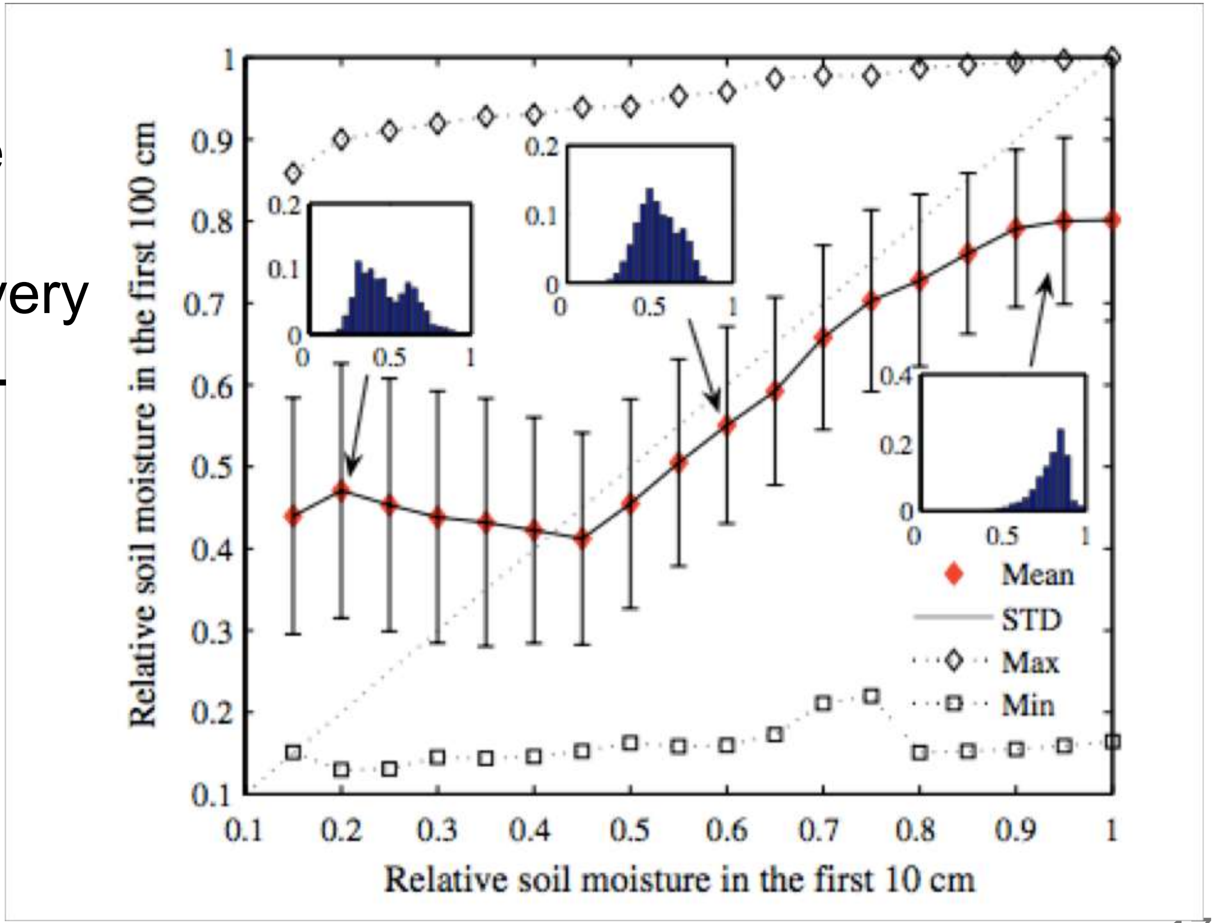

Manfreda et al. (AWR - 2007)

Soil Moisture Analytical Relationship (SMAR)

The schematization proposed assumes the soil composed of two layers, the first one at the surface of a few centimeters and the second one below with a depth that may be assumed coincident with the rooting depth of vegetation (of the order of 60–150 cm).

This may allow the derivation of a function of the soil moisture in one layer as a function of the other one.

$$s_2(t_j) = s_w + (s_2(t_{j-1}) - s_w)\, e^{-a(t_j - t_{j-1})} + (1 - s_w) b\, y(t_j)(t_j - t_{j-1})$$

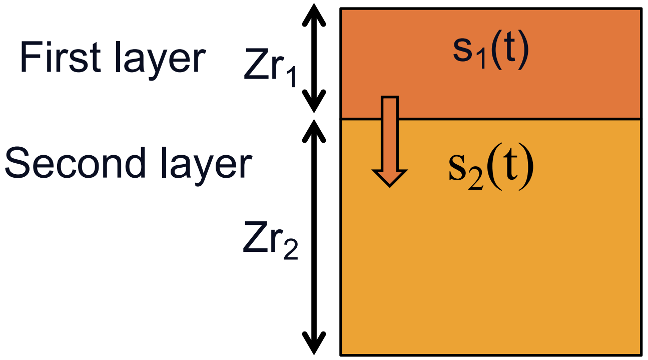

Manfreda et al. (HESS - 2014)

Sensitivity of SMAR's parameters

The derived root zone soil moisture (S_{RZ}) is plotted changing the soil water loss coefficient (**A**), the depth of the second soil layer (**B**), and the soil textures (**C**).

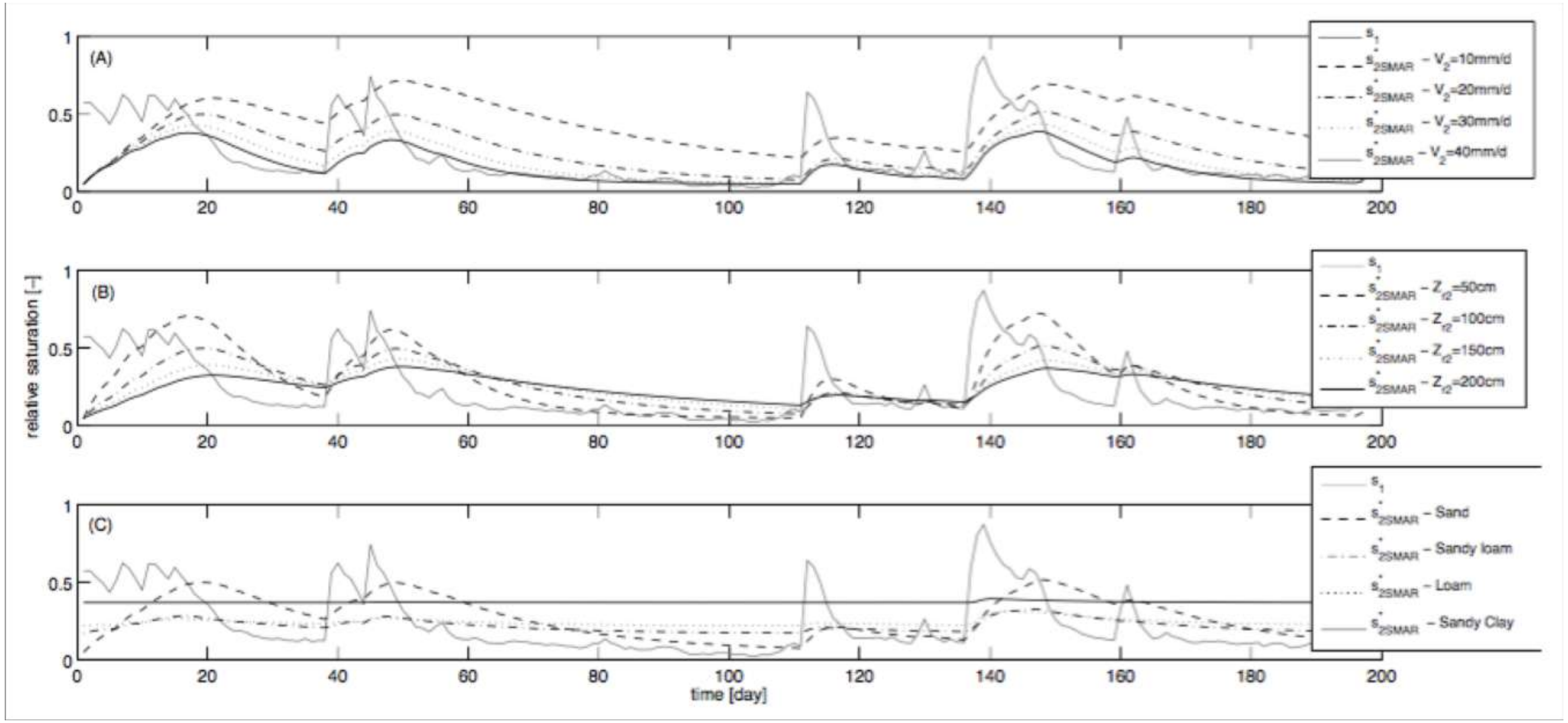

Manfreda et al. (HESS - 2014)

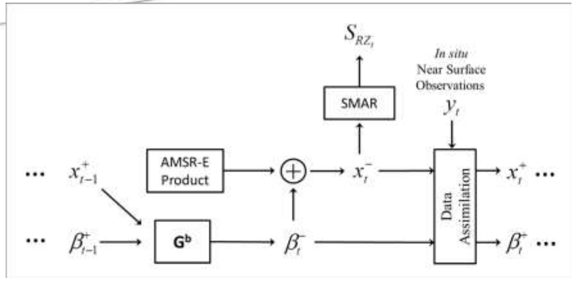

SMAR-EnKF optimization and prediction

Root mean square errors ranging from 0.014 - 0.049 [cm^3 cm^{-3}].

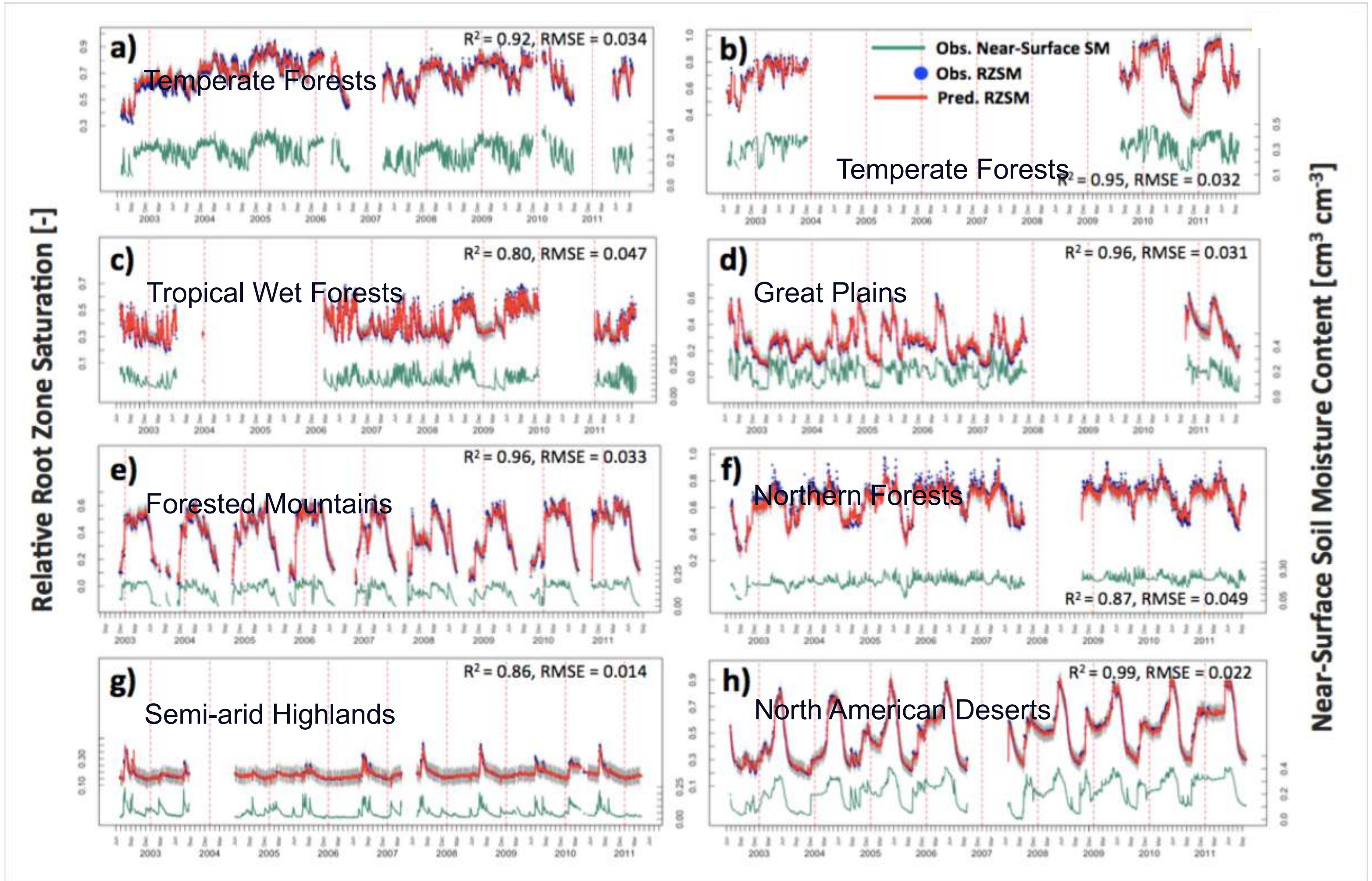

(Baldwin et al., J. Hydr., 2017)

COST EUROPEAN COOPERATION IN SCIENCE & TECHNOLOGY

Stream flow monitoring with UAS Particle Tracking Velocimetry (PTV)

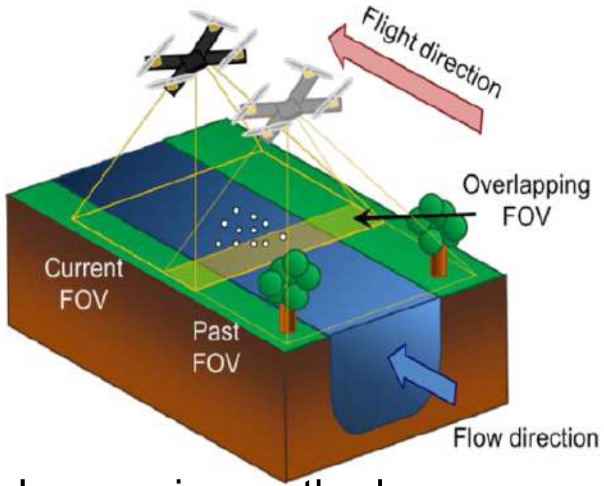

Lagrangian method
(Tauro et al., 2016)

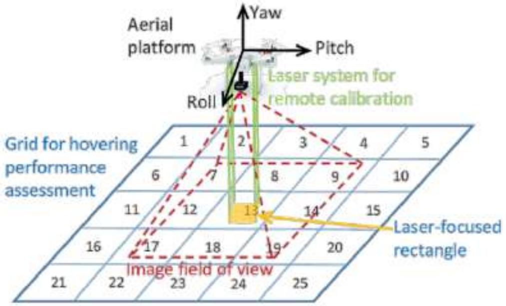

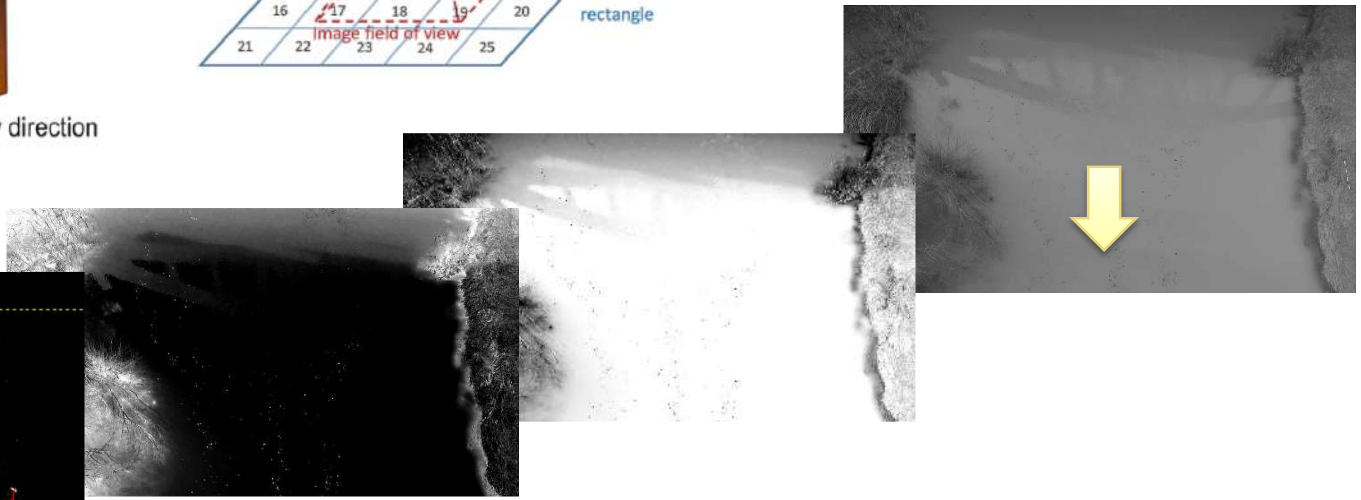

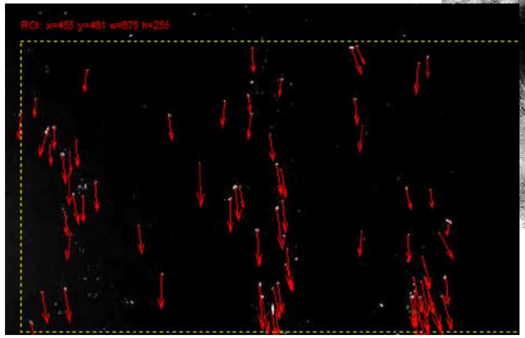

Image processing

Particle Tracking

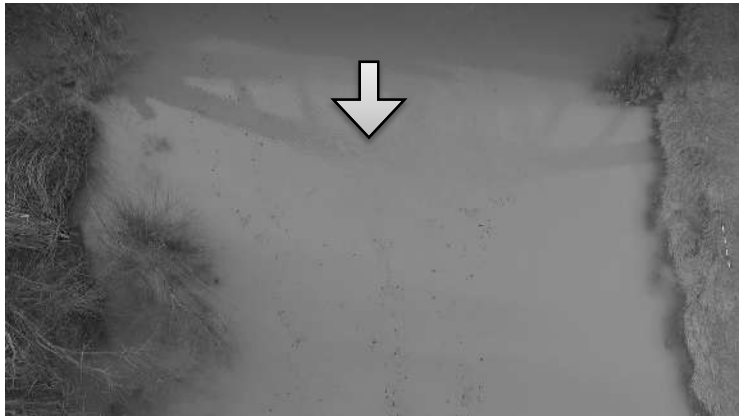

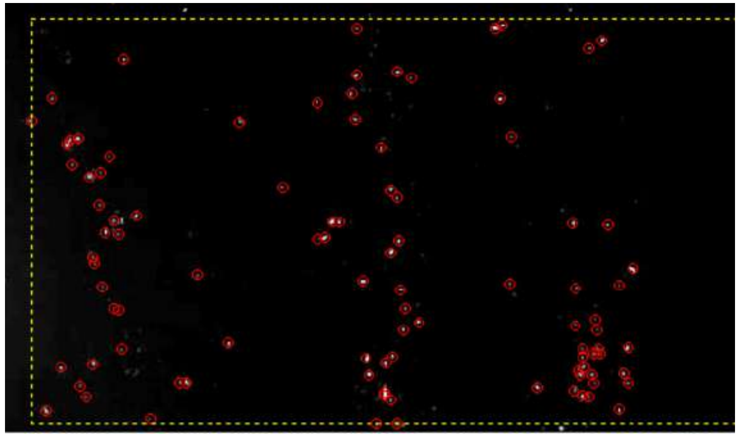

Particle detection

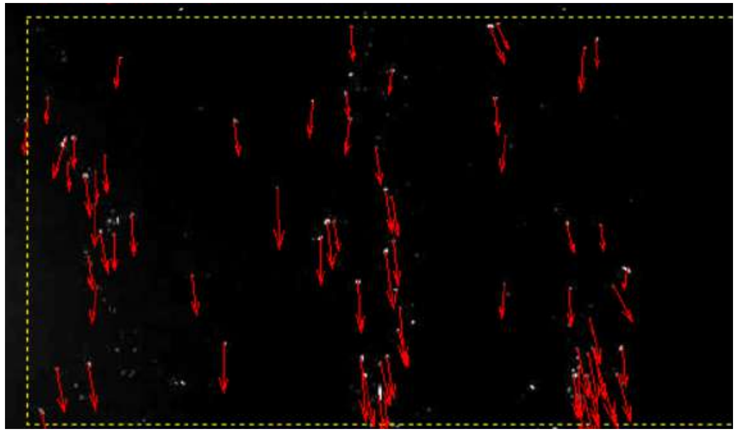

Velocity vectors

Monitoring River Systems

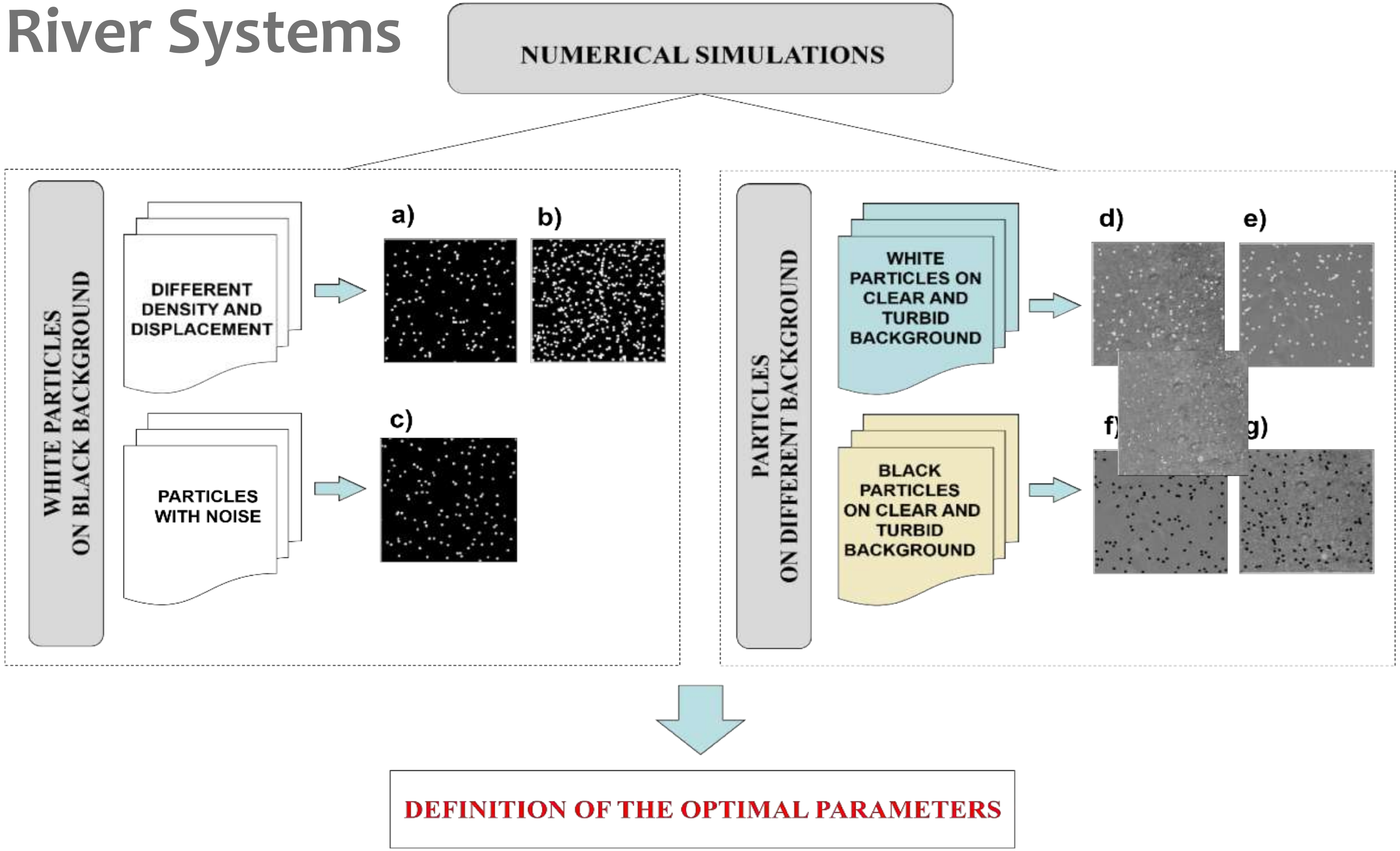

(Dal Sasso et al., E.M.A. 2018)

Optimal parameter settings for PTV techniques

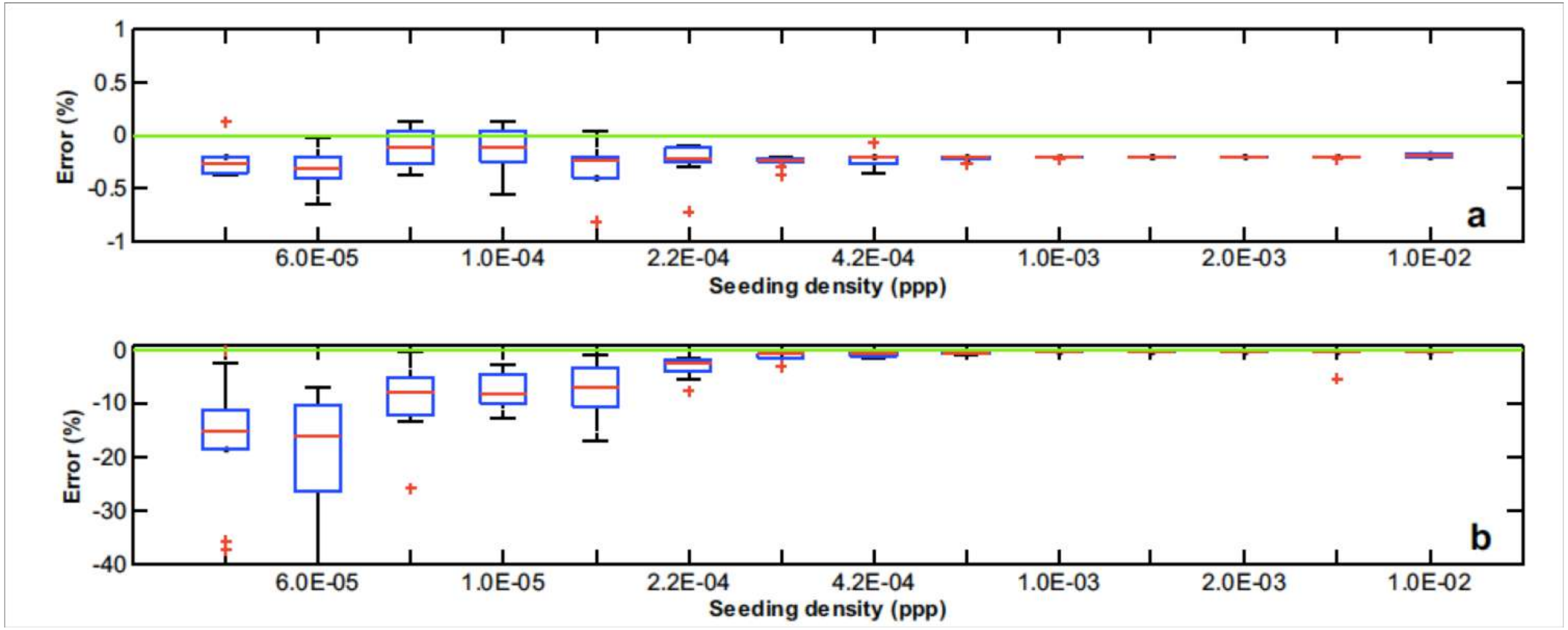

Box plot of the relative error for the different densities investigated in the configurations: a ideal condition, b real condition

(Dal Sasso et al., E.M.A. 2018)

Image Velocimetry Techniques: Intro

Image Velocimetry

2-D flow velocity field derived using an optical camera mounted on a quadcopter hovering over a portion of the Bradano river system in southern Italy. One of the images used for the analysis is shown as a background, where surface features used by flow tracking algorithms are highlighted in the insets (a, b).

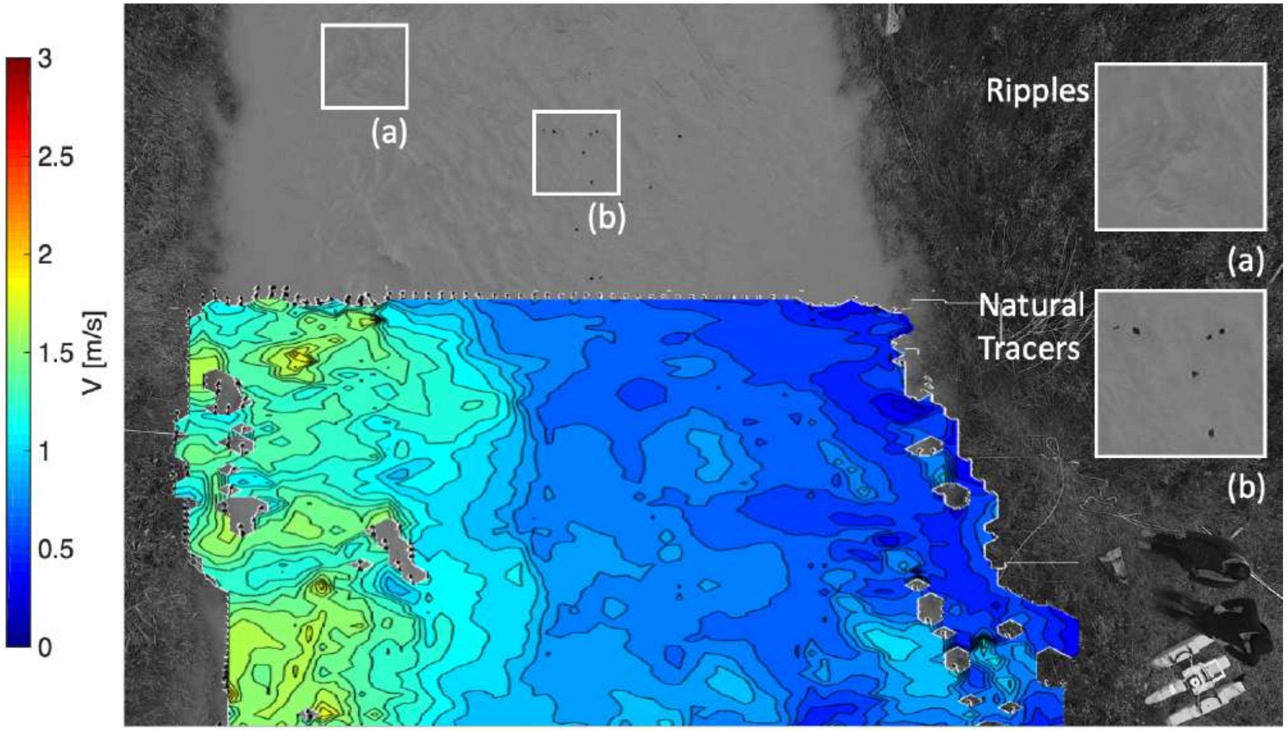

Surface Flow Velocity

Charcoal

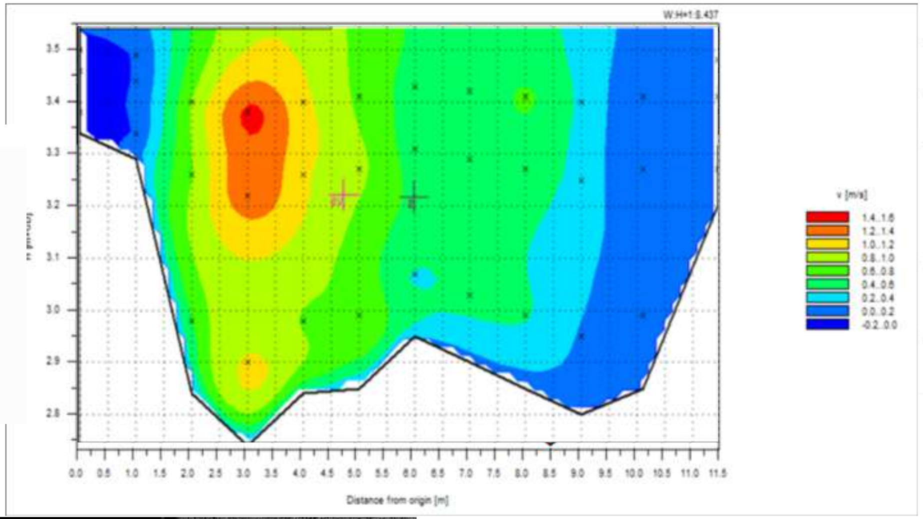

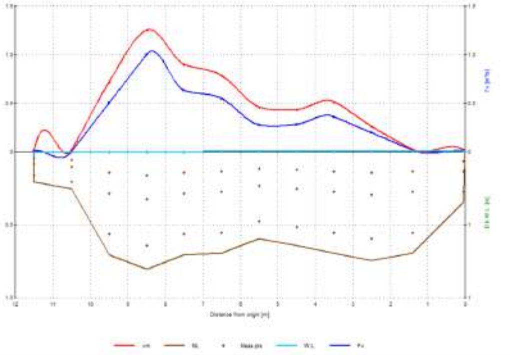

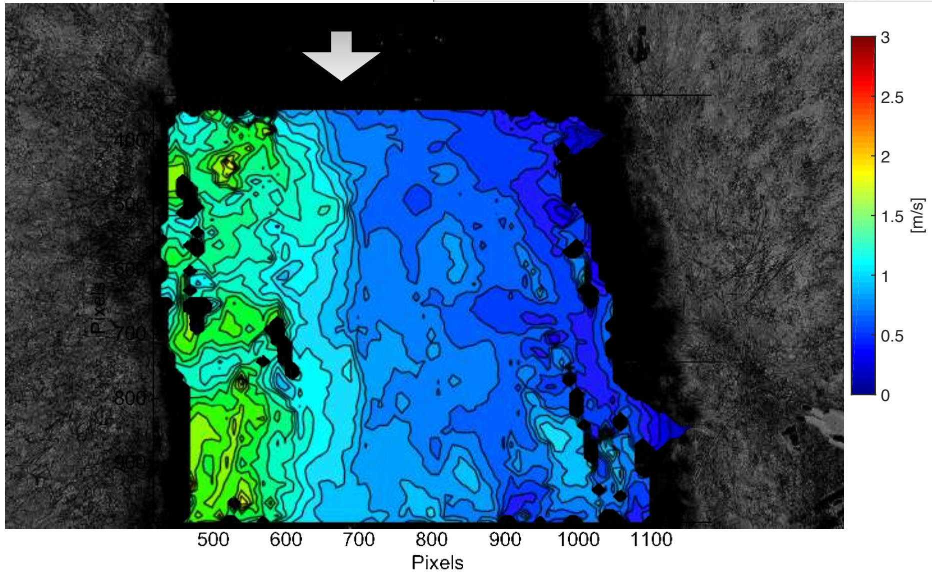

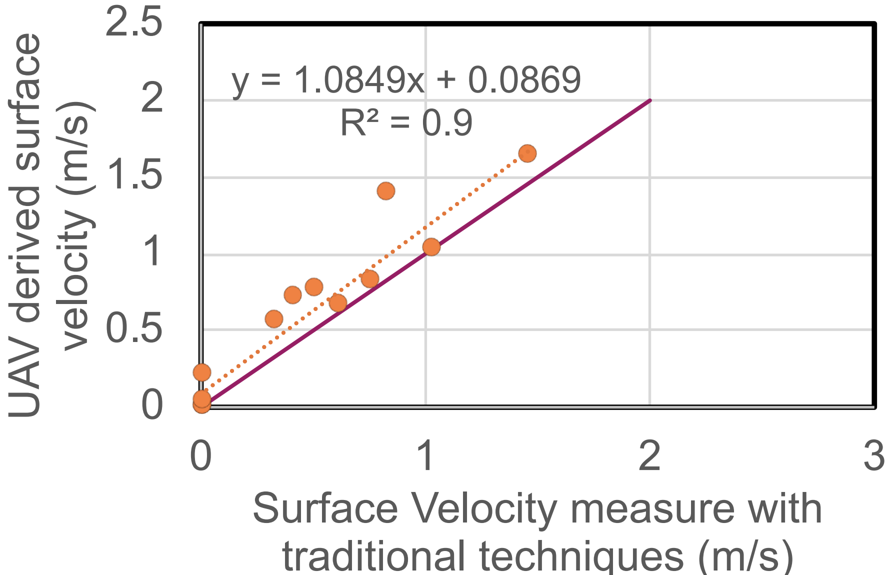

EUROPEAN COOPERATION IN SCIENCE & TECHNOLOGY

Field Experience with UAS

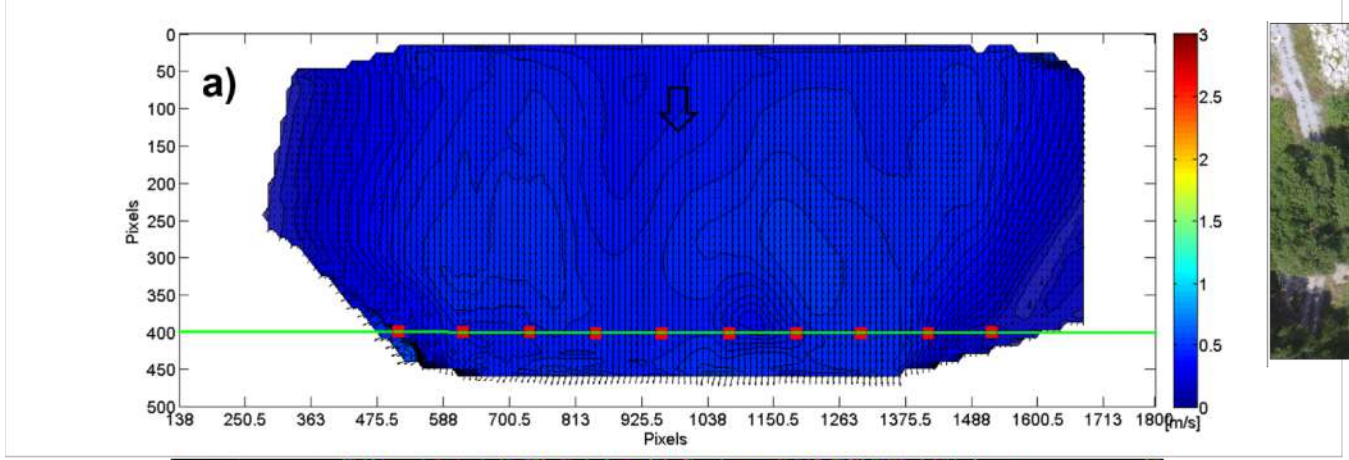

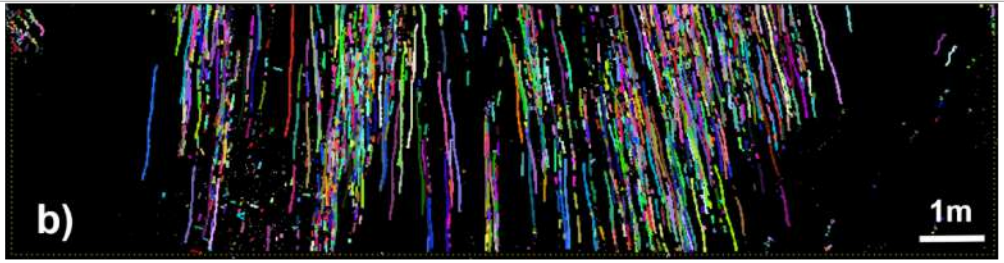

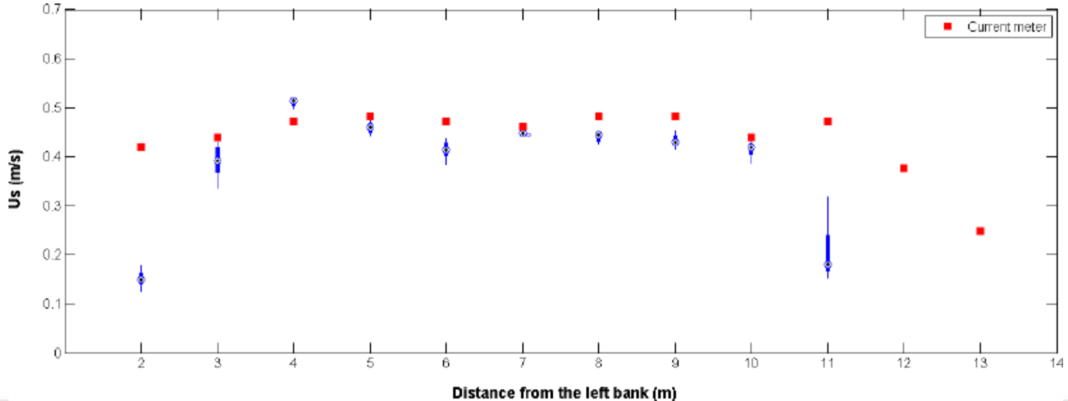

Validation with current meters

EUROPEAN COOPERATION IN SCIENCE & TECHNOLOGY

Stream Flow Monitoring – Data Collection for Benchmarking Optical Techniques

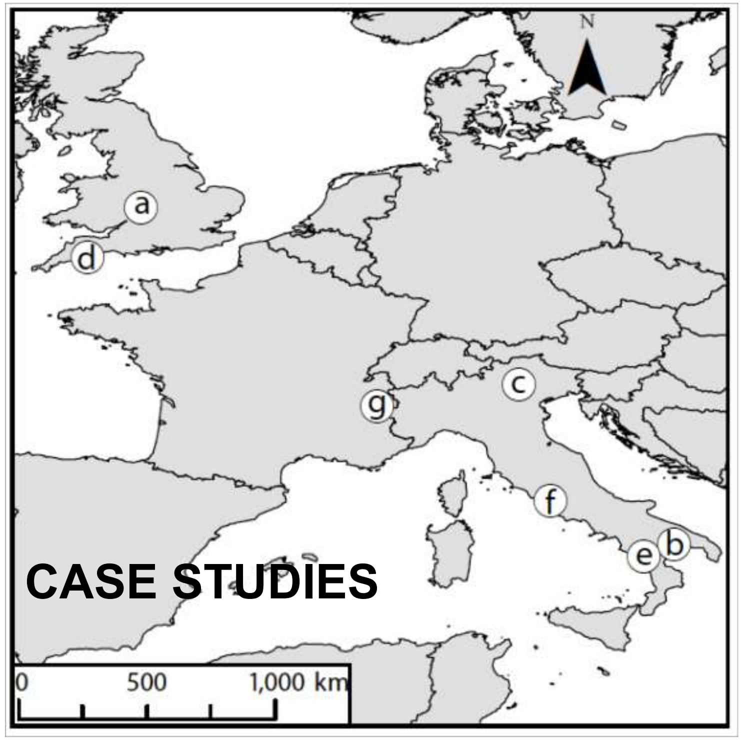

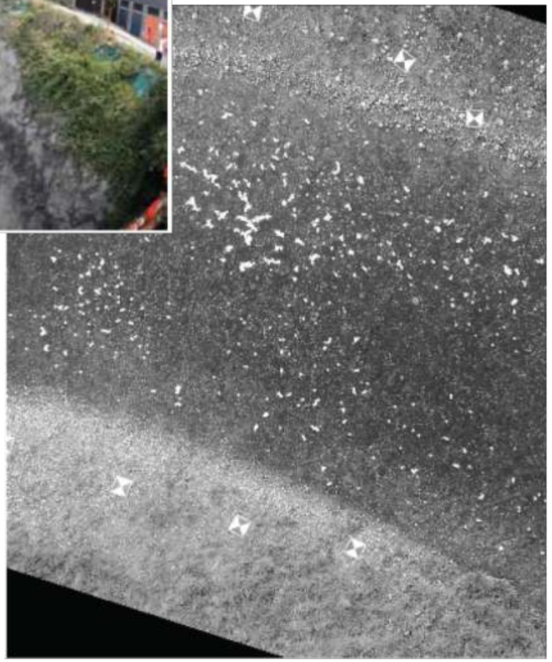

Stream Flow Monitoring – Data Collection

Original Video File Name: [River]_[Country][ddmmyearhhmmUTC].mov
Camera Model:
Platform used (gaugecam, drone, mobile, etc.):
Camera setting (autofocus, field of view, ISO, stabilization, …):
Video resolution (4000x2000, …)
Video frequency (Hz):
Presence of tracers and type:
Optional Info
Lumen:
Wind speed and orientation:
Case Study
River Name:
River Basin Drainage Area (km^2):
Cross-Section Coordinates (Lat, Long WGS84):
Flow regime (low, medium, high):
Ground-true availability (yes or not):
File Format (mov, avi, mp4, etc.):
Reference paper:
Processed Data
File Name of Processed Frames: [River]_[Country][ddmmyearhhmmUTC].zip
Number of frames:
Frame rate (Hz):
Pixel dimension:
Pre-processing actions (contrast correction, channel used, orthorectification, stabilization, etc.):

The Use of Discharge DATA: FRCs

FRCs are generally obtained using curve fitting methods with river stage (*H*) and discharge (*Q*) observations.

The most common equation is:

$$Q = \alpha(H - h_0)^{\beta}$$

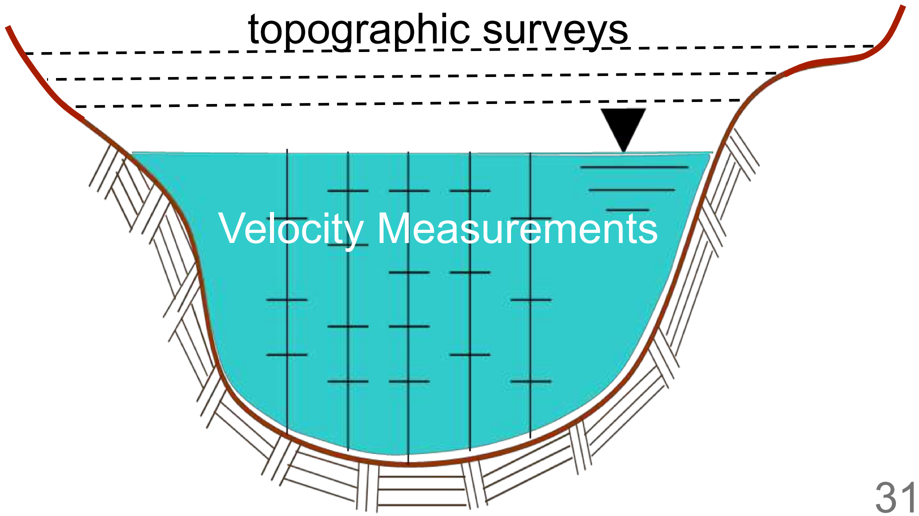

The Key Idea

Decomposing the parameter calibration according to the existing processes leads to more reliable model calibrations.

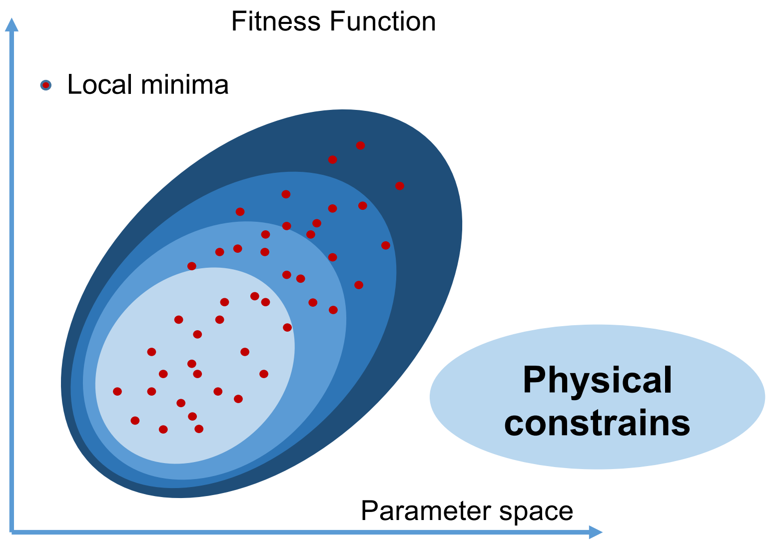

Impact of physical information on the parameter space domain

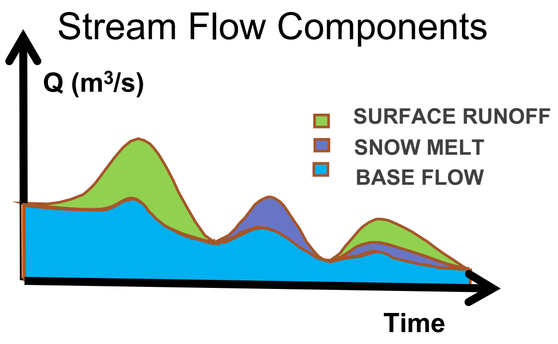

Model Performances

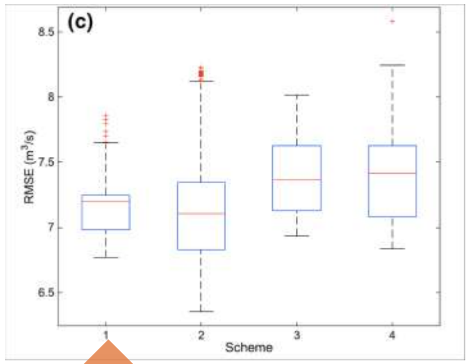

Including physical info

Manfreda et al. (HP - 2018)

The V Ω Method

The rating curve can be obtained as the product of two functions:

$$Q = V(H - h_0)\Omega(H - h_0)$$

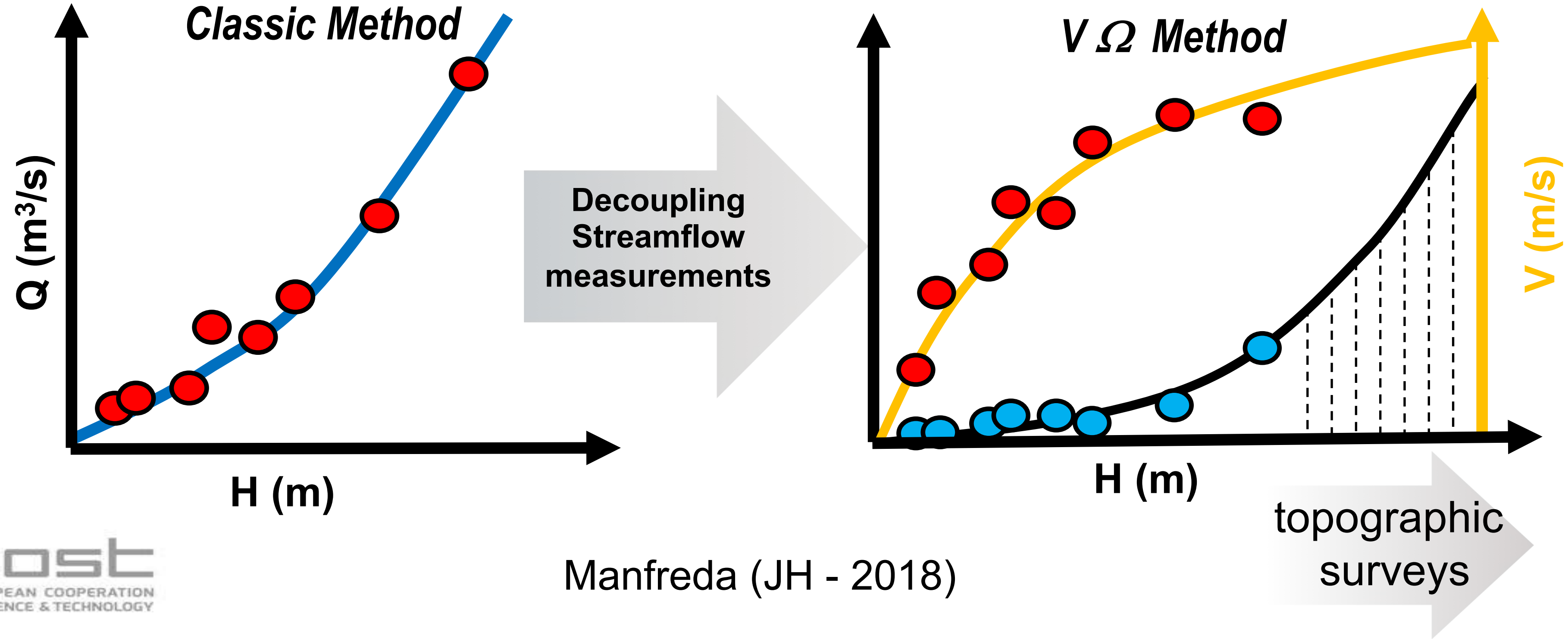

Manfreda (JH - 2018)

Comparison of the two methodologies

- FRCs derived with different permutation of the same dataset;
- Comparison is made on the calibration dataset and on the data excluded from the calibration.

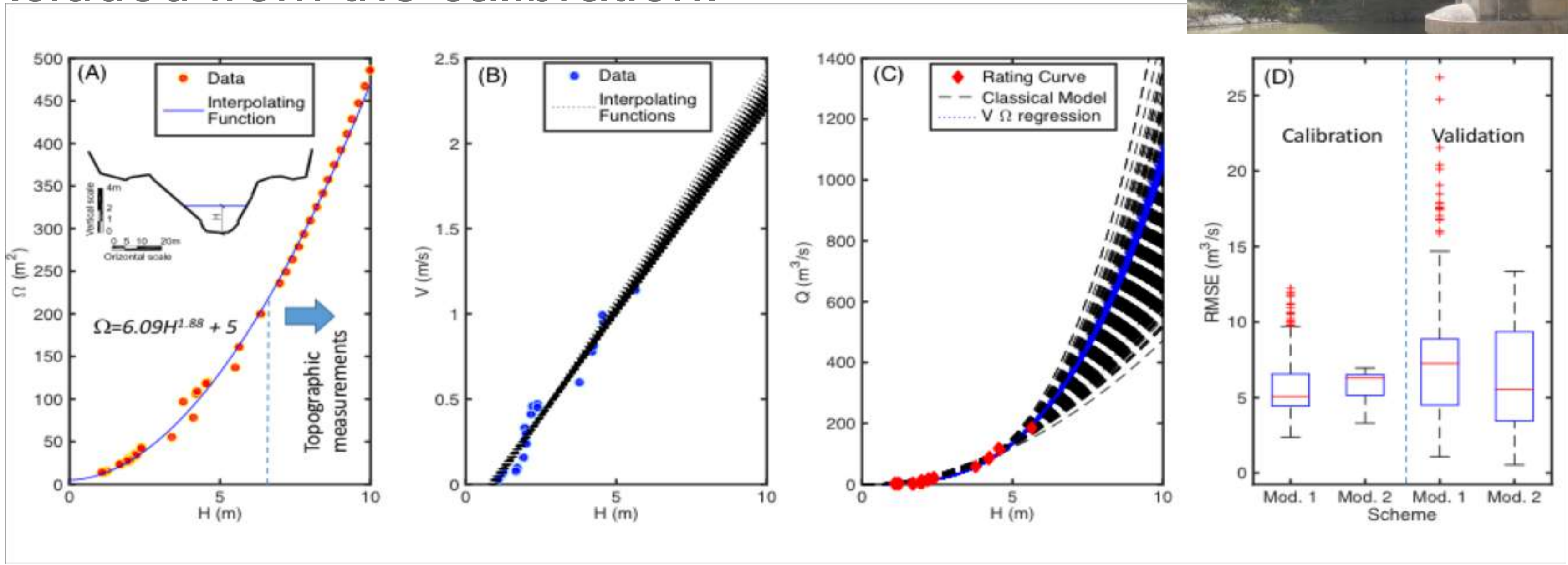

Manfreda (JH - 2018)

Conclusion

- UAS-based remote sensing provides new advanced procedures to monitor key variables, including vegetation status, soil moisture content, and stream flow.
- The detailed description of such variables will increase our capacity to describe water resource availability and assist agricultural and ecosystem management.
- The wide range of applications testifies to the great potential of these techniques, but, at the same time, the variety of methodologies adopted is evidence that there is still need for harmonization efforts.

Related Publications

- Manfreda and McCabe (2019). ***Emerging earth observing platforms offer new insights into hydrological processes***, Hydrolink.
- Perks, Hortobágyi, Le Coz, Maddock, Pearce, Tauro, Dal Sasso, Grimaldi, Manfreda (2019) **Towards harmonization of image velocimetry techniques for determining open-channel flow**, Earth system science data (in preparation).
- Manfreda, Dvorak, Mullerova, Herban, Vuono, Arranz Justel, Perks (2019) ***Assessing the Accuracy of Digital Surface Models Derived from Optical Imagery Acquired with Unmanned Aerial Systems***, Drones.
- Manfreda, ***On the derivation of flow rating-curves in data-scarce environments***, Journal of Hydrology, 2018.
- Dal Sasso, Pizarro, Samela, Mita, and Manfreda (2018) ***Exploring the optimal experimental setup for surface flow velocity measurements using PTV***, Environmental Monitoring and Assessment.
- Manfreda, McCabe, Miller, Lucas, Pajuelo Madrigal, Mallinis, Ben-Dor, Helman, Estes, Ciraolo, Müllerová, Tauro, De Lima, De Lima, Frances, Caylor, Kohv, Maltese (2018), ***On the Use of Unmanned Aerial Systems for Environmental Monitoring***, Remote Sensing.
- Baldwin, Manfreda, Keller, and Smithwick, Predicting root zone soil moisture with soil properties and satellite near-surface moisture data at locations across the United States, Journal of Hydrology, 2017.
- Manfreda, Brocca, T. Moramarco, F. Melone, and J. Sheffield, ***A physically based approach for the estimation of root-zone soil moisture from surface measurements***, Hydrology and Earth System Sciences, 18, 1199-1212, 2014.
- Manfreda, Lacava, Onorati, Pergola, Di Leo, Margiotta, and Tramutoli, ***On the use of AMSU-based products for the description of soil water content at basin scale***, Hydrology and Earth System Sciences, 15, 2839-2852, 2011.


HydroLAB

Università per Stranieri di Perugia

UAS Photogrammetry

Prof. Salvatore Manfreda

Associate Professor of Water Management and Ecohydrology - http://www2.unibas.it/manfreda

Chair of the COST Action Harmonious - http://www.costharmonious.eu

COST EUROPEAN COOPERATION IN SCIENCE & TECHNOLOGY

Funded by the Horizon 2020 Framework Programme of the European Union

UNIVERSITA' DEGLI STUDI DELLA BASILICATA

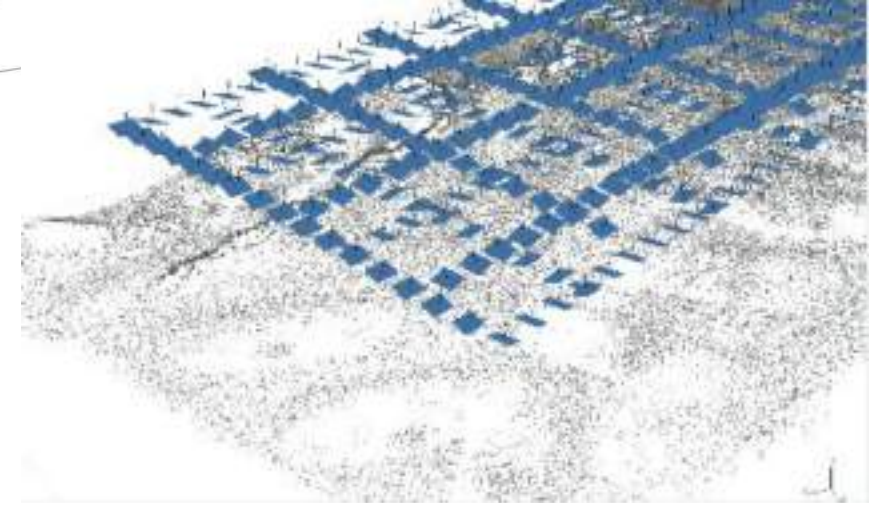

Outline

Principle of Photogrammetry

Surface from Motion Algorithms

UAS photogrammetry
- Georeferencing
- Direct and GCP-based georeferencing
- Using check points and assessing accuracy

•UAS-based DSM accuracy assessment and survey strategies

•Introduction to the exercise

What is Photogrammetry?

Derived from Greek terms:
- Photos = light
- Gramma = to draw
- Metron= to measure

Fundamentally: The process of extracting metric information or measurements from imagery

COST
EUROPEAN COOPERATION IN SCIENCE & TECHNOLOGY

Why is this useful?

Treat imagery as maps –make direct, reliable measurements

ORTHOIMAGE or **ORTHOMOSAIC**

• Necessary for topographic mapping
• Digital elevation models (DEMs)
• Combines geometric and semantic properties of imagery

Applications:

• topographic and thematic mapping
• change detection
• feature extraction

•3D building & city modelling
•3D visualisation
•military applications

How is this achieved?

Relief displacement

- Elevated objects displaced outwards from centre
- Effect of ‘building lean’

Tilt distortion

- Image plane not truly level (effect of tilt at time of capture)
- Imaged terrain must be rectified to remove this distortion

Relief Displacement

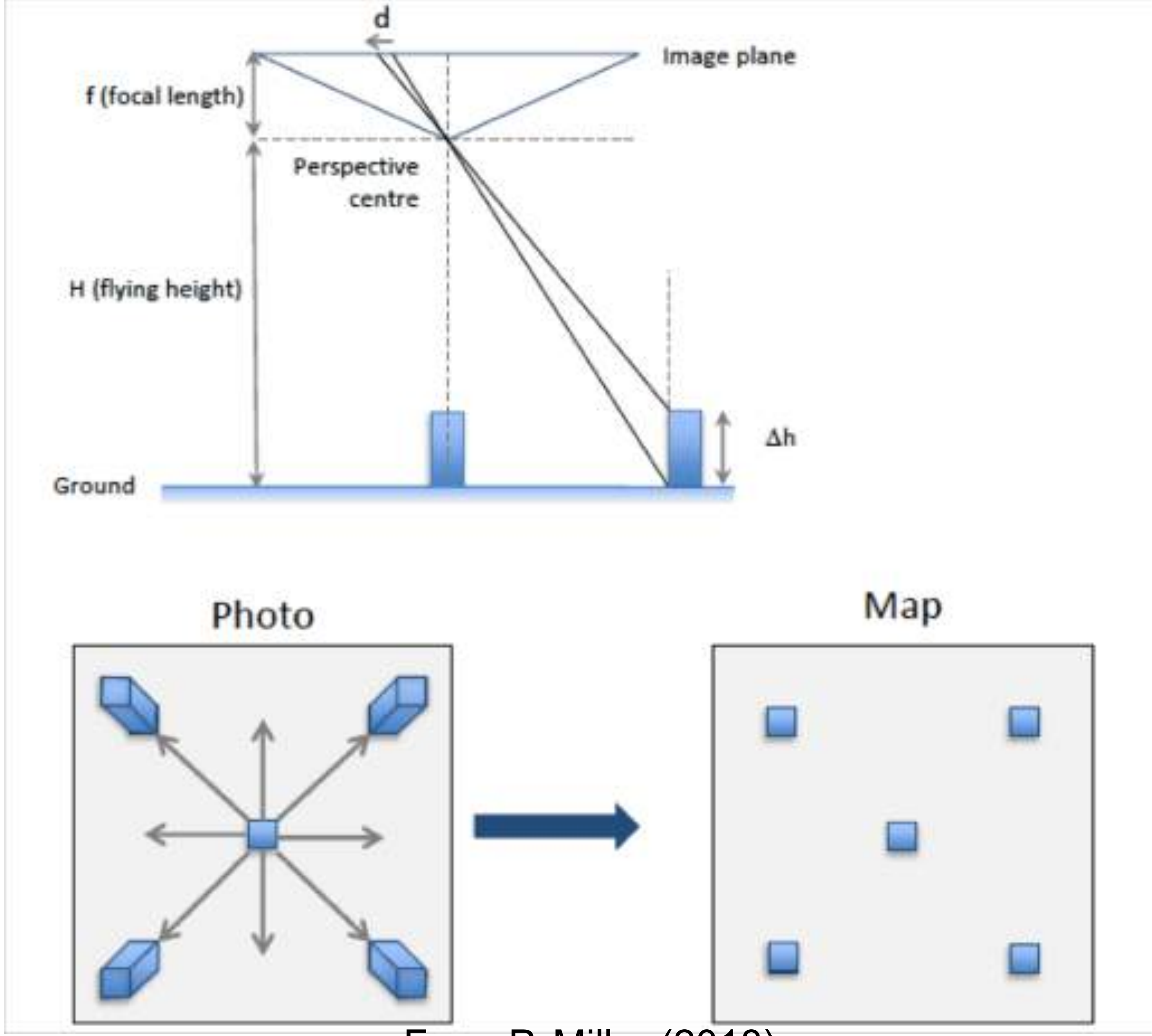

From P. Miller (2018)

Tilt Distorsion

- **Rectification to remove tilt distortion**
- Ideally minimised at time of capture, but some effects still remain

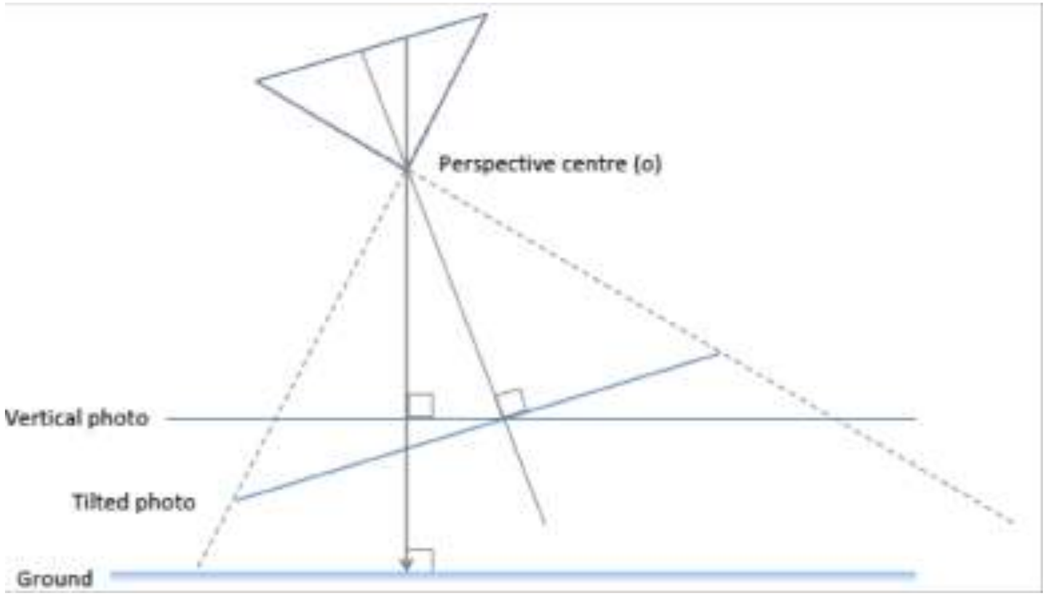

COST
EUROPEAN COOPERATION IN SCIENCE & TECHNOLOGY

Stereo Photogrammetry

- 3D (x,y,z) measurement: overlapping (stereo) imagery

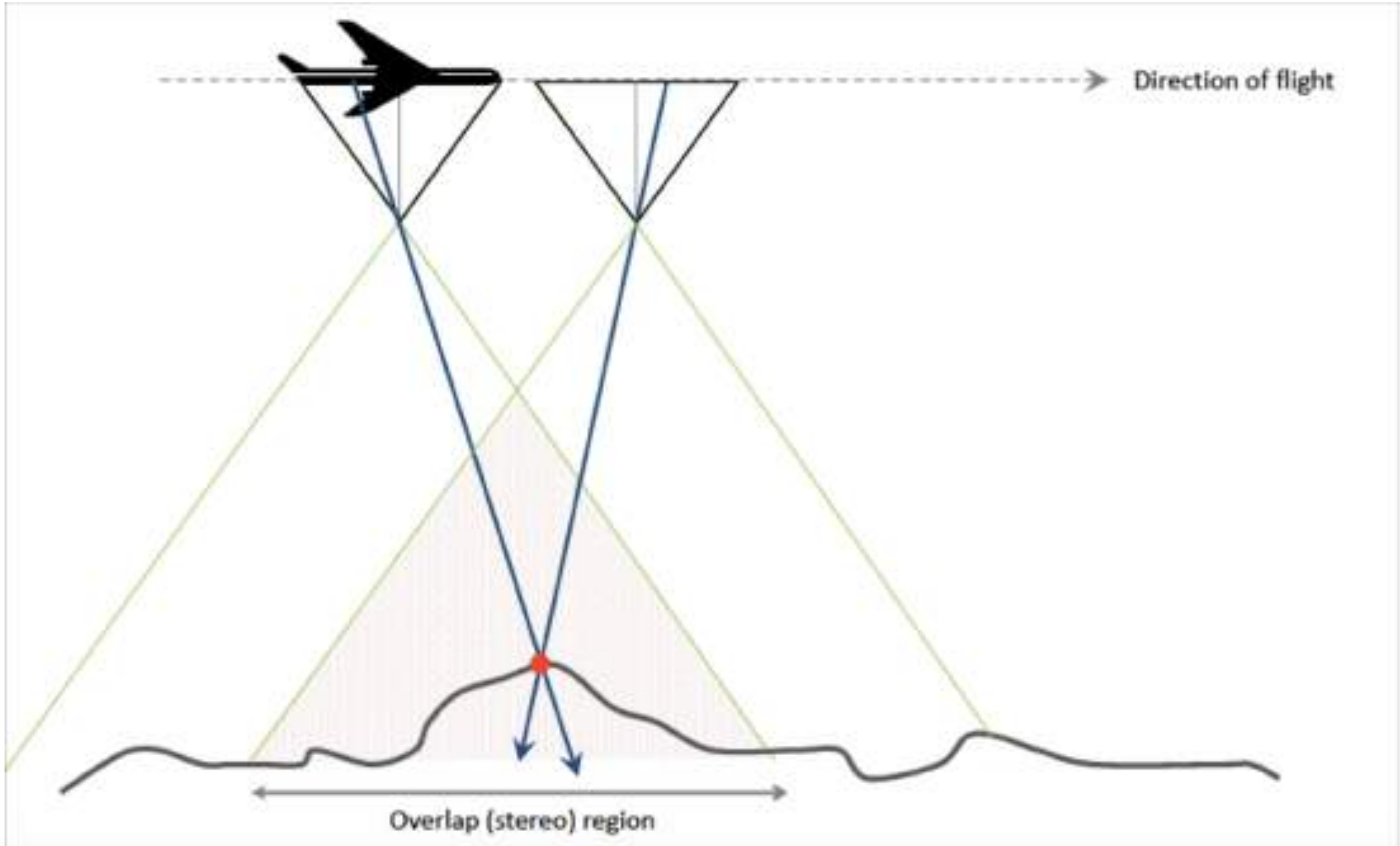

EUROPEAN COOPERATION IN SCIENCE & TECHNOLOGY

Parallax

- Pa = $x_a – x'_a$
- Pa = parallax of point A
- X_a= x coord of A on left photo
- x'_a= x coord of A on right photo

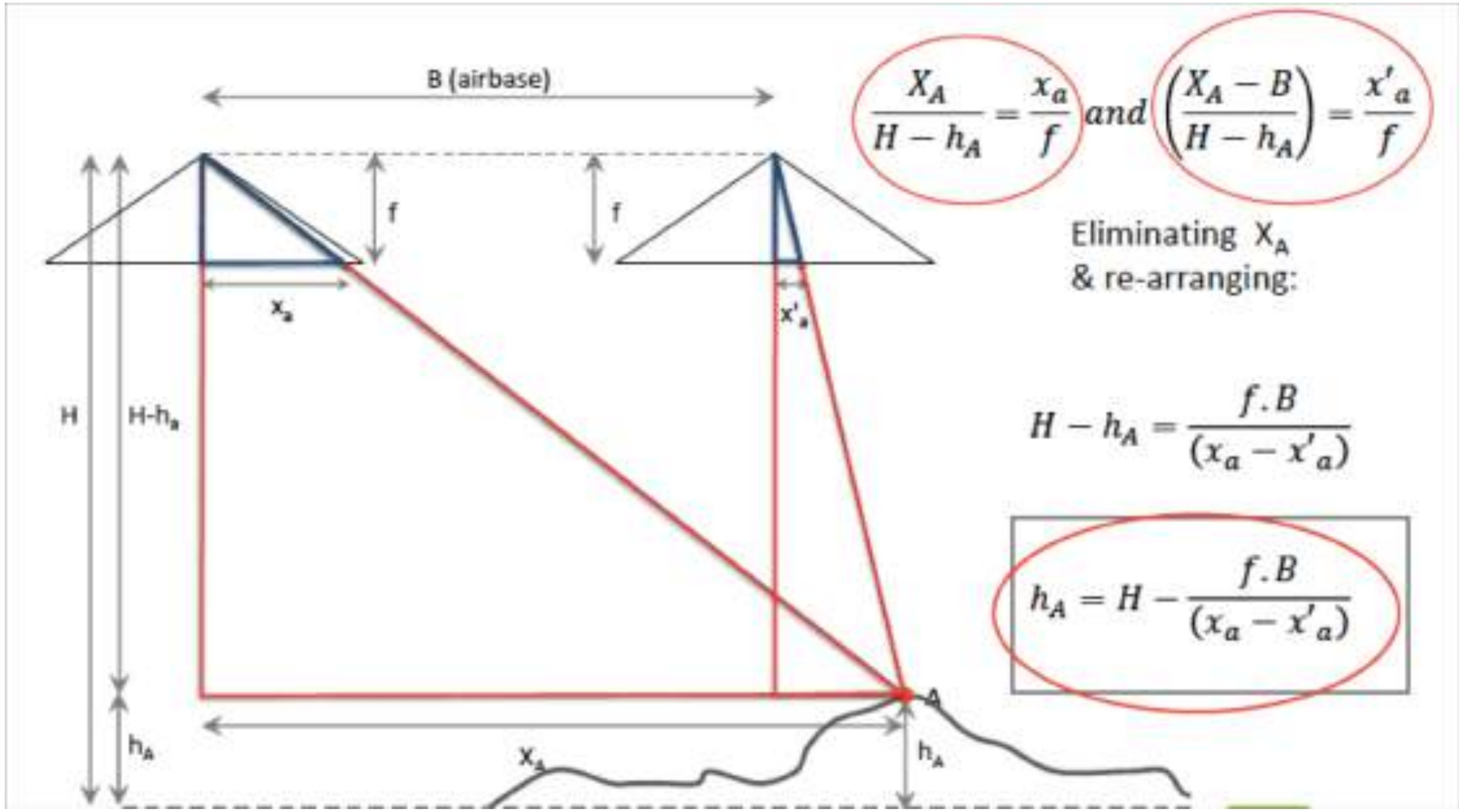

Parallax as a function of height

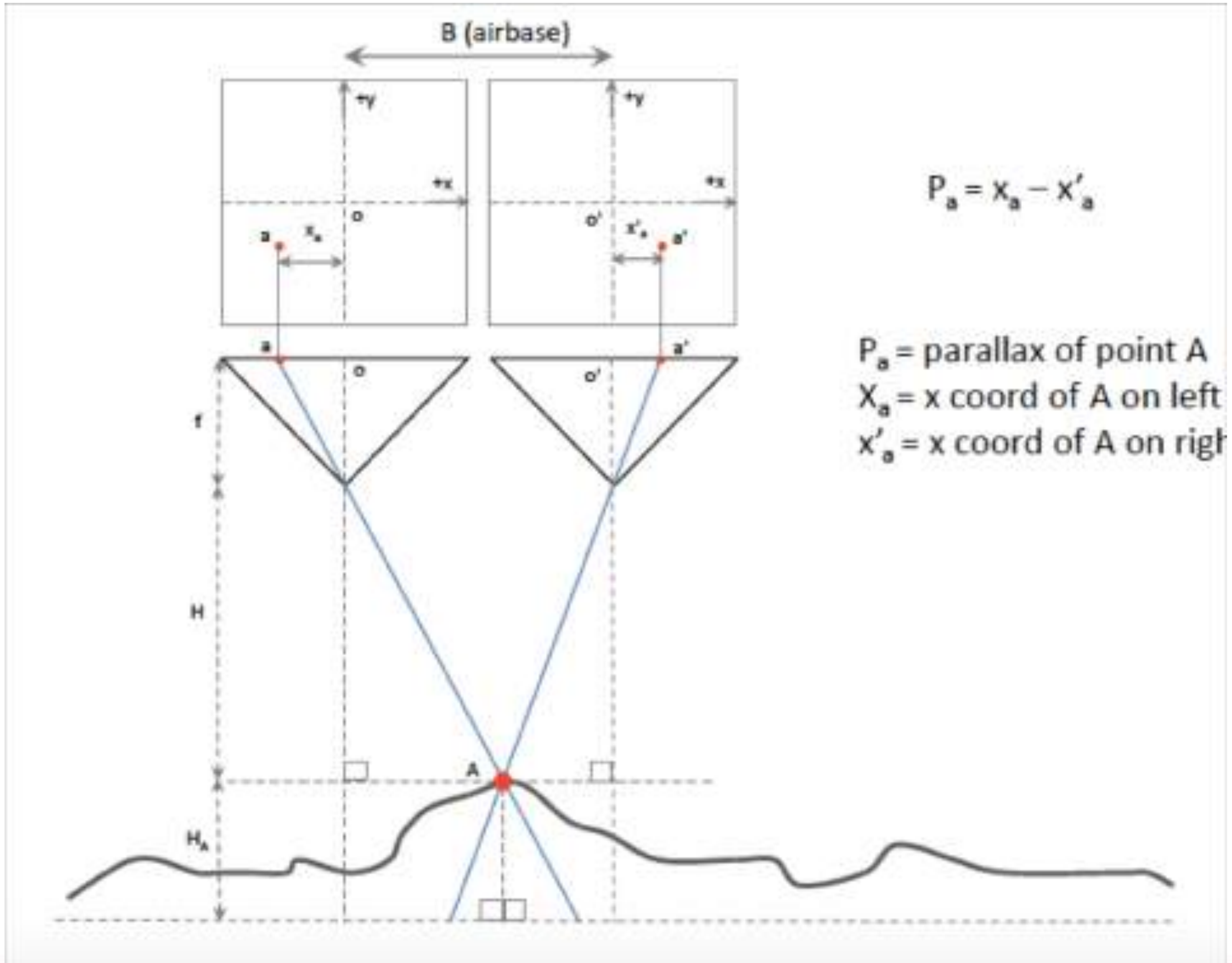

Space Resection

- If three or more points with known 3D ground coordinates are observed in an image, the camera position and orientation can be determined
- {X, Y, Z, ω, ϕ, κ}

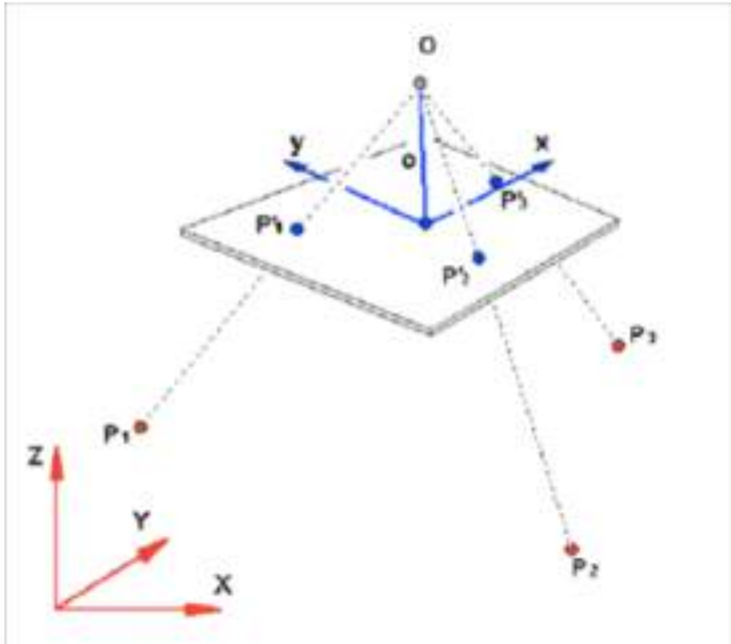

Aerial Photogrammetry

- Most common application
- Relies on ‘near-vertical’ imagery captured from airborne camera

VERTICAL CASE

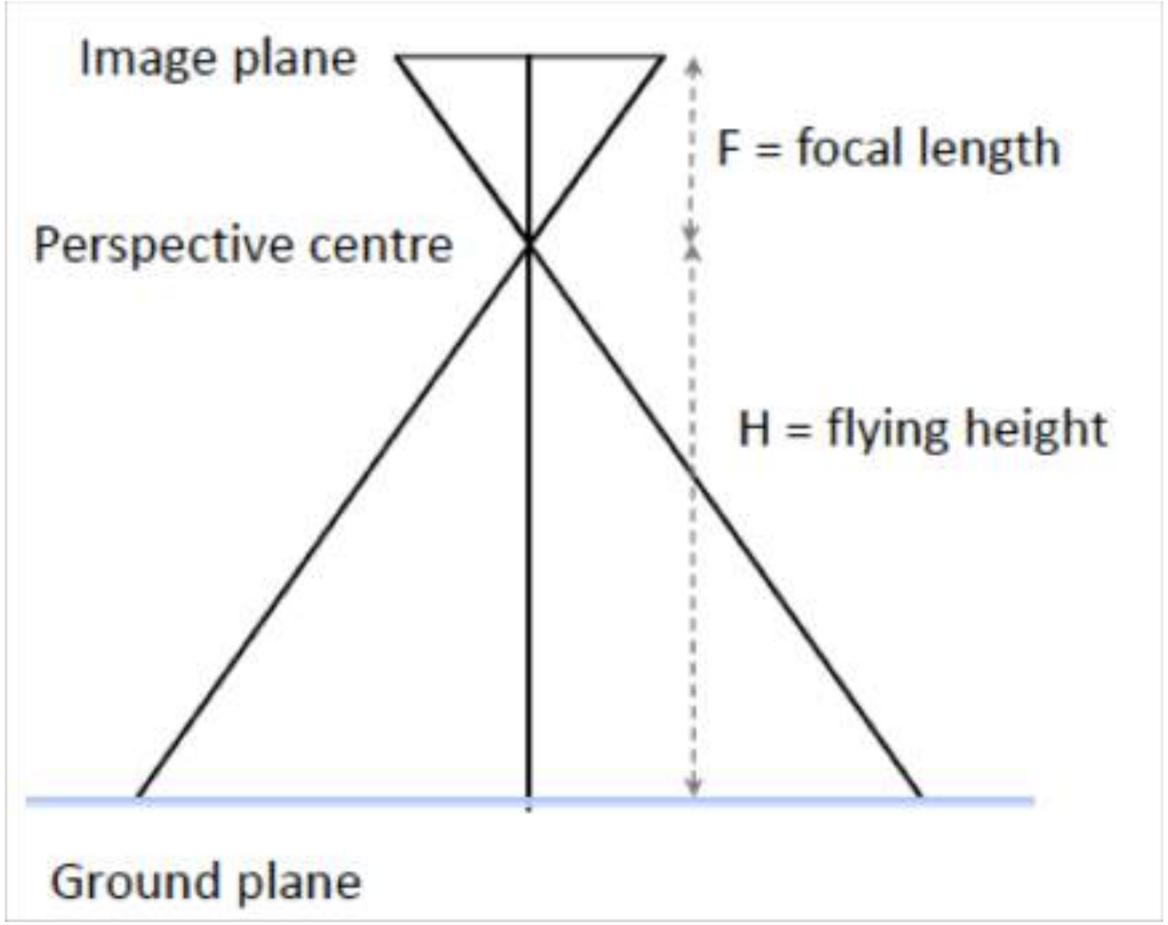

Lens Distortion

- Distortion increases with distance from centre of lens
- Metric cameras: few microns (µm)
- Non-metric: 20 –several hundred microns

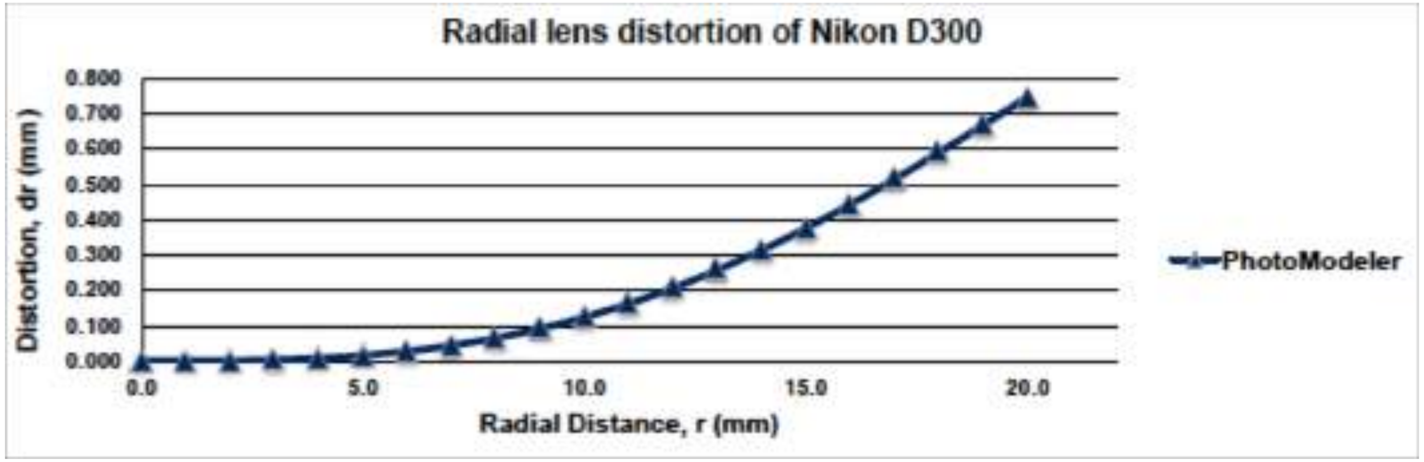

Relative Orientation

- Relative orientation between camera centres. Offsets in XYZ
- Model coordinate system

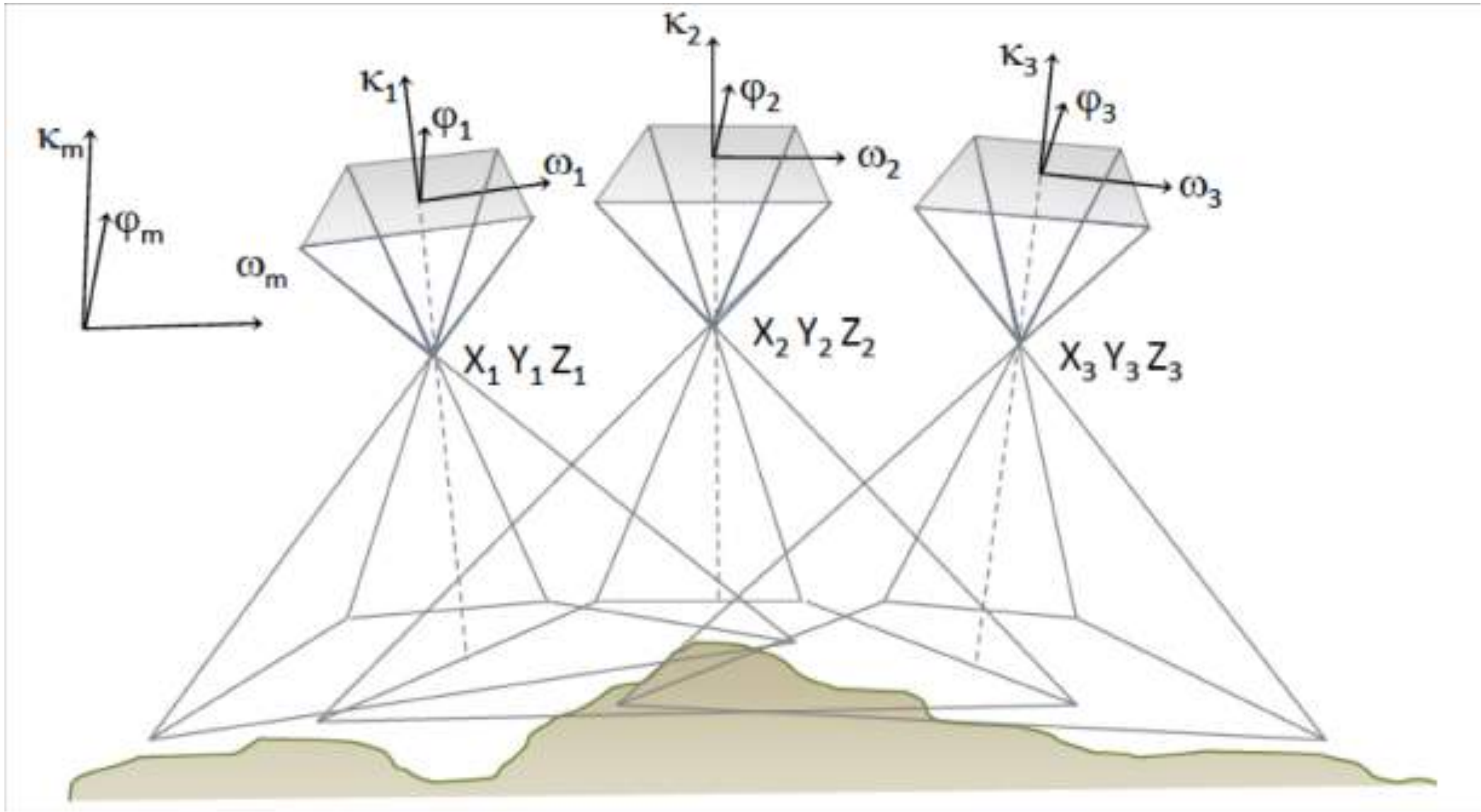

Intersection

- If a point is observed in two or more cameras of known relative position and orientation, the 3D coordinates of the point can be determined

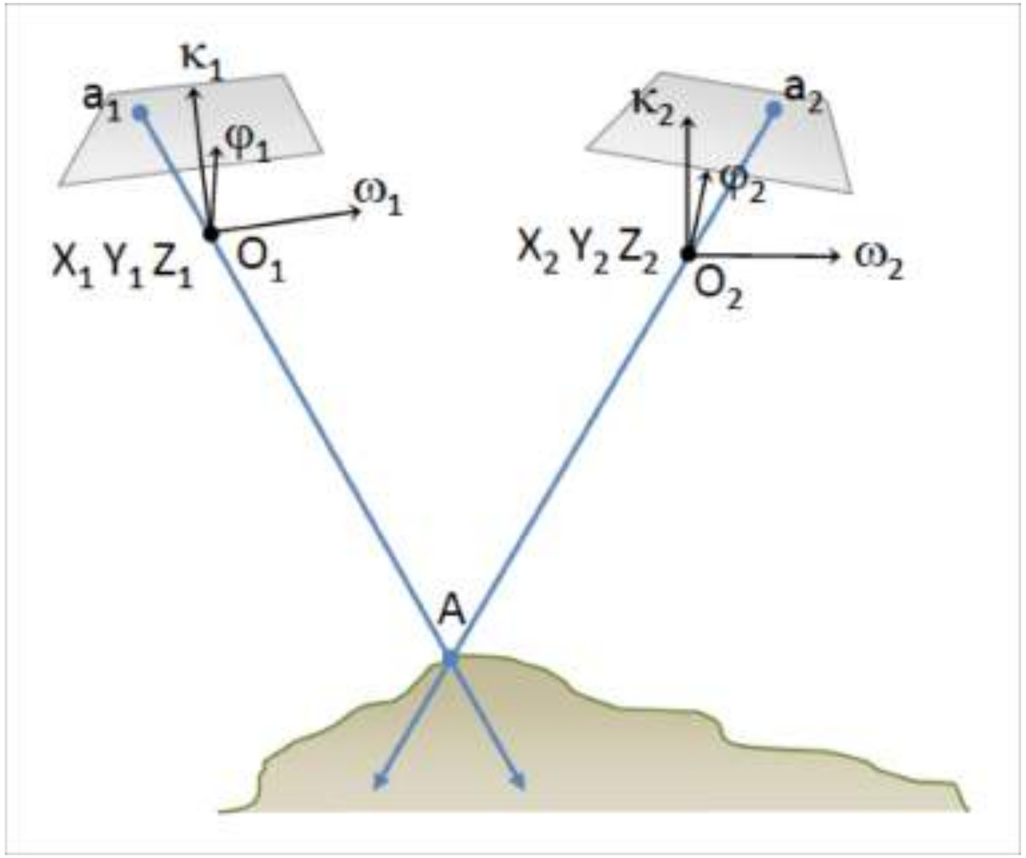

RO: Tie Points

- Identify corresponding points in overlap (stereo) region
- Mathematical solution of intersection of light ‘rays’
- Transformation to stereomodelsystem 3D model coordinates

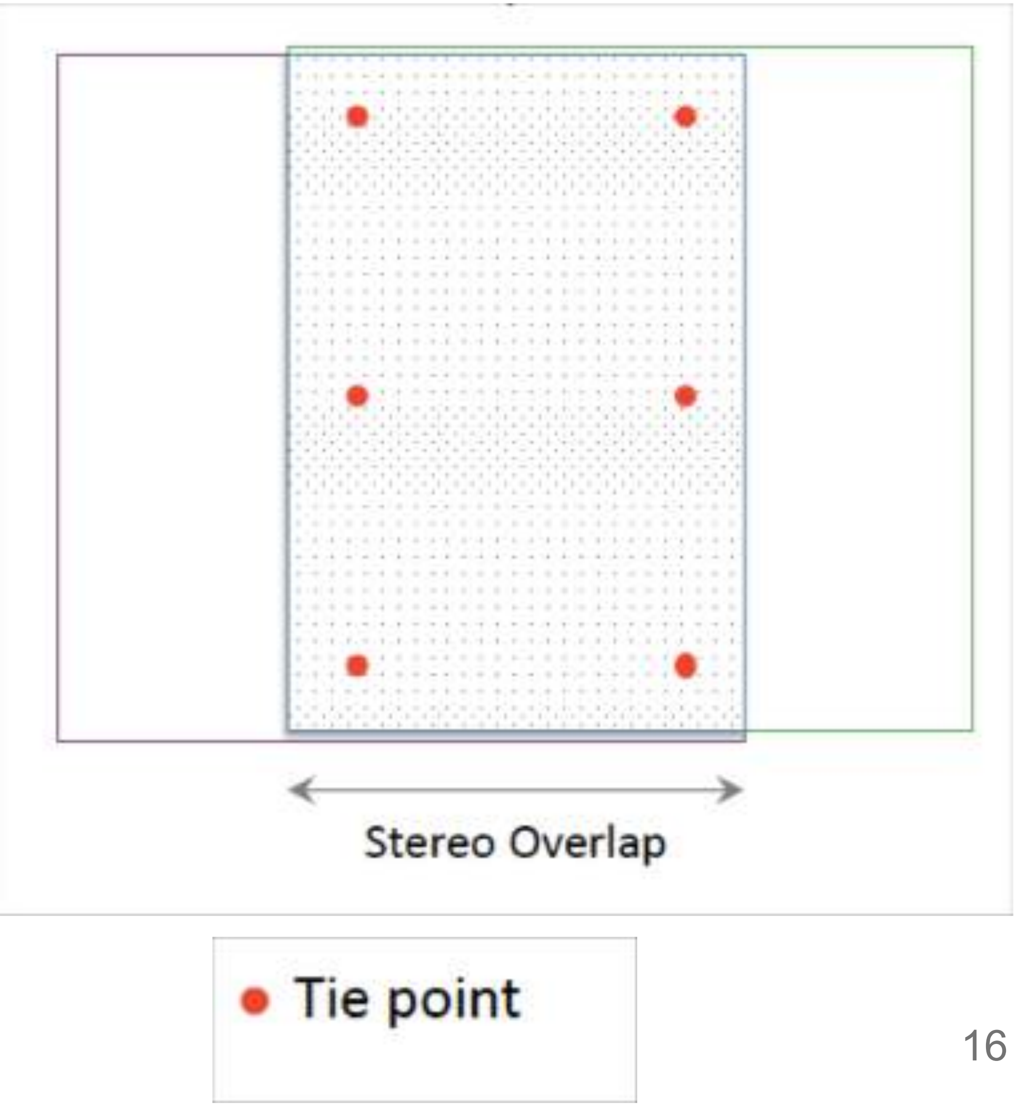

EUROPEAN COOPERATION IN SCIENCE & TECHNOLOGY

Absolute Orientation

Goal: transform stereomodelto ground coordinate system

Approach

- Ground control points (GCPs) measured in field (e.g. by GNSS)
- Natural targets or pre-marked
- Clearly visible in imagery
- Measure 3D model coordinates of GCPs
- Relate the two systems –**3D conformal transformation**

Requirements

- Minimum: 2 PLAN & 3 HEIGHT points
- 2 points to **scale**and **orientate** the model
- 3 points to **level**
- Always add redundancy and measure more GCPs

Digital Photogrammetry

- Employs powerful **Digital Photogrammetric Workstations (DPW)**
- Very expensive
- Skilled photogrammetric operator
- Very robust & rigorous
- Incorporates **stereo viewing** system
- Solves using **bundle adjustment**
- Oriented images matched to **extract DSM**
- DSM then used to ortho-rectify imagery to generate **orthophoto**or **orthomosaic**
- **Digital Photogrammetry**

Bundle (block) Adjustment

In practice this is how we solve for exterior orientation

- A simultaneous least squares adjustment of all model parameters. Minimises residuals (errors).

Inputs:

- Tie point observations
- Ground control point observations & coordinates
- Camera geometry

Outputs:

- Tie point positions
- Camera position and orientations
- Camera parameters (optionally)
- Parameter uncertainty & overall accuracy of solution

Photogrammetry from UAS

Aim: Derive quantitative geospatial information from imagery

- Not a new challenge
- BUT, UAV platforms present new opportunities

Attractions

- Flexible data collection over small to medium extents
- Delivers DEMs & ortho-imagery at very high spatial resolutions
- Cost effective -relatively low initial investment
- Ease of uptake for standard application

- **Photogrammetry from UAS**

Photogrammetry: ease of application?

Historically

- Complex software workflows
- Careful parameterisation
- Expensive software/hardware and difficult to access
- Highly specialist -skilled operators

Present Situation

- Development of **structure-from-motion**(SfM), enabled through dense image matching developments (multi-view stereo)
- Low cost & quite ‘black box’
- Little expertise required

→ **Bundle adjustment central to both approaches**

COST EUROPEAN COOPERATION IN SCIENCE & TECHNOLOGY

SfM Software

Proprietary

- Agisoft Photoscan
- Pix4D
- nFramesSURE
- …

Open Source

- VisualSFM
- Micmac
- PMVS/CMVS
- Bundler
- Apero/MicMac
- …

Photogrammetric Block Capture

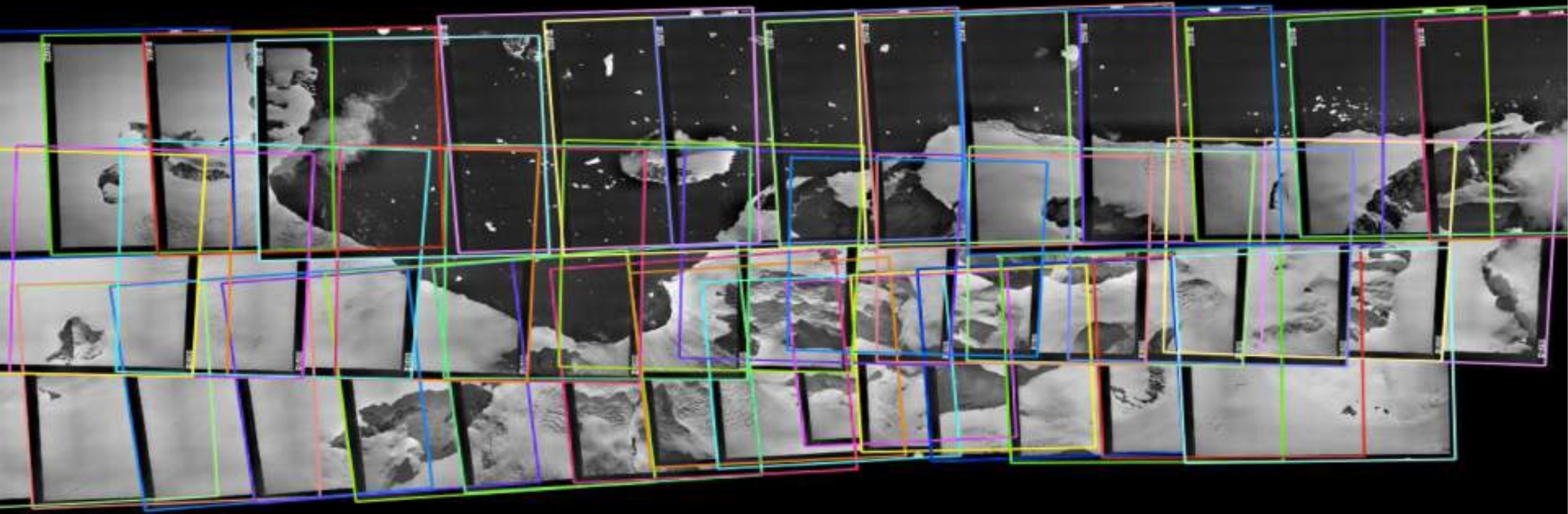

Strip = sequential exposures in a single flightline
Block = multiple strips to build up area coverage

Flight Planning

- Sequential overlaps
- Parallel flightlines
- Height above ground
- Consider effect of wind
- Time for UAV to turn
- Auto-triggering best
- Include cross-strips
- Some oblique images

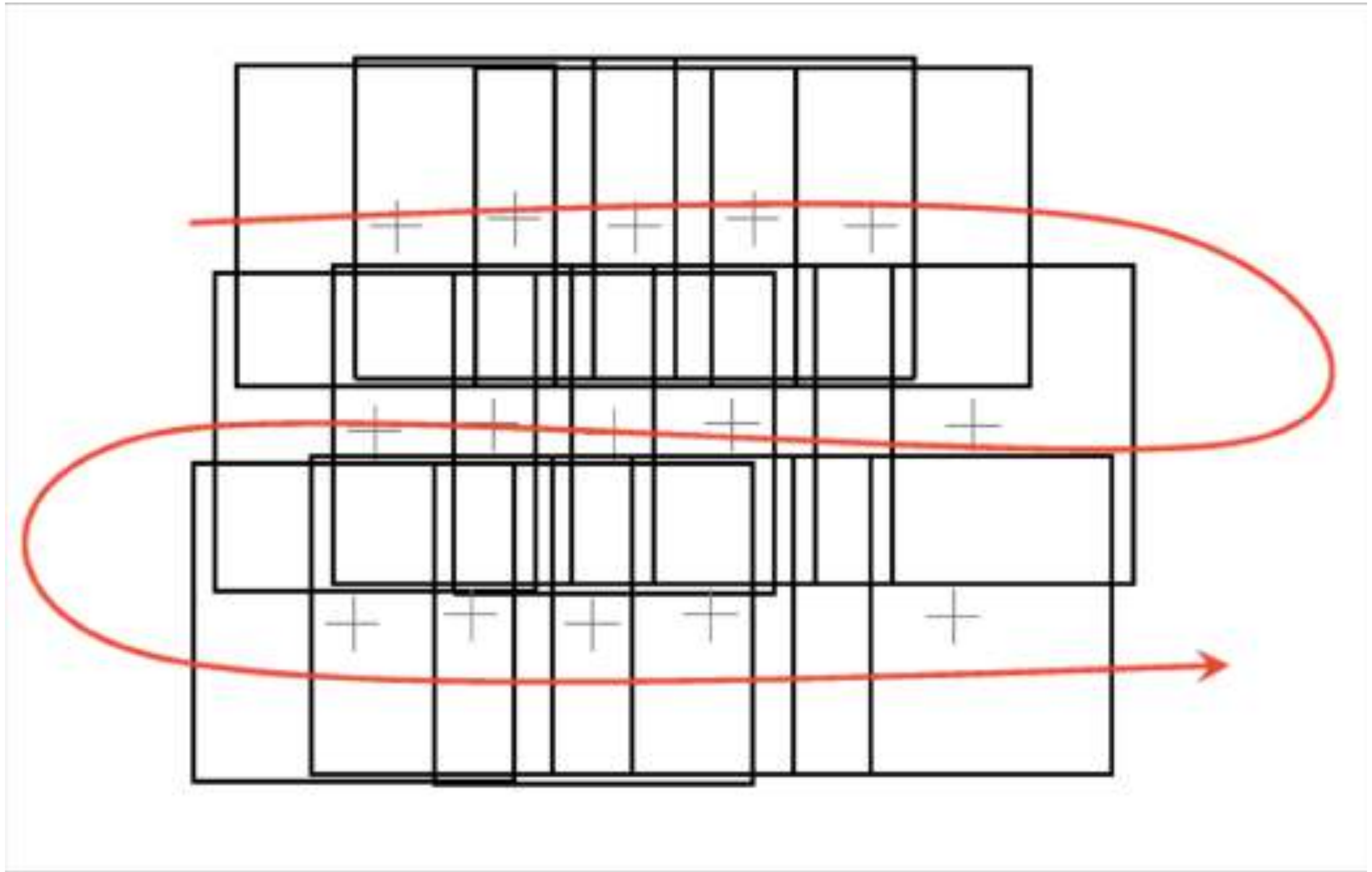

Photogrammetry from UAS

Match sensor size, focal length, flying height to GSD

Overlaps for stereo coverage (SfM)

- 80% forward overlap
- 60% sidelap

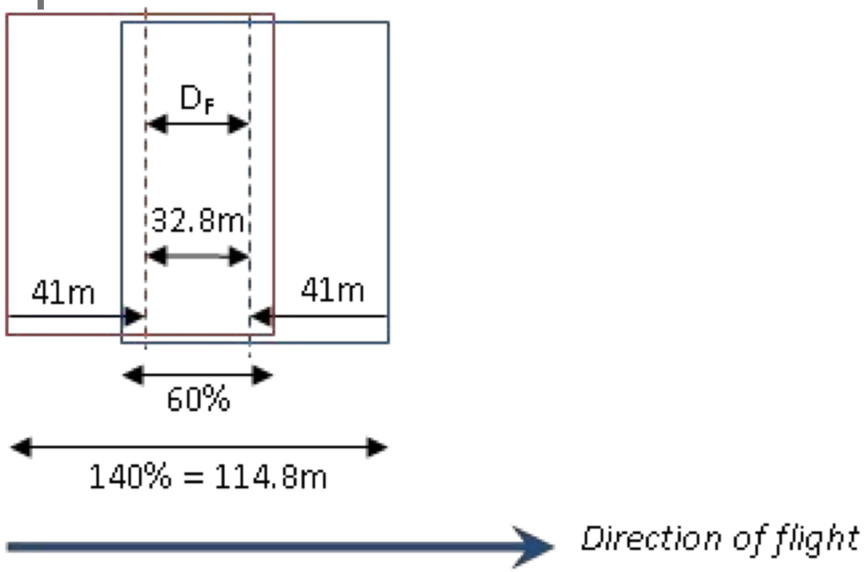

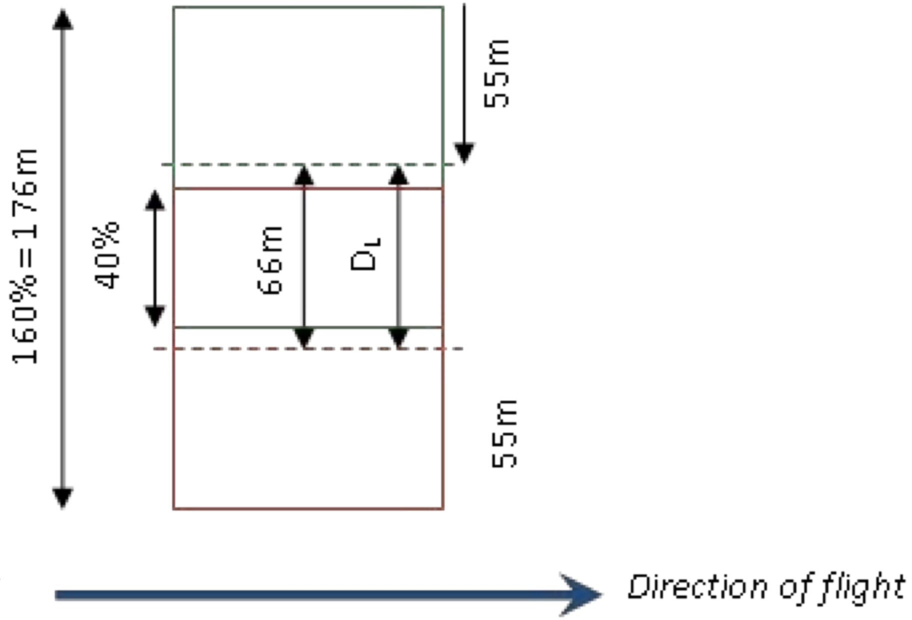

COST EUROPEAN COOPERATION IN SCIENCE & TECHNOLOGY

Ground Control Points

Well distributed in plan and height

Well distributed across area of interest

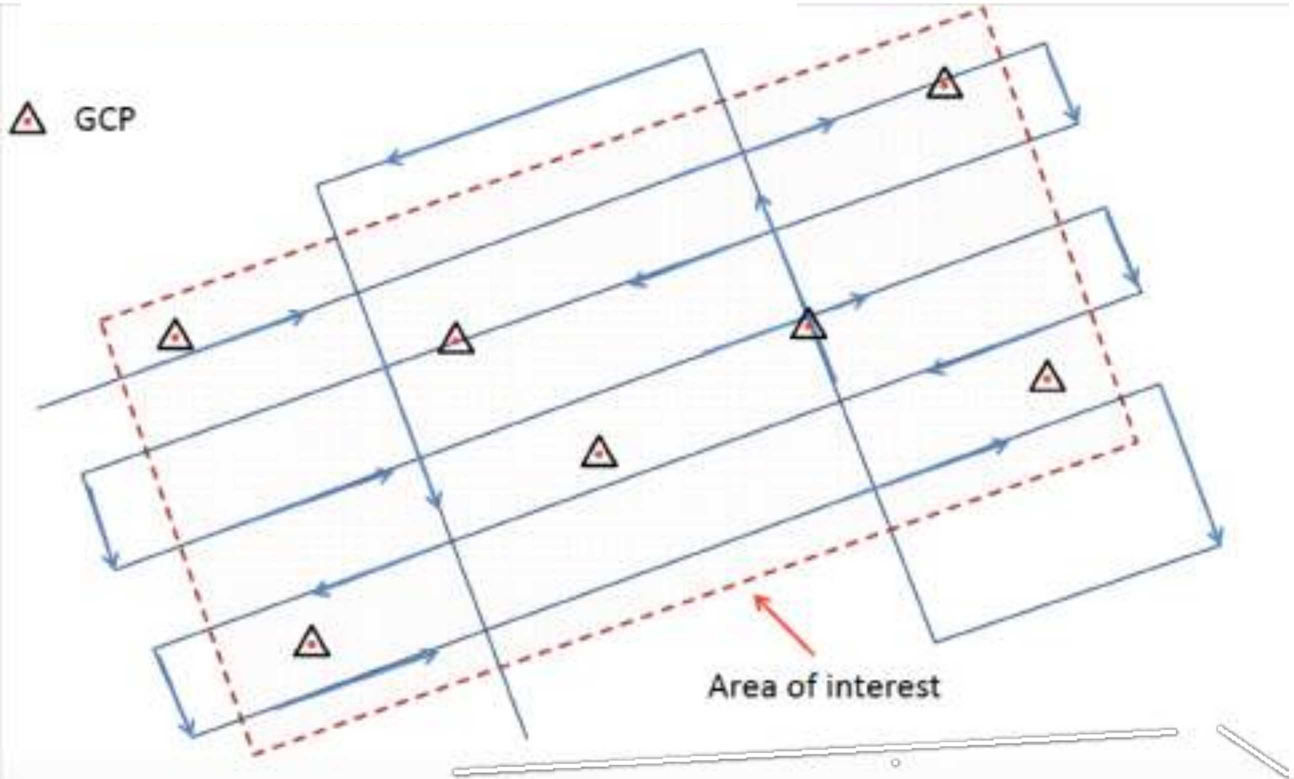

GCP Targets

- **Pre-marked** best for precise observations
- Must be large enough to be visible in images (link to GSD)
- Must be small/distinct enough for precise location at image scale
- Measured through GNSS (post-processed) or total station
- Positional accuracy must fit to purpose of study

EUROPEAN COOPERATION IN SCIENCE & TECHNOLOGY

Hands on a Flight Planning

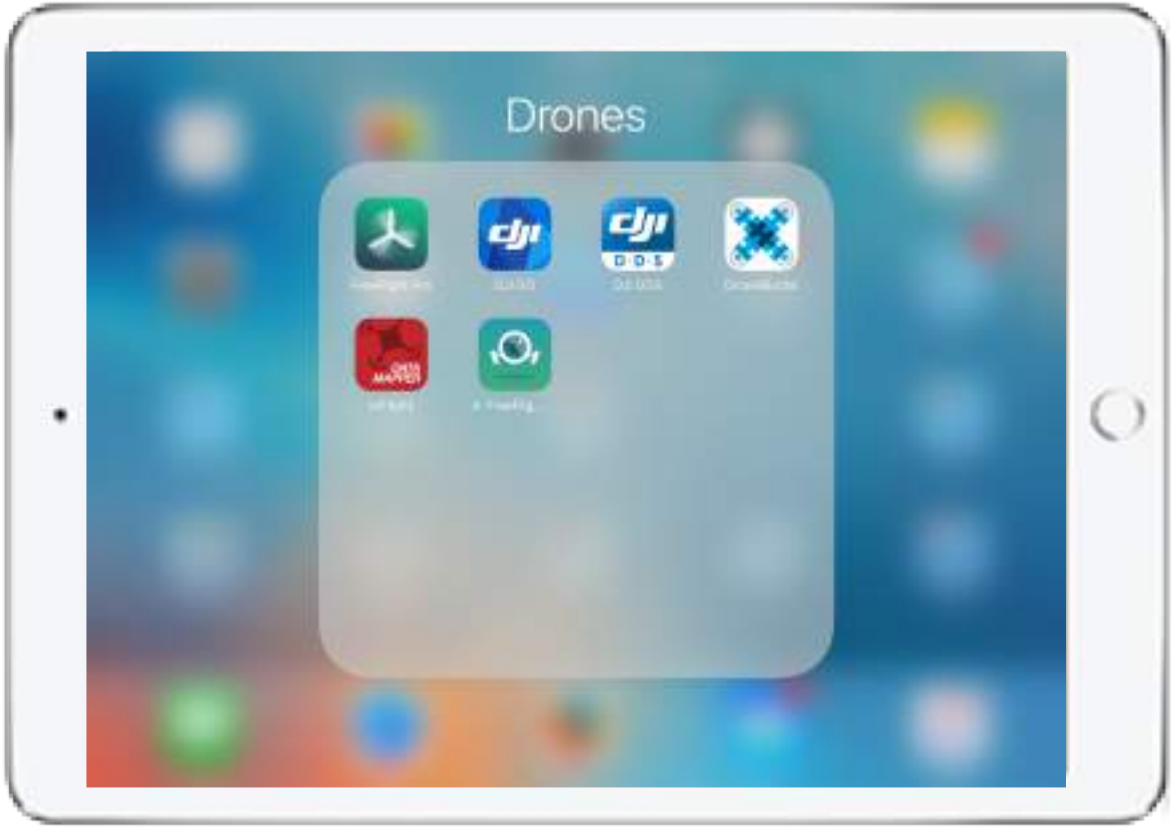

Flight planning: Data Mapper

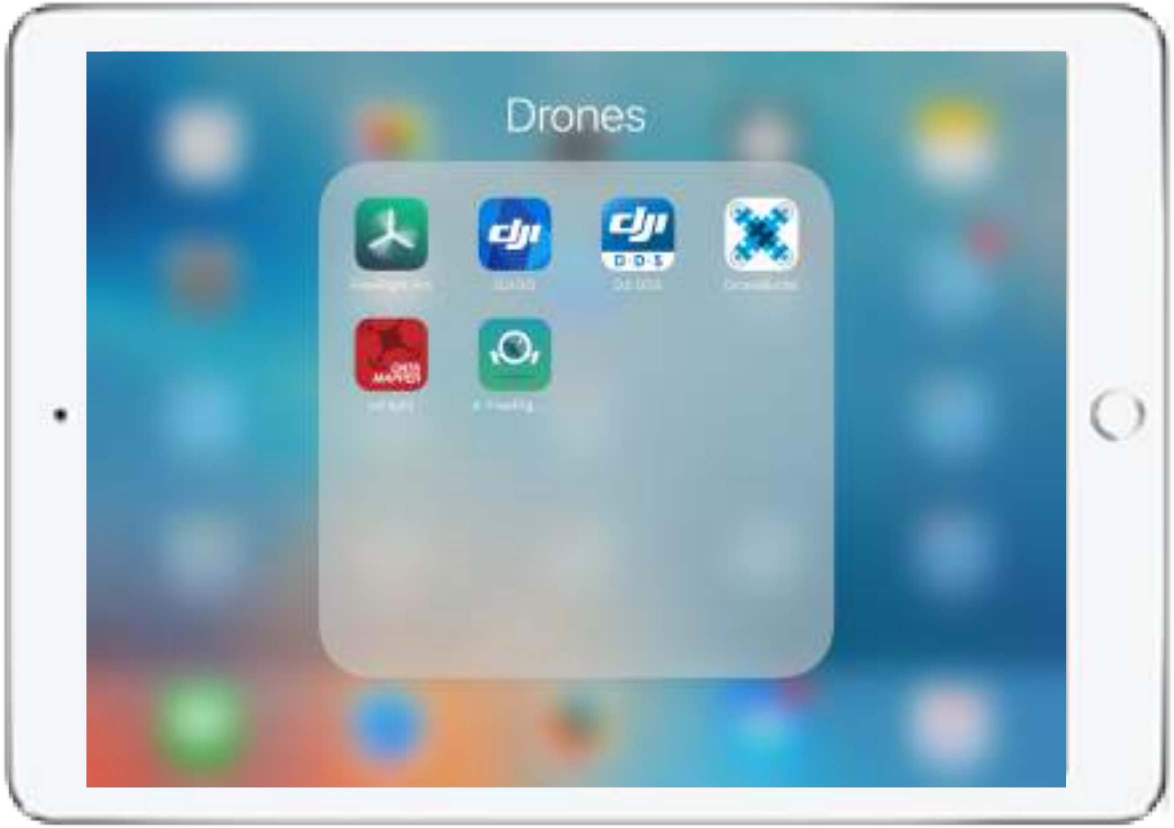

Definition of the Study Area

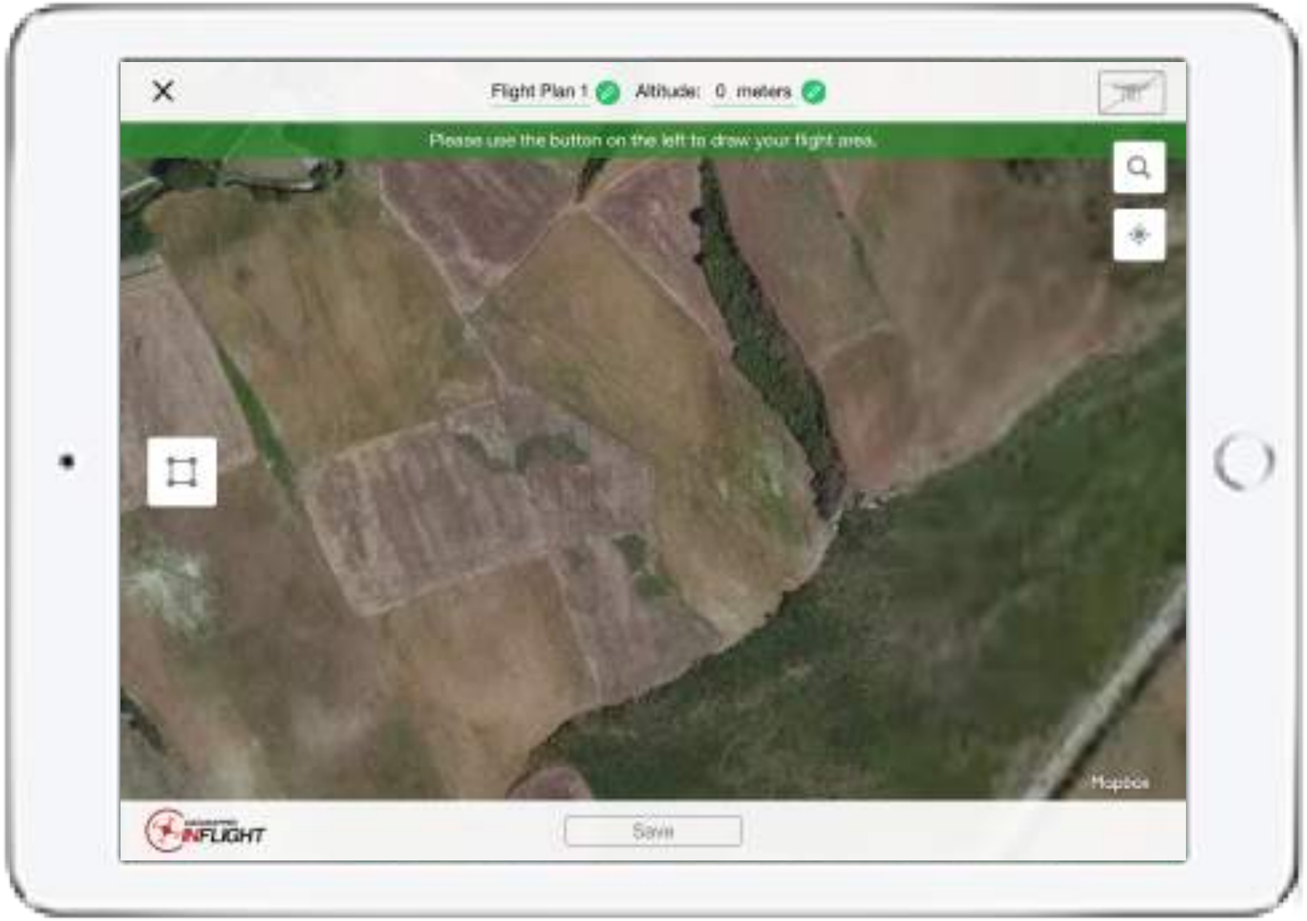

Selection the Study Area

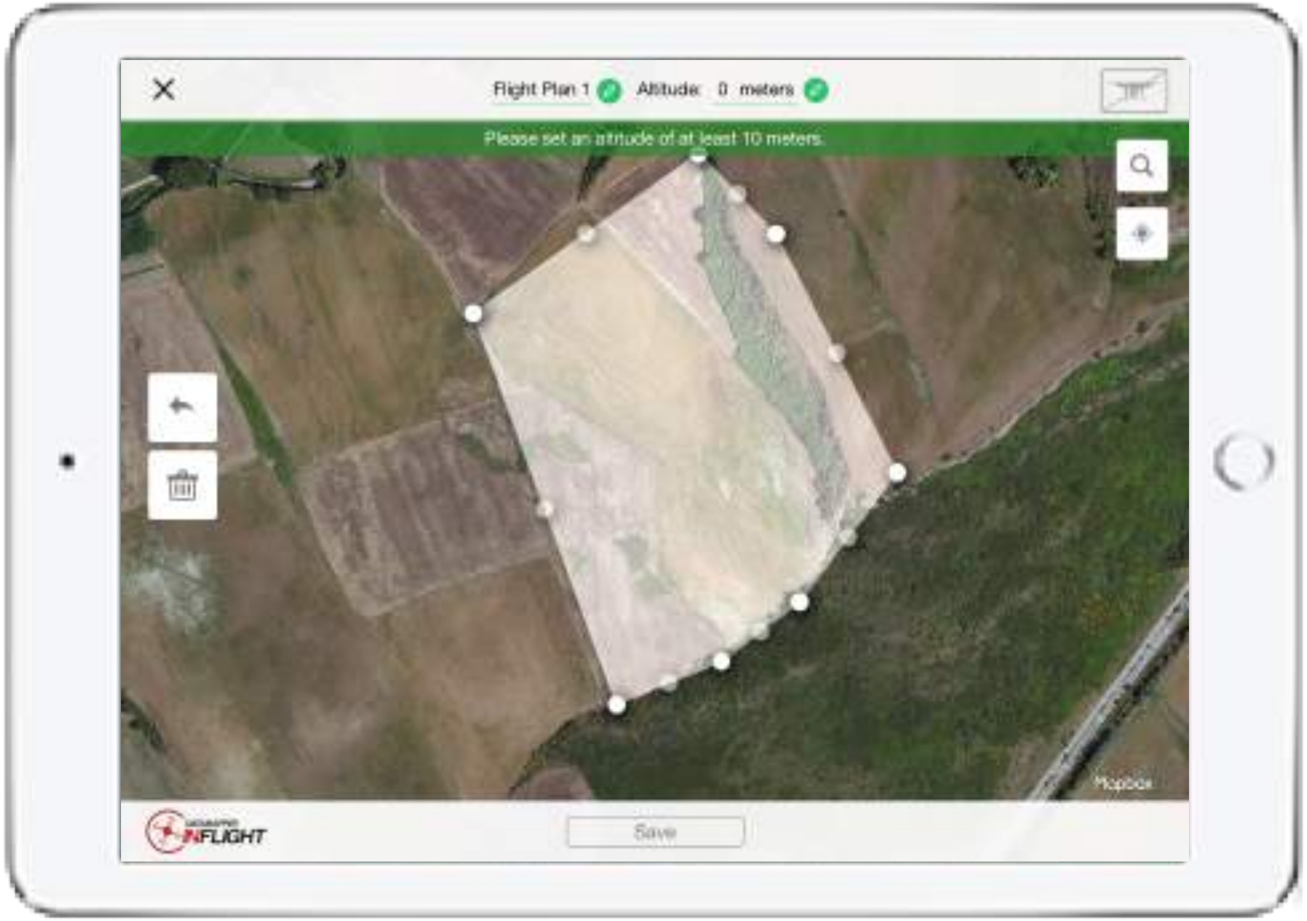

Flight Settings

Plaght Plan

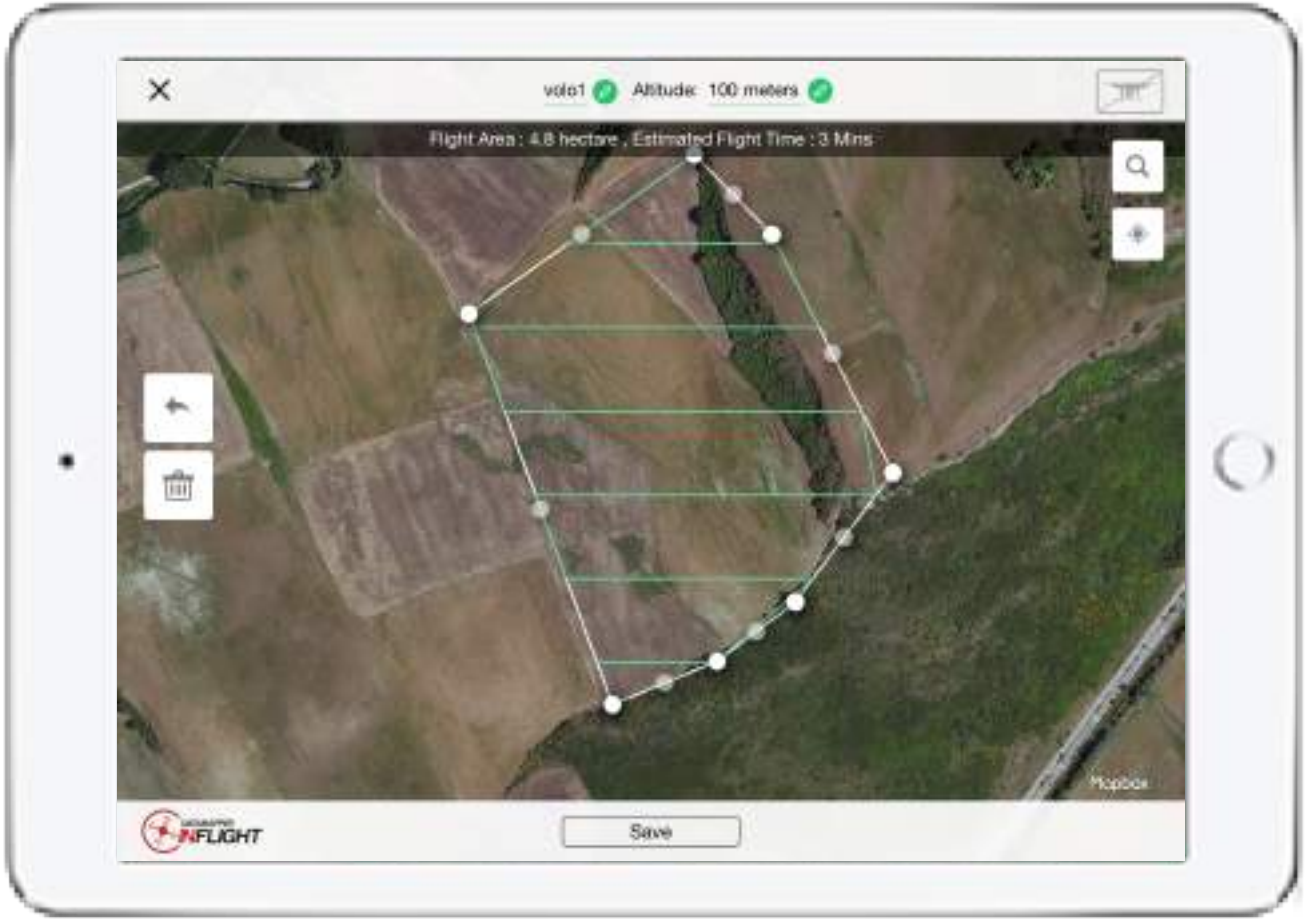
volo1
Altitude: 100 meters
Flight Area : 4.8 hectare , Estimated Flight Time : 3 Mins
Mapbox
INFLIGHT
Save

Photoscan 3D Modelling

1) photo alignment with high accuracy;
2) optimizing alignment,
3) dense cloud building,
4) mesh building using a dense cloud,
5) texture building with the default blending mode,
6) tiled model building,
7) DSM building using the default settings,
8) orthomosaic generation.

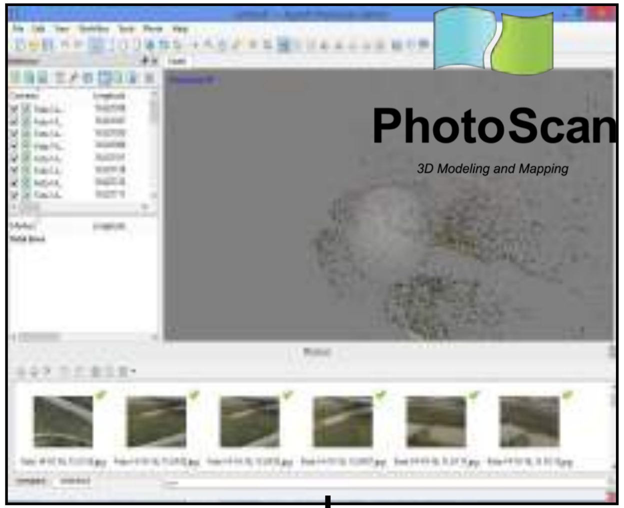

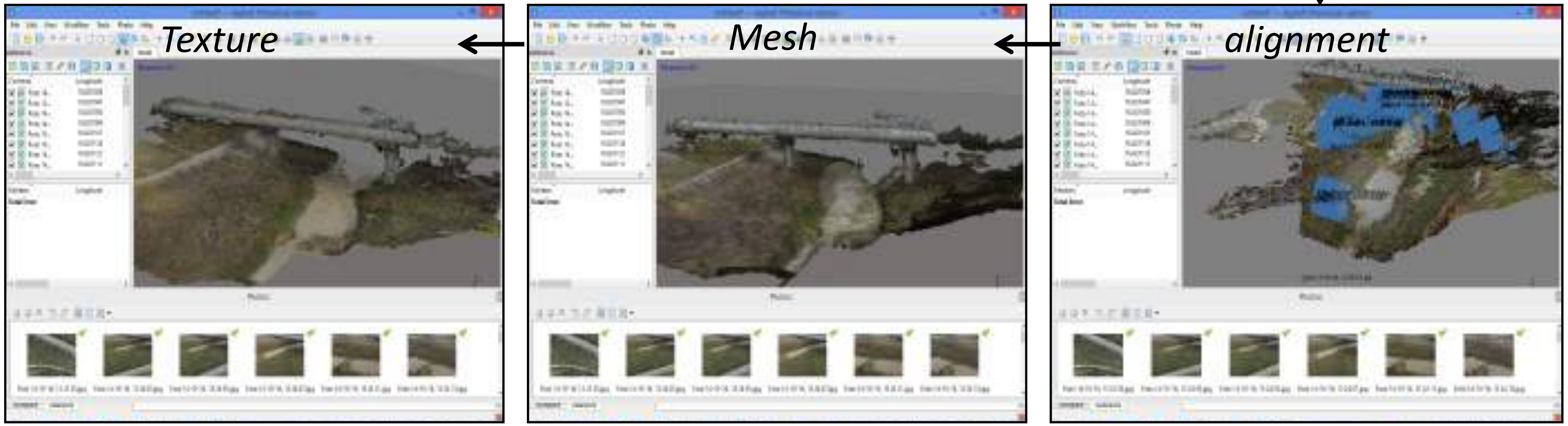

Photos Allignment

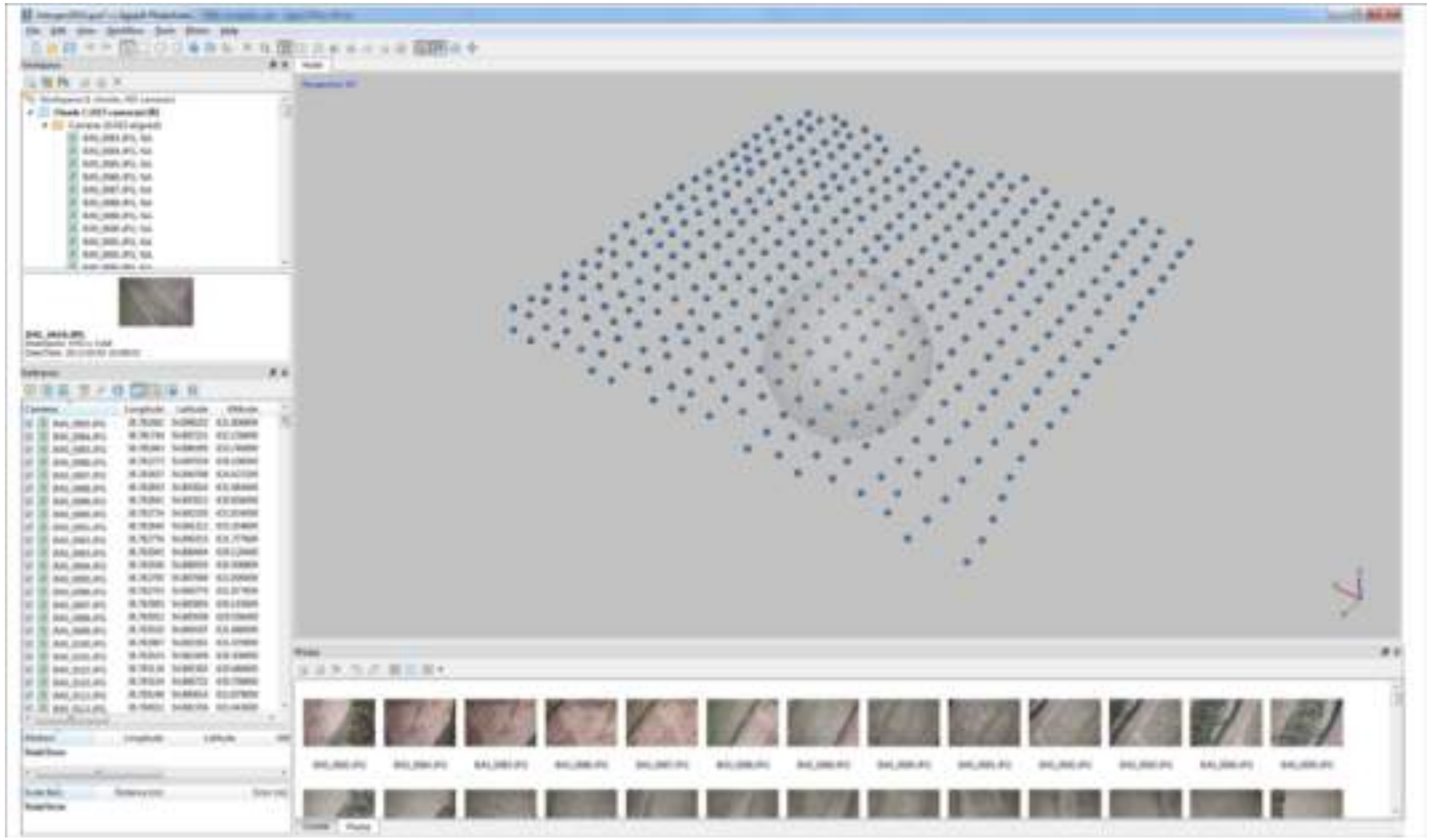

PhotoScan
3D Modeling and Mapping

Cloud Point

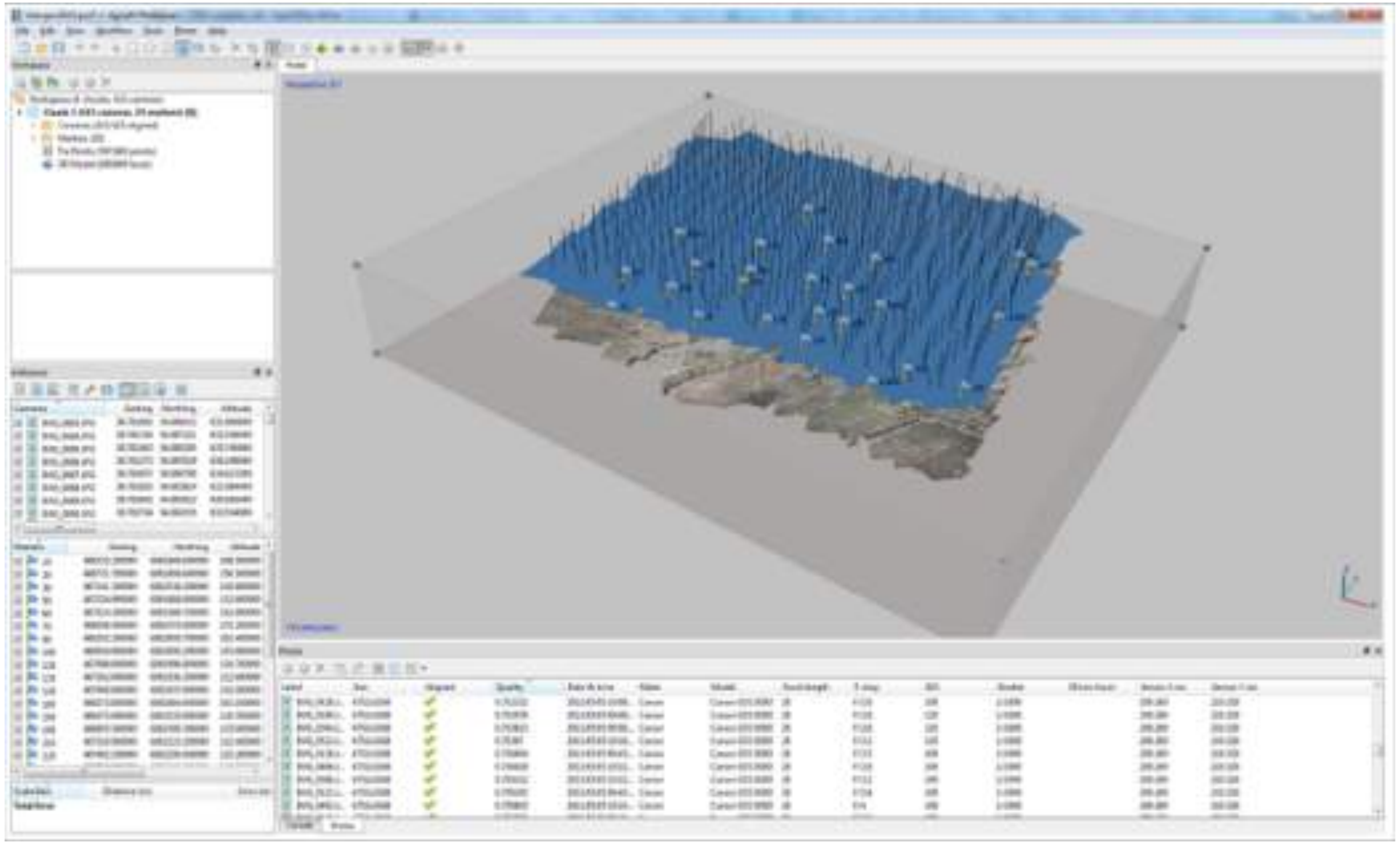

cost
EUROPEAN COOPERATION IN SCIENCE & TECHNOLOGY

Tiled Mesh

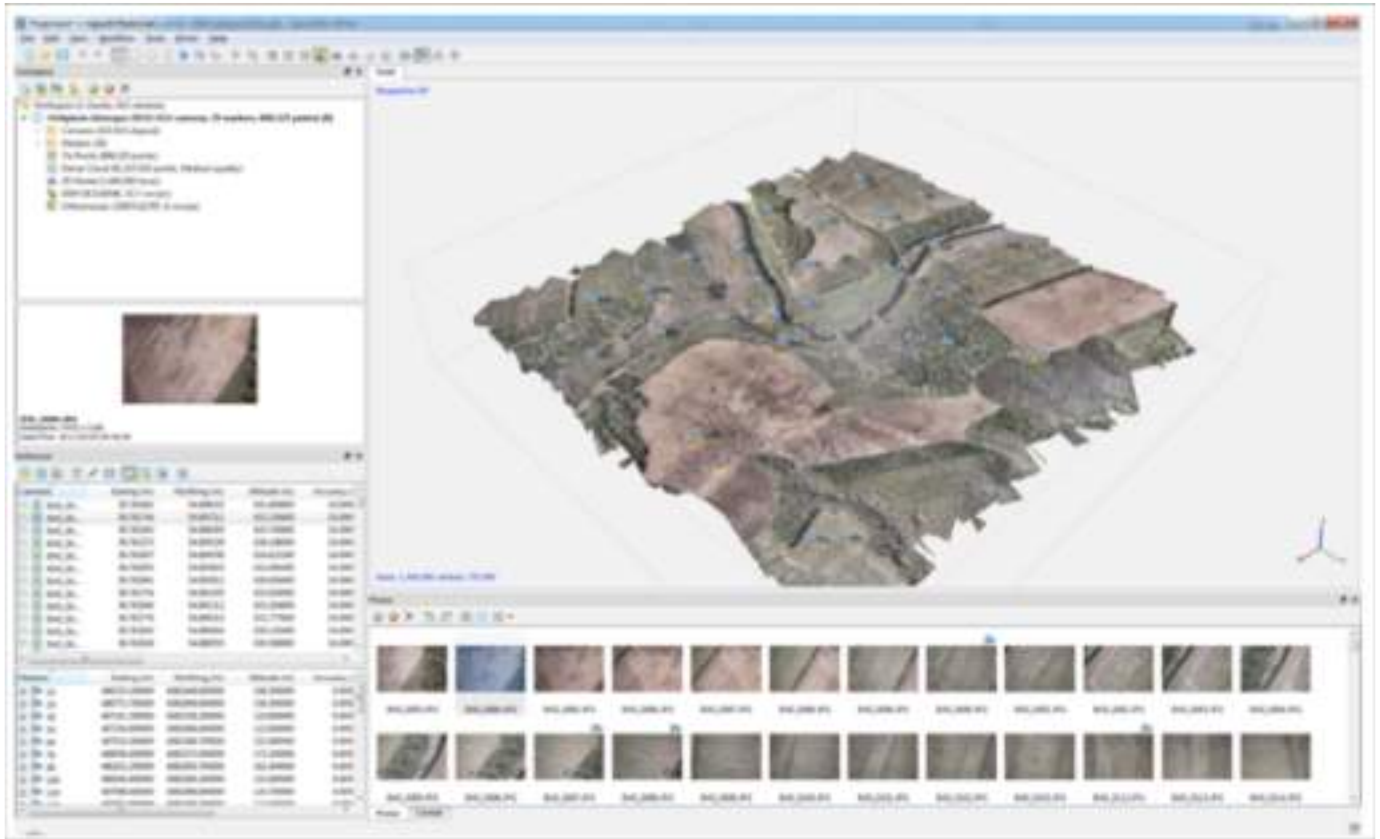

Digital Elevation Model

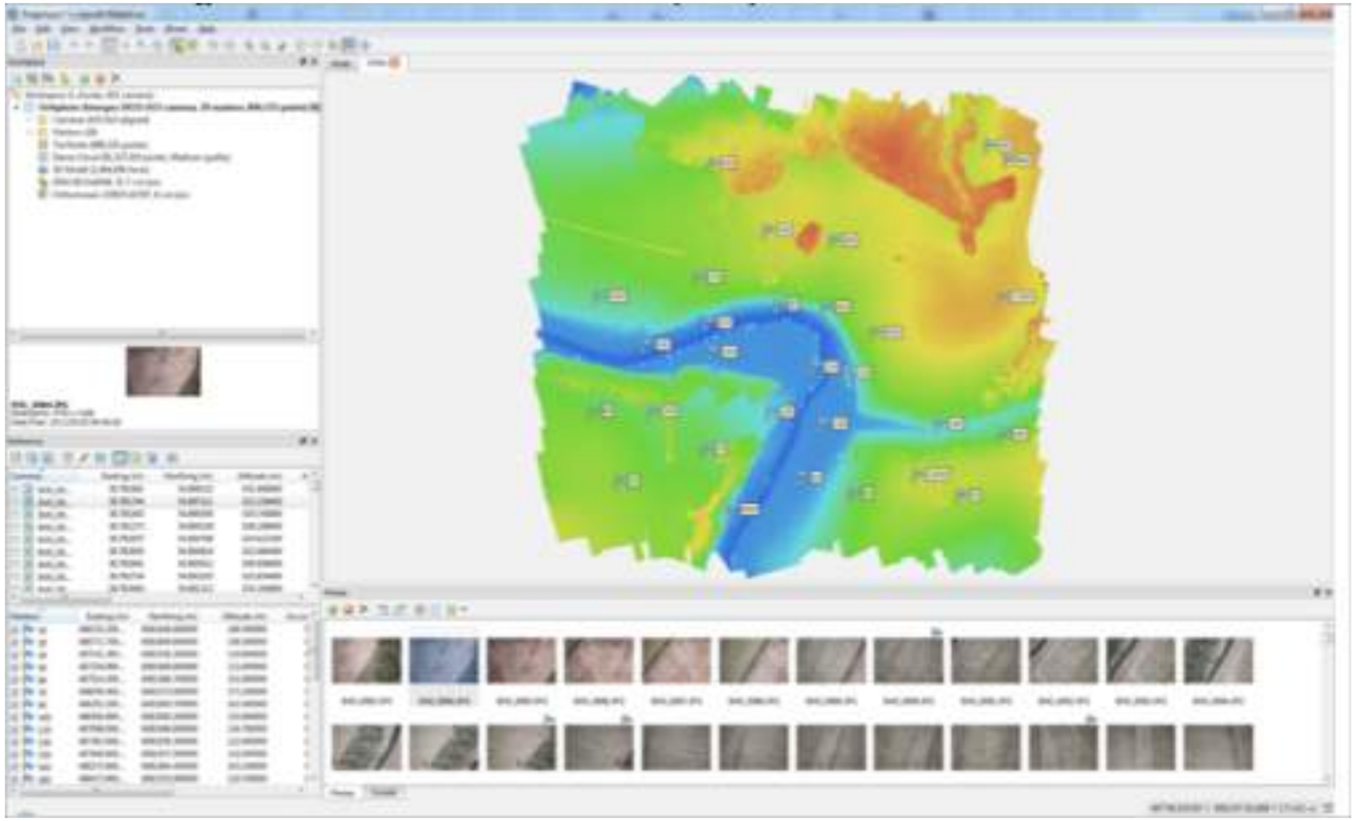

UAS-based DSM

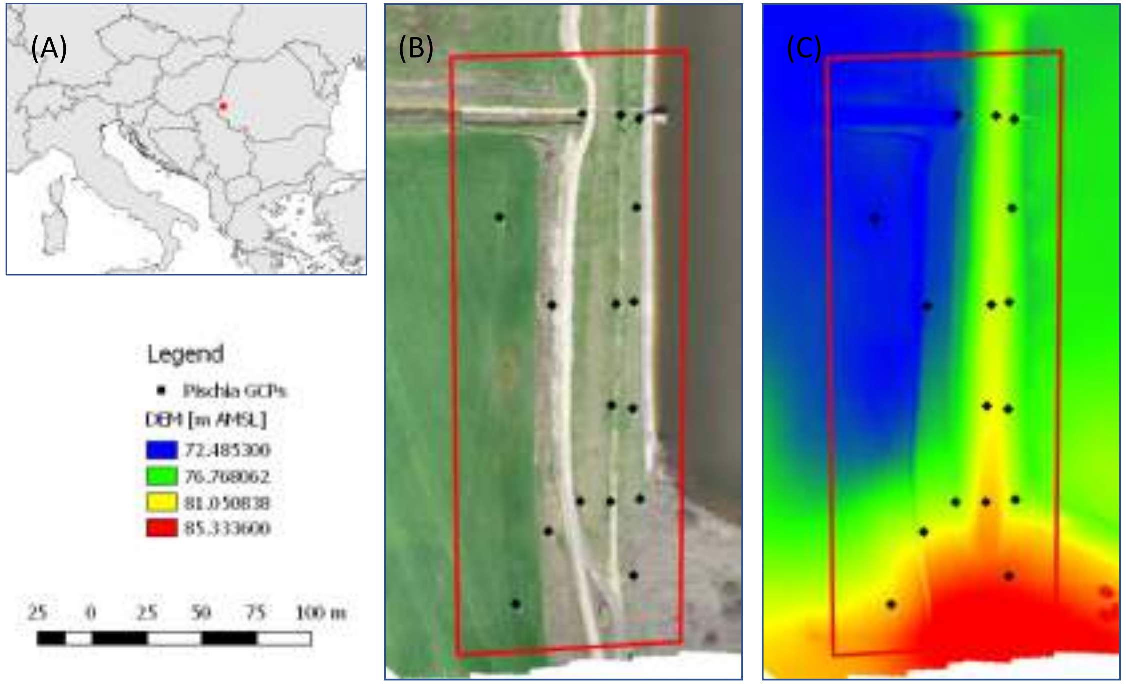

A) Position of the study area within Europe (45.927N, 21.335E).
B) Description of the study area and distribution of the GCPs.
C) UAS-derived DSM of the area

drones

Assessing the Accuracy of Digital Surface Models Derived from Optical Imagery Acquired with Unmanned Aerial Systems

From Manfreda et al., Drones 2019

DSM accuracy in terms of planar and vertical RMSE as a function of the GCPs density

Reference	Area (ha)	Number of GCPs	AGL (m)	$RMSE_{X,Y}$ (cm)	$RMSE_Z$ (cm)	RMSE Total (cm)
Rock et al. [2011]	N/A	1042	50–550	N/A	5.5	N/A
Tahar [2013]	150	8–9	N/A	50.0	78.0	N/A
Mancini et al. [2013]	2.75	18	40	0.8	10.0	N/A
Hugenholtz et al. [2013]	4.5	28	200	18	29	N/A
Lucieer et al. [2014]	0.75	39	N/A	7.4	6.2	N/A
Cryderman et al. [2014]	7.12	11	118	3.3	3.1	4.6
Gómez–Candón et al. [2014]	1.0	11–45	30–100	N/A	N/A	0.29–0.12
Uysal et al. [2015]	5.0	27	60	N/A	6.62	N/A
Kung et al. [2011]	210.0	19	262	38	107	125
Agüera-Vega et al. [2017]	17.64	4–15–20	120	7–4.5–1.7	33–5.8–4.7	N/A
Koci et al. [2017]	41–45–72	6–7	100	N/A	30.9–68.7–95.9	N/A
James et al. [2017]	7.5	4–27	100	4.9	N/A	1.6
Oniga et al. [2018]	1.0	3–40	28–35	4.5–8.9	6.6–4.0	7.4–7.9

(Manfreda et al., Drones 2019)

DSM accuracy in terms of planar and vertical RMSE as a function of the GCPs density

- The errors observed in the **vertical precision are systematically higher compared with the horizontal precision**, and decrease more slowly with an increase in GCPs.

- The **planar error** tends to stabilize after **reaching 5 GCP/ha, whereas 10 GCPs/ha** are needed to reach the same condition for **vertical** precision.

- We need to find new strategies to improve DSM accuracy, especially vertical accuracy.

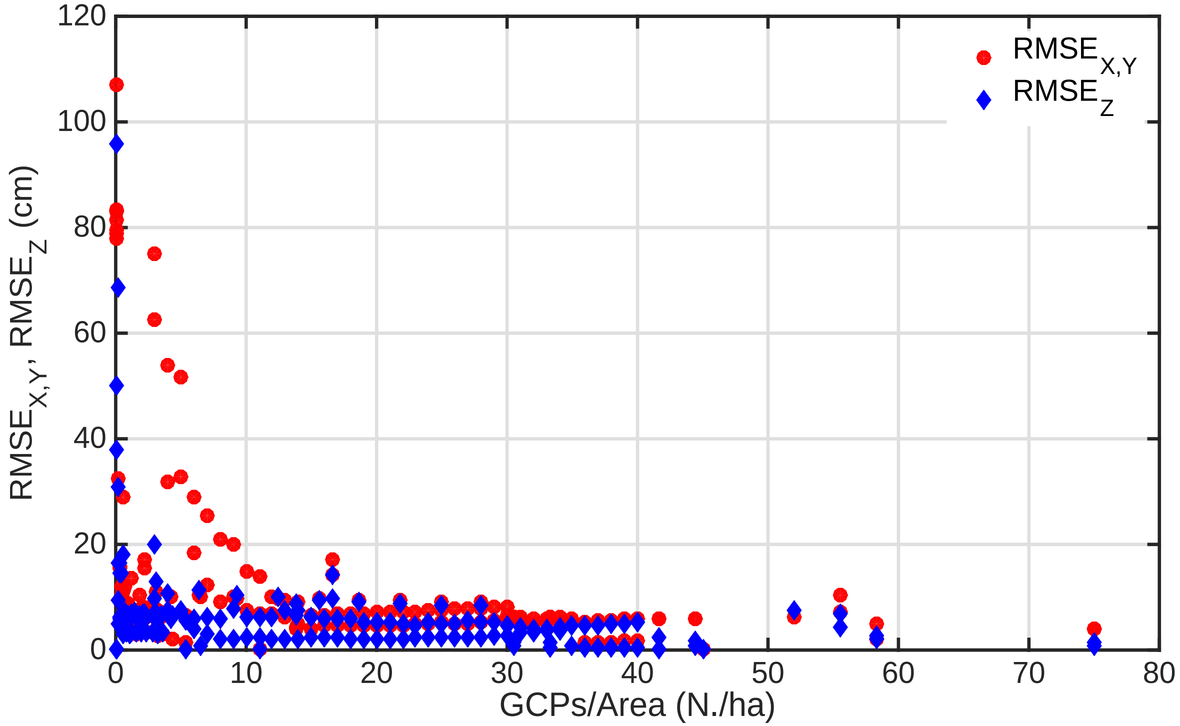

(Manfreda et al., Drones 2019)

Data Collection with a low-cost UAS

Characteristics of the different surveys: flight pattern, AGL at the take-off, average AGL, camera tilt, GSD, and number of images.

DJI Phantom 4 Pro quadcopter

Fligth	Fligth plan	Level Above the Ground (m)	Camera Tilt (degree)	Avg GSD (cm/px)	Images
N.1	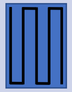	60	0°	1.9	276
N.2		60	0°	1.9	268
N.3		60	70°	-	271
N.4		60	20°	2.0	273
N.5	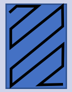	60	0°	1.9	257
N.6	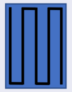	120	0°	3.3	85

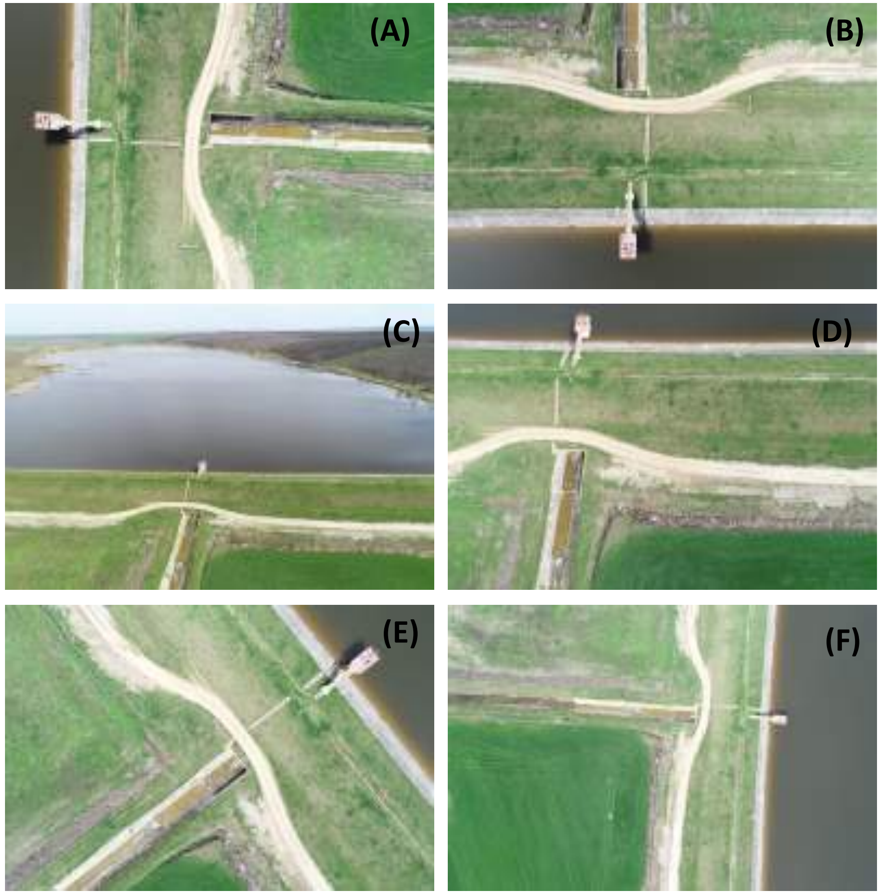

UAS data Collection: Ground Contro Points

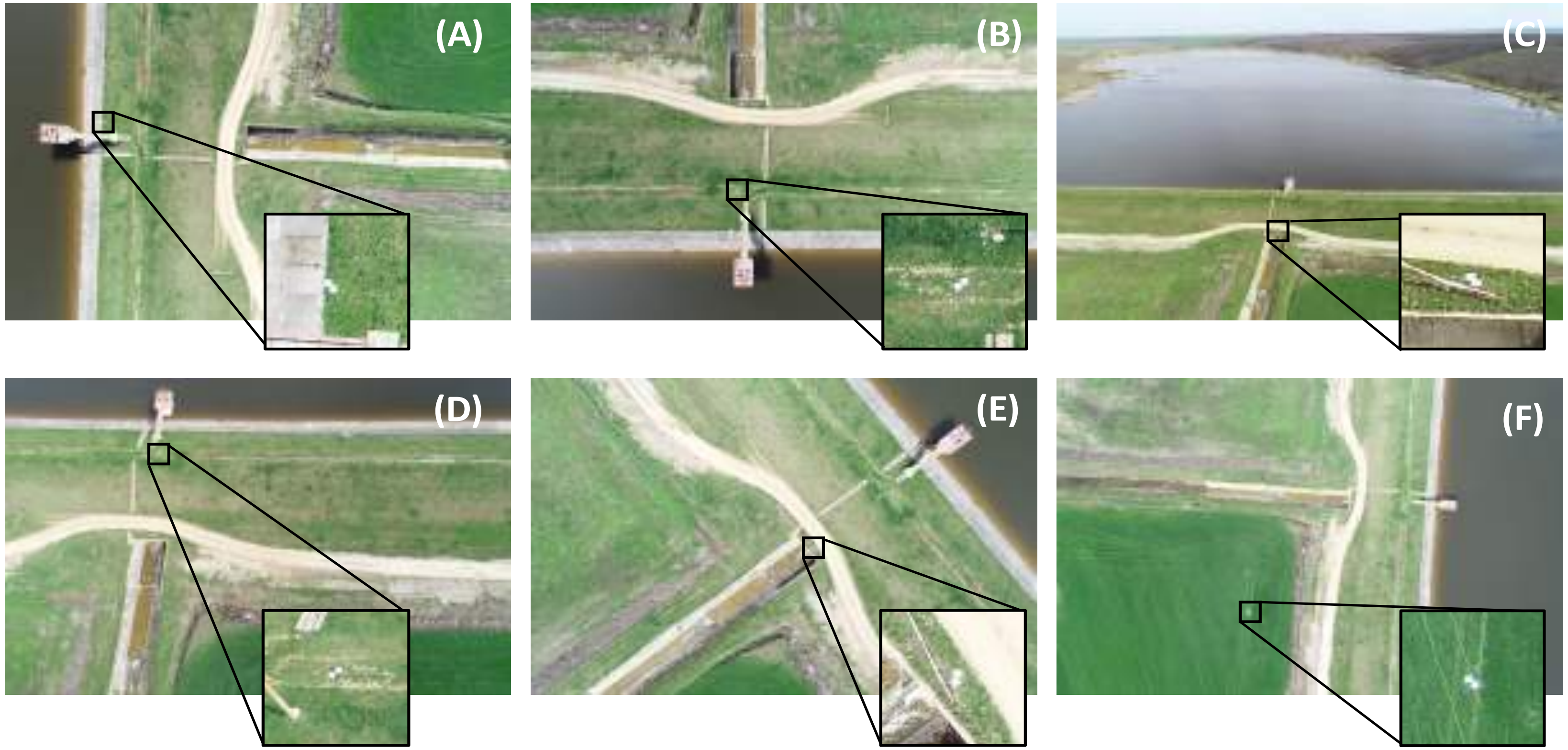

UAS derived 3D dense point cloud derived from a UAS based survey of an earthen dam next to the village of Pișchia (Timisoara, Romania)

From Manfreda and McCabe, Hydrolink 2019

Mesh Model derived from a UAS-based survey

From Manfreda and McCabe, Hydrolink 2019

Tiled Model derived from a UAS-based survey

Such data provide the framework for development of high-resolution flood modeling, urban watershed mapping and civil engineering design and map updating.

From Manfreda and McCabe, Hydrolink 2019

DSM Accuracy without GCPs

Fligth	Fligth plan	Camera Tilt (degree)
N.1	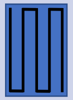	0°
N.2		0°
N.3	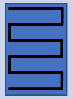	70°
N.4		20°
N.5	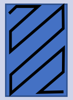	0°
N.6	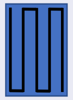	0°

Performances
Good
Medium
Low

Planar Coordinates—RMSEx,y (m)						
Flight	N.1	N.2	N.3	N.4	N.5	N.6
N.1	4.47					
N.2	2.39	2.03				
N.3	136.05	1497.25	-			
N.4	**1.64**	3.08	3835.20	7.75		
N.5	2.09	1.95	15042.56	8.05	7.15	
N.6	3.06	3.35	1750.11	8.63	6.94	19.70

Elevation—RMSEz (m)						
Flight	N.1	N.2	N.3	N.4	N.5	N.6
N.1	82.90					
N.2	81.18	78.72				
N.3	80.32	56.94	-			
N.4	79.21	76.94	15.51	75.02		
N.5	77.90	77.86	**7.70**	73.35	71.86	
N.6	78.79	75.48	20.25	72.85	70.27	59.75

Relative Elevation—RMSEz (m)						
Flight	N.1	N.2	N.3	N.4	N.5	N.6
N.1	1.06					
N.2	0.39	0.37				
N.3	3.74	19.55	-			
N.4	0.55	0.42	5.88	**0.11**		
N.5	0.39	0.25	8.00	0.47	0.26	
N.6	0.22	0.94	13.85	0.80	0.40	3.44

Planar and vertical—RMSE (m)						
Flight	N.1	N.2	N.3	N.4	N.5	N.6
N.1	4.59					
N.2	2.42	2.06				
N.3	136.10	1497.38	-			
N.4	**1.73**	3.11	3835.20	7.75		
N.5	2.13	1.97	15042.56	8.06	7.15	
N.6	3.07	3.48	1750.16	8.67	6.95	20.00

RMSE and Number of GCPs

RMSE of the 3D model as a function of the number of GCPs adopted. A) $RMSE_{X,Y}$; B) $RMSE_{Z}$; C) $RMSE_{X,Y,Z}$ for the combination of flights N.1 and N.4.

A sharp increase in DSM accuracy can be observed, moving from 3–4 GCPs to 5–6 GCPs.

The magnitude of planar errors seems to be fairly stable after five GCPs. Vertical errors are always larger and tend to be more stable after six GCPs

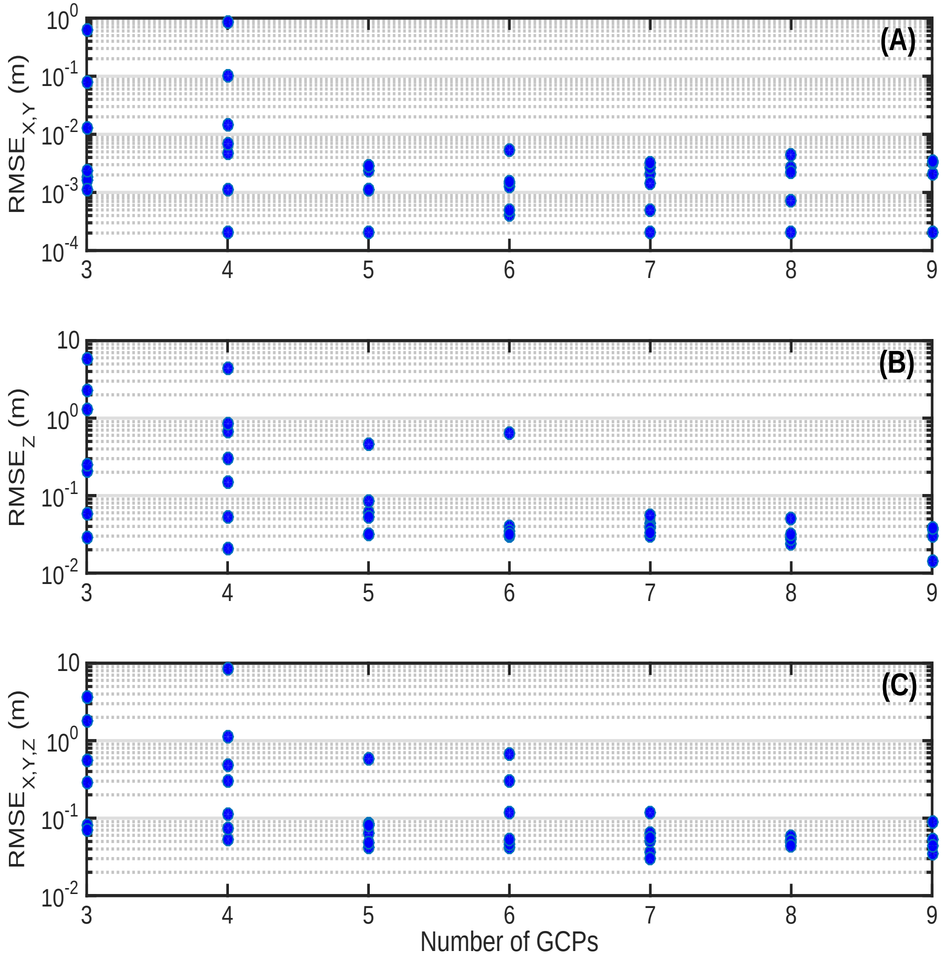

RMSE and Number of GCPs

Comparison of results obtained changing the number of GCPs and adopting a single flight or a two flights dataset on the plane (A) and z-axes (B).

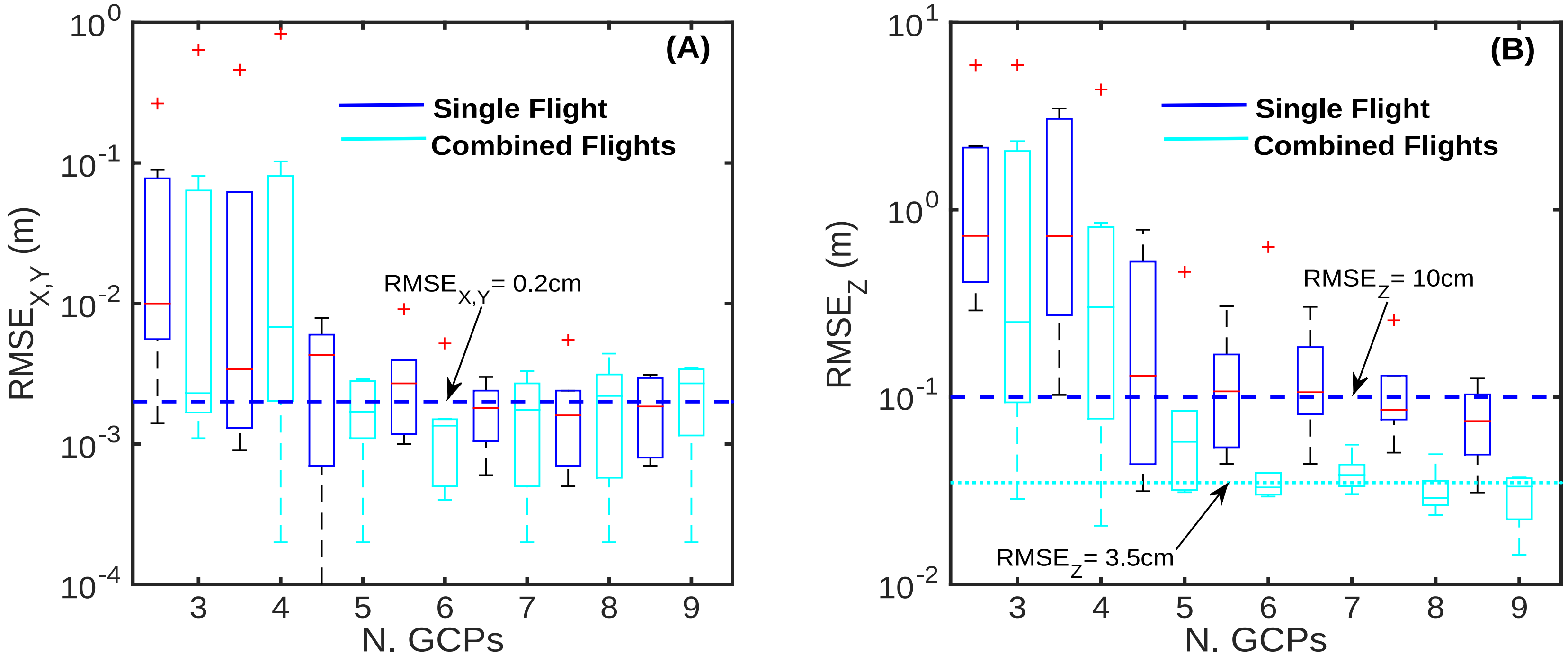

(Manfreda et al., Drones 2019)

Spatial Distribution of GCPs

RMSE of the 3D model as a function of the mean distance between GCPs obtained for the flight N.2 (A, B) and for the combination of flights N.1 and N.4 (C, D).

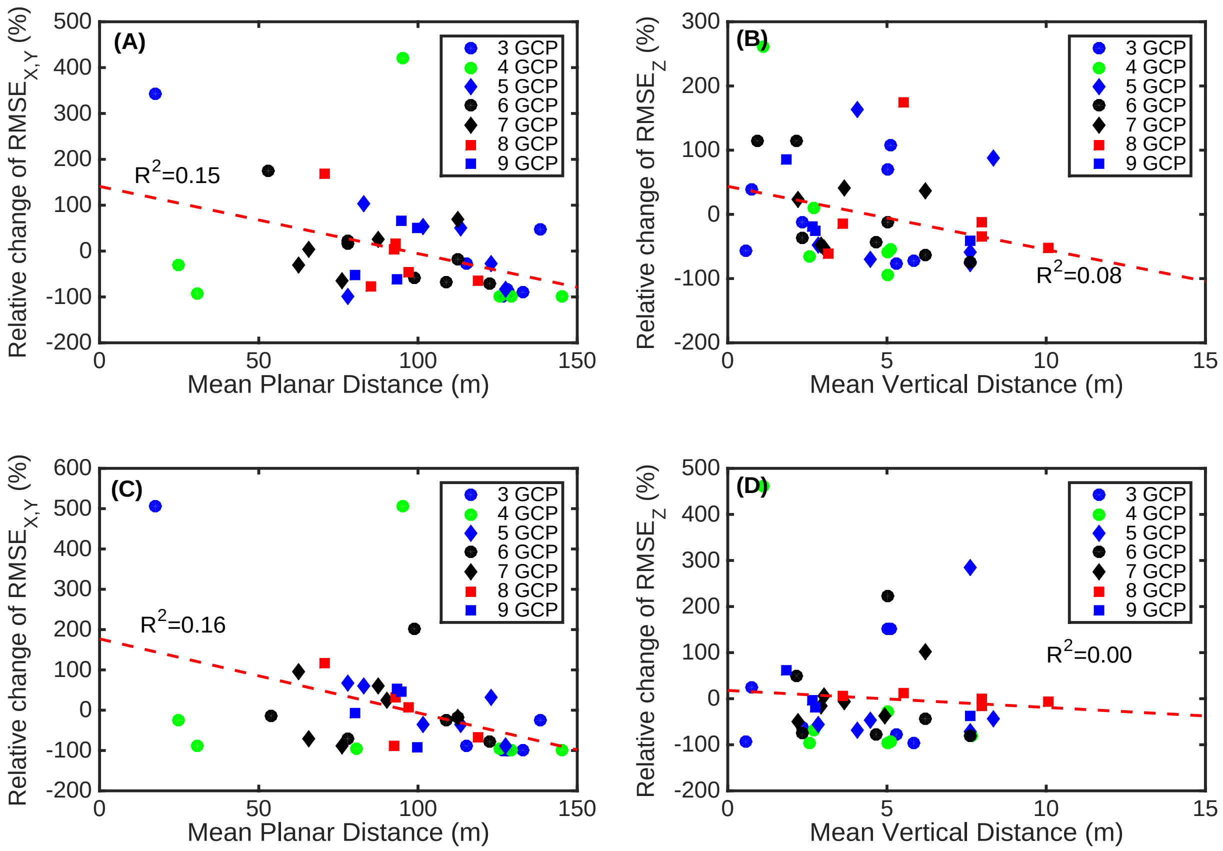

(Manfreda et al., R.S. 2018b)

Conclusions 1/2

- UAS-derived orthomosaics can produce a planar accuracy of a few centimeters, whereas the vertical accuracy of DSMs is always lower. This is likely due to the fact that most UASs adopt a camera in a zenithal position that provides more accurate description of planar features. Vertical measurements are generally more complex, but also critical for studies of change detection.
- The flight plan and camera configuration may significantly impact the overall quality of the resulting DSM. Therefore, it should be planned thoroughly to produce the best depiction of the entire area. For instance, a transversal survey with respect to a given structure provides better description and quality of the resulting 3D surface.

Conclusions 2/2

- The use of a tilted camera can improve the amount of information (retrieved number of points) for inclined surfaces, providing higher DSM elevation accuracy. The tilted camera images increases the robustness of the geometrical model, providing a possible strategy to reduce the total number of GCPs adopted over a given area. This can be beneficial especially in inaccessible areas.
- The combination of several flights may be extremely beneficial for DSM accuracy. This may increase redundancy of information and improve the overall quality of the results, exploiting the benefits derived by different flight plans and camera configurations.
- The planar and vertical accuracies can be improved by increasing the number of GCPs. In particular, the quality of the 3D model tends to increase when both the relative plane and vertical distances of the GCPs increase. It is therefore convenient to evenly spread GCPs in space. In many cases, such ideal settings are not possible. In such cases, our results suggest adopting a combination of flights that are less sensitive to this parameter in the final vertical accuracy of the DSM.

Related Publications

- Manfreda and McCabe (2019). ***Emerging earth observing platforms offer new insights into hydrological processes***, Hydrolink.
- Perks, Hortobágyi, Le Coz, Maddock, Pearce, Tauro, Dal Sasso, Grimaldi, Manfreda (2019) **Towards harmonization of image velocimetry techniques for determining open-channel flow**, Earth system science data (in preparation).
- Manfreda, Dvorak, Mullerova, Herban, Vuono, Arranz Justel, Perks (2019) ***Assessing the Accuracy of Digital Surface Models Derived from Optical Imagery Acquired with Unmanned Aerial Systems***, Drones.
- Manfreda, ***On the derivation of flow rating-curves in data-scarce environments***, Journal of Hydrology, 2018.
- Dal Sasso, Pizarro, Samela, Mita, and Manfreda (2018) ***Exploring the optimal experimental setup for surface flow velocity measurements using PTV***, Environmental Monitoring and Assessment.
- Manfreda, McCabe, Miller, Lucas, Pajuelo Madrigal, Mallinis, Ben-Dor, Helman, Estes, Ciraolo, Müllerová, Tauro, De Lima, De Lima, Frances, Caylor, Kohv, Maltese (2018), ***On the Use of Unmanned Aerial Systems for Environmental Monitoring***, Remote Sensing.
- Baldwin, Manfreda, Keller, and Smithwick, Predicting root zone soil moisture with soil properties and satellite near-surface moisture data at locations across the United States, Journal of Hydrology, 2017.
- Manfreda, Brocca, T. Moramarco, F. Melone, and J. Sheffield, ***A physically based approach for the estimation of root-zone soil moisture from surface measurements***, Hydrology and Earth System Sciences, 18, 1199-1212, 2014.
- Manfreda, Lacava, Onorati, Pergola, Di Leo, Margiotta, and Tramutoli, ***On the use of AMSU-based products for the description of soil water content at basin scale***, Hydrology and Earth System Sciences, 15, 2839-2852, 2011.

Università per Stranieri di Perugia

UAS-based Mapping: Examples

Prof. Salvatore Manfreda

Associate Professor of Water Management and Ecohydrology - http://www2.unibas.it/manfreda

Chair of the COST Action Harmonious - http://www.costharmonious.eu

cost EUROPEAN COOPERATION IN SCIENCE & TECHNOLOGY

Funded by the Horizon 2020 Framework Programme of the European Union

UNIVERSITA' DEGLI STUDI DELLA BASILICATA

Example of Applications: Orthomosaic Timisoara (Romania)

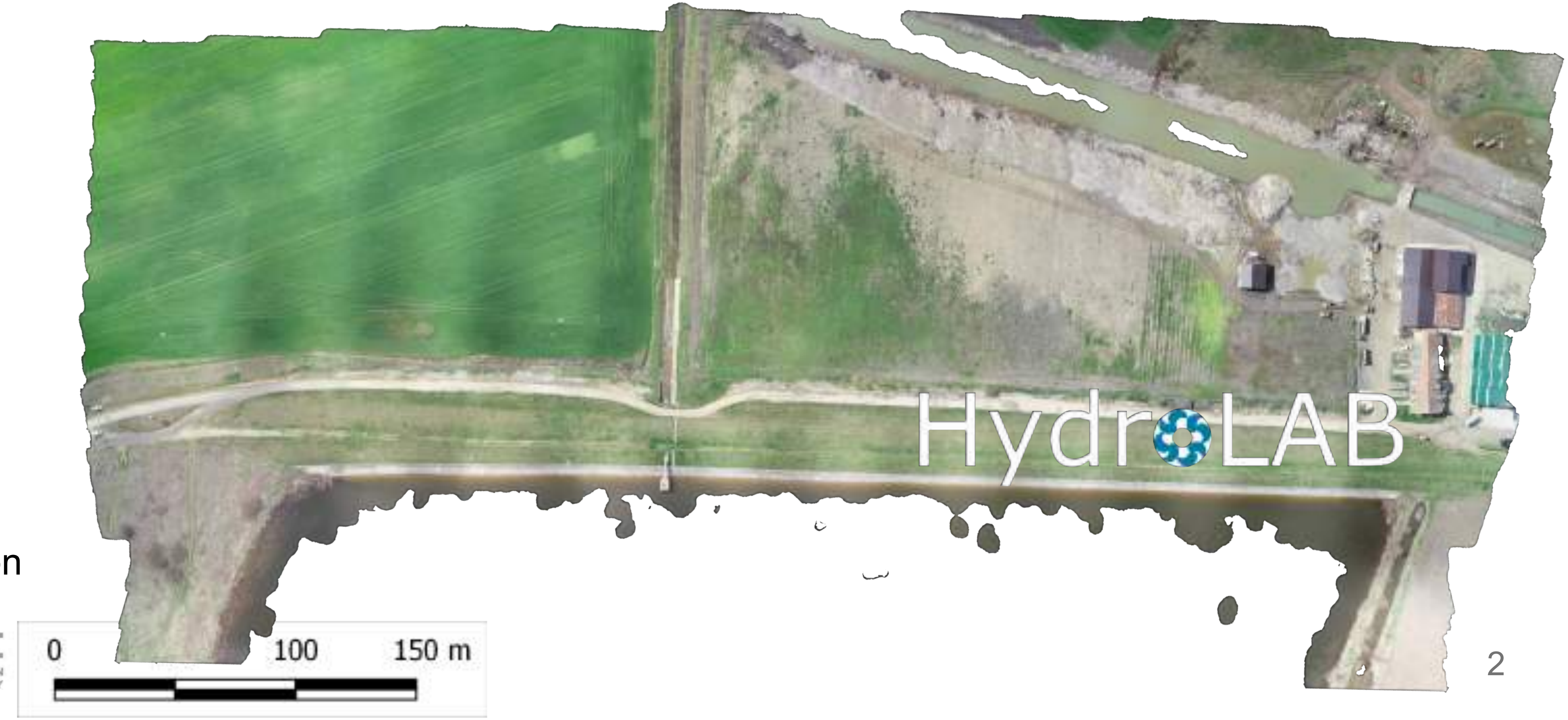

Orthomosaic
1 cm resolution

Example of Applications: Orthomosaic Diga Saetta (Potenza)

Example of Applications: Orthomosaic Iran Neshabur

RGB Orthomosaic
5 cm resolution

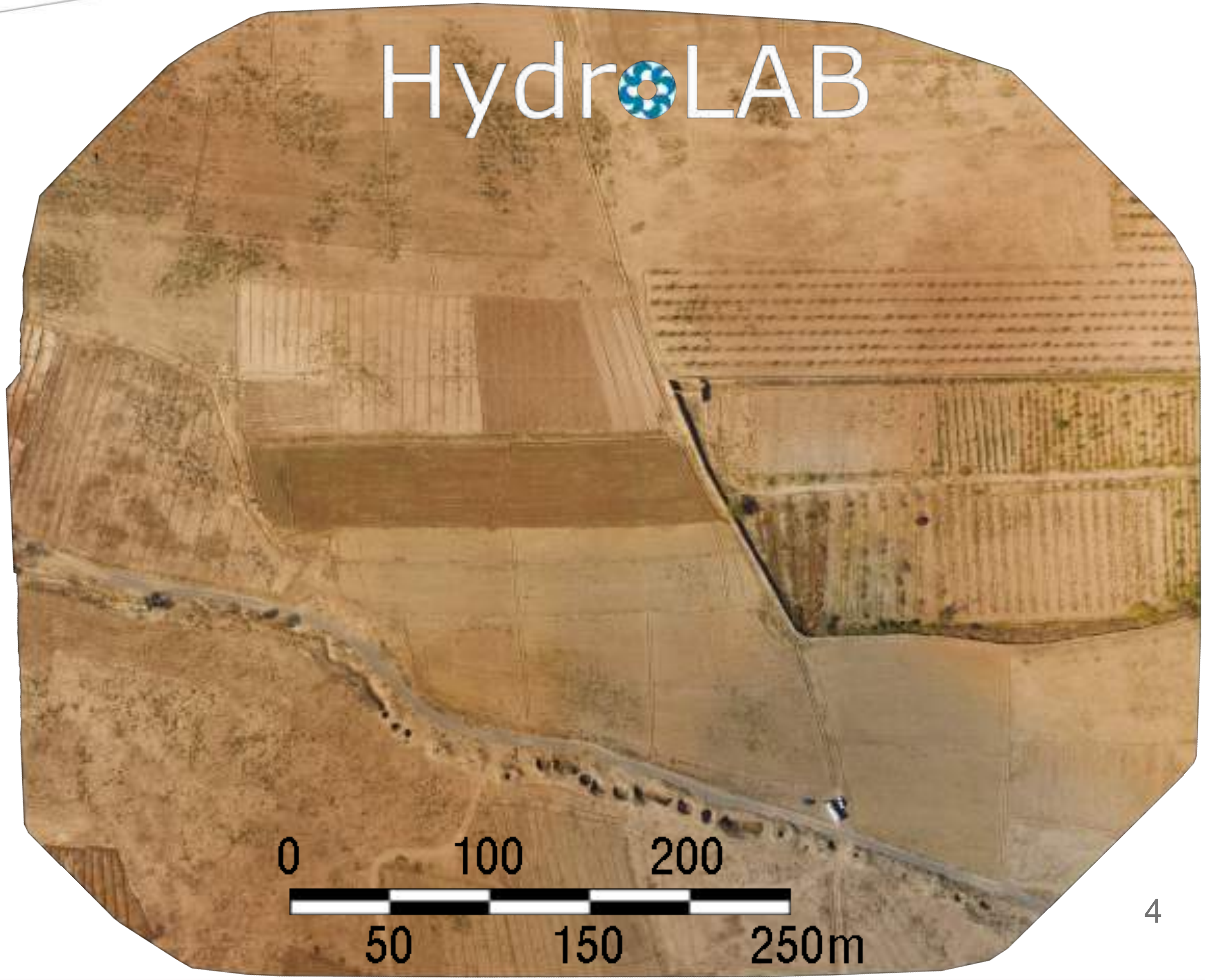

COST
EUROPEAN COOPERATION IN SCIENCE & TECHNOLOGY

Example of Applications: Orthomosaic Iran Neshabur

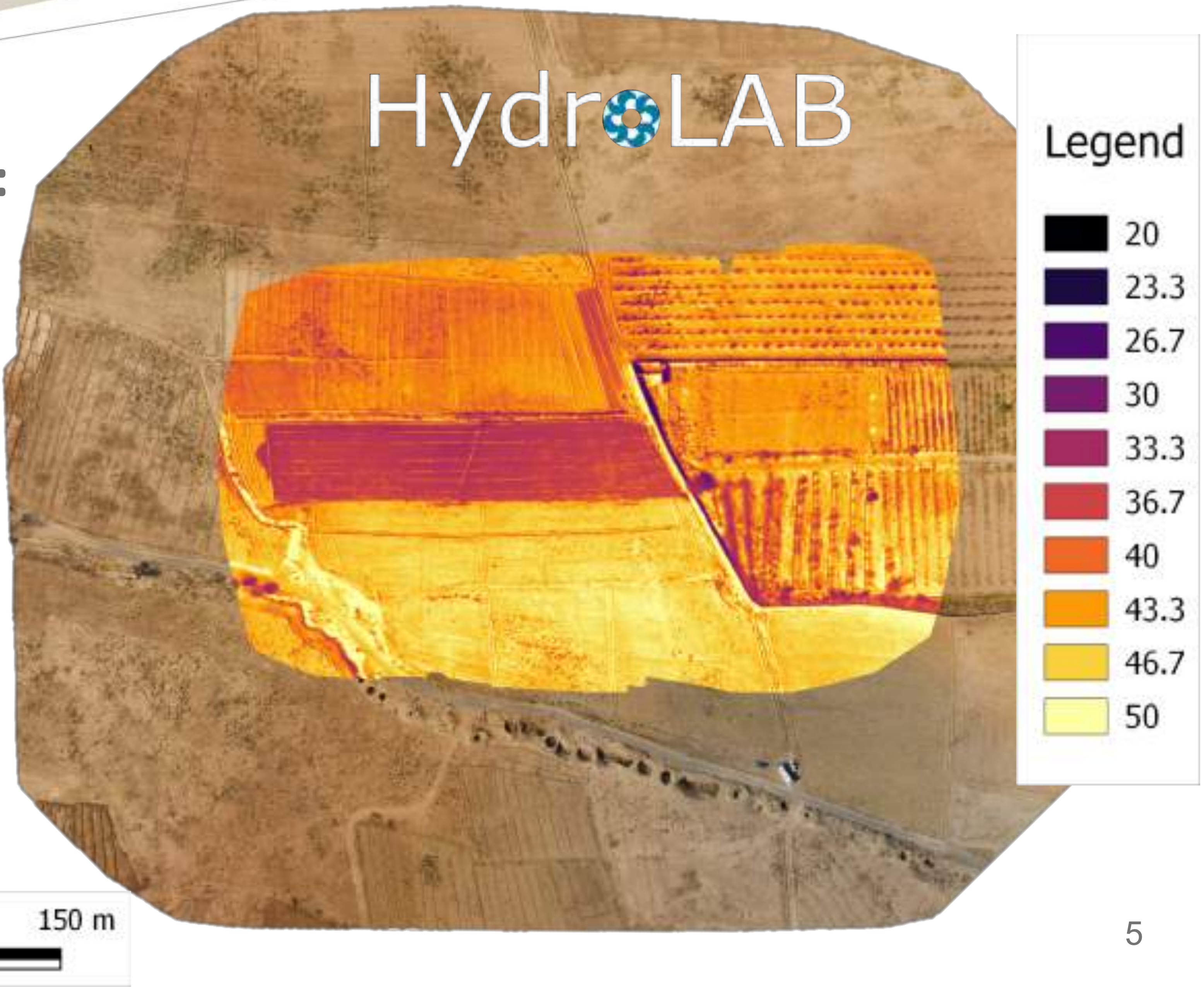

Thermal mosaic
19 cm resolution

EUROPEAN COOPERATION IN SCIENCE & TECHNOLOGY

Example of Applications: Orthomosaic Monteforte

RGB-based Indices

$$TGI = R_{GREEN} - 0.39 * R_{RED} - 0.61 * R_{BLUE}$$

GLI = (2 x G - R - B) / (2 x G+R+B)

$$NGRDI = \frac{GREEN - RED}{GREEN + RED}$$

RGB Orthomosaic
4 cm resolution

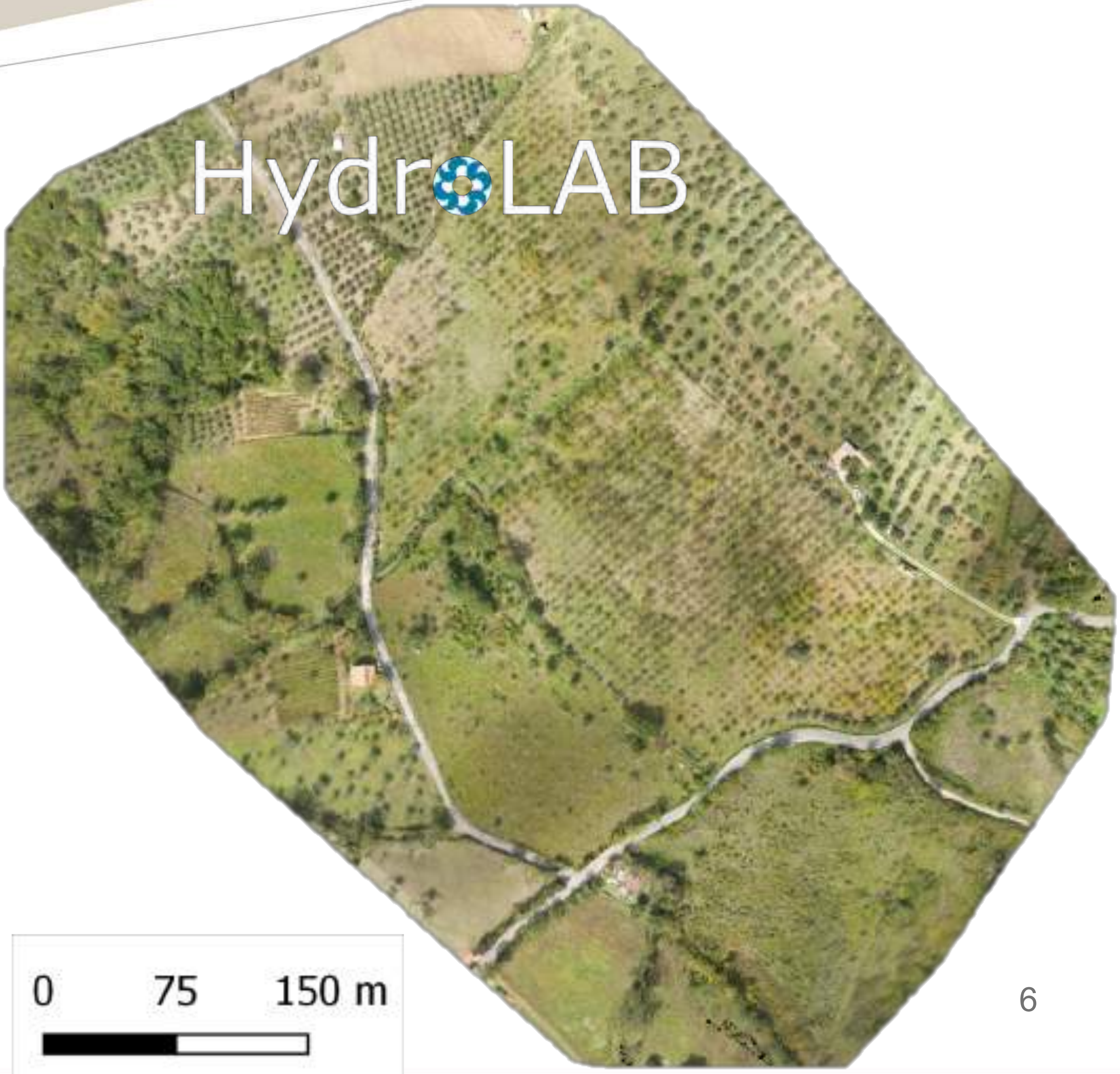

COST EUROPEAN COOPERATION IN SCIENCE & TECHNOLOGY

Example of Applications: Orthomosaic Monteforte

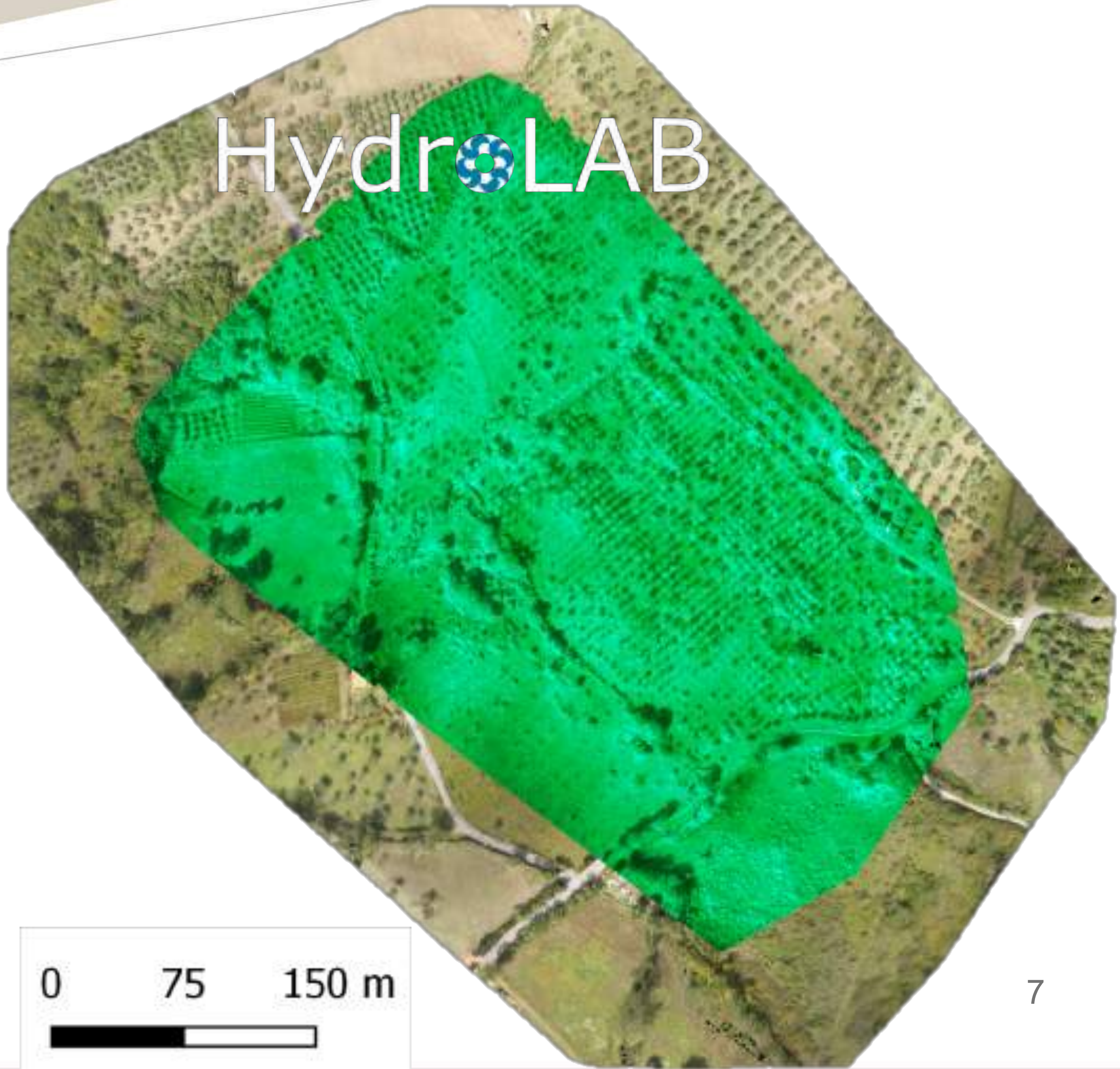

Multi-spectral mosaic
5 cm resolution

Example of Applications: Orthomosaic Monteforte

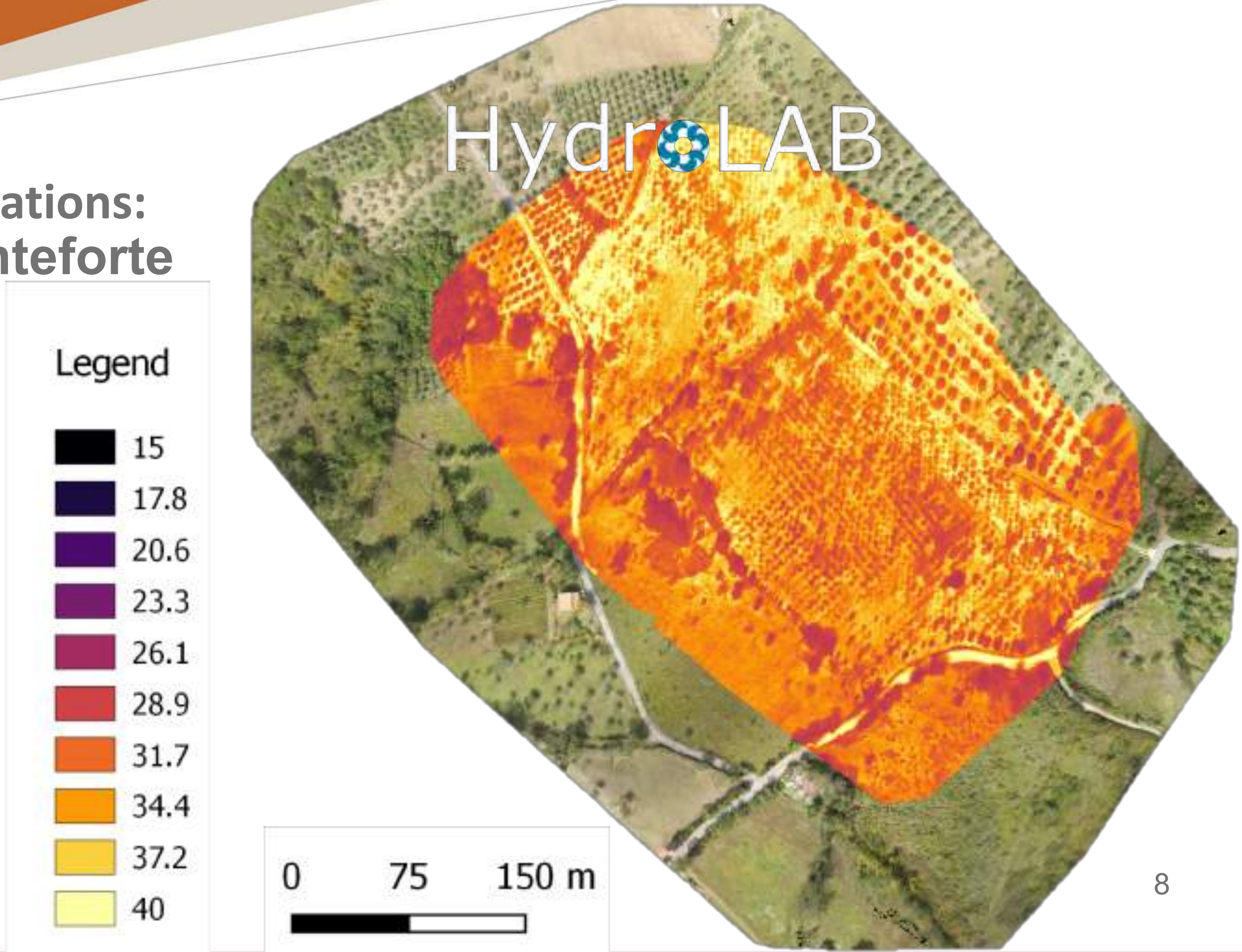

Thermal mosaic
17 cm resolution

Example of Applications: Orthomosaic Cantine del Notaio Maschito)

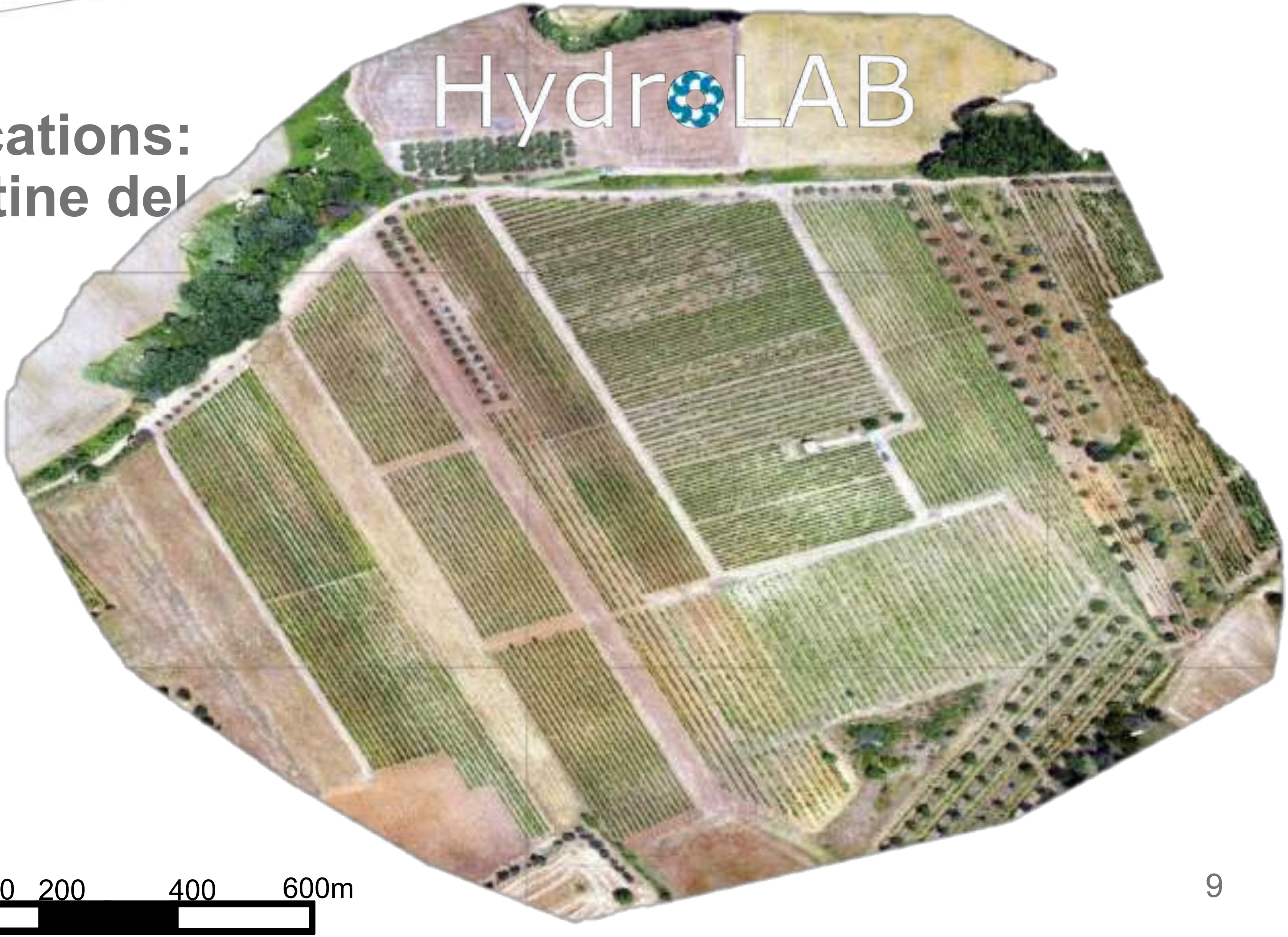

0 100 200 400 600m

Example of Applications: Orthomosaic Cantine del Notaio Maschito)

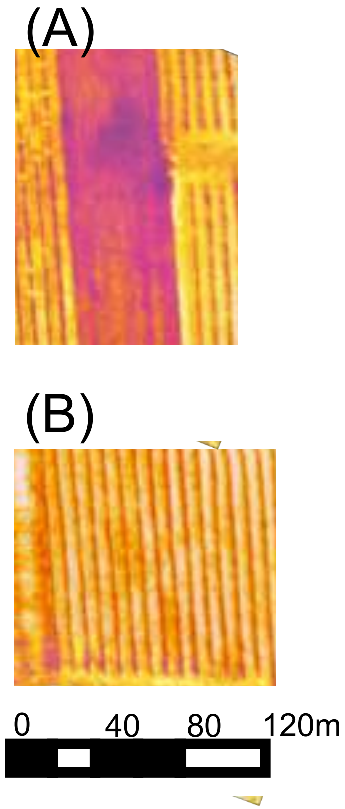

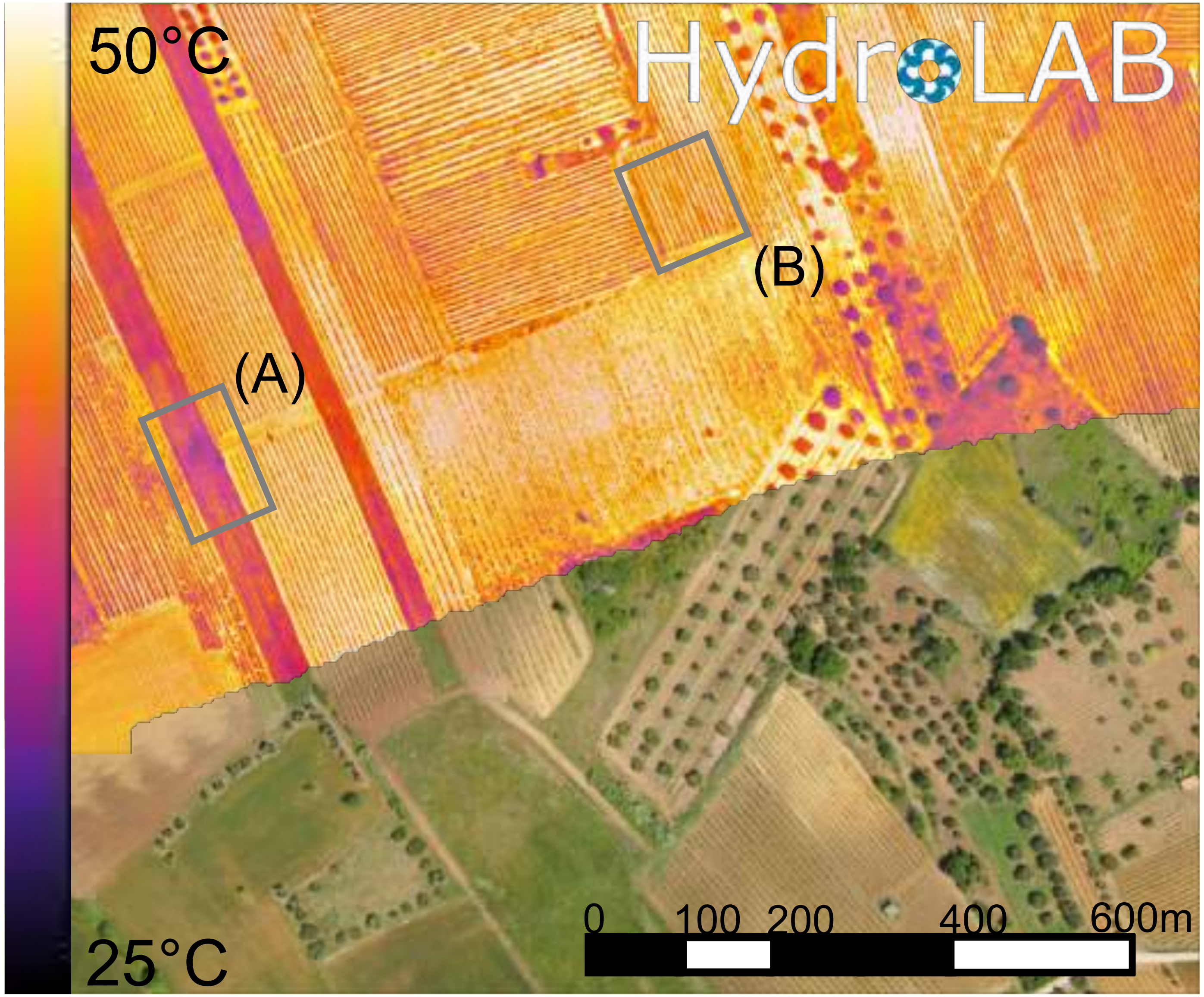

Example of Applications: Orthomosaic Murgia Timone (Matera)

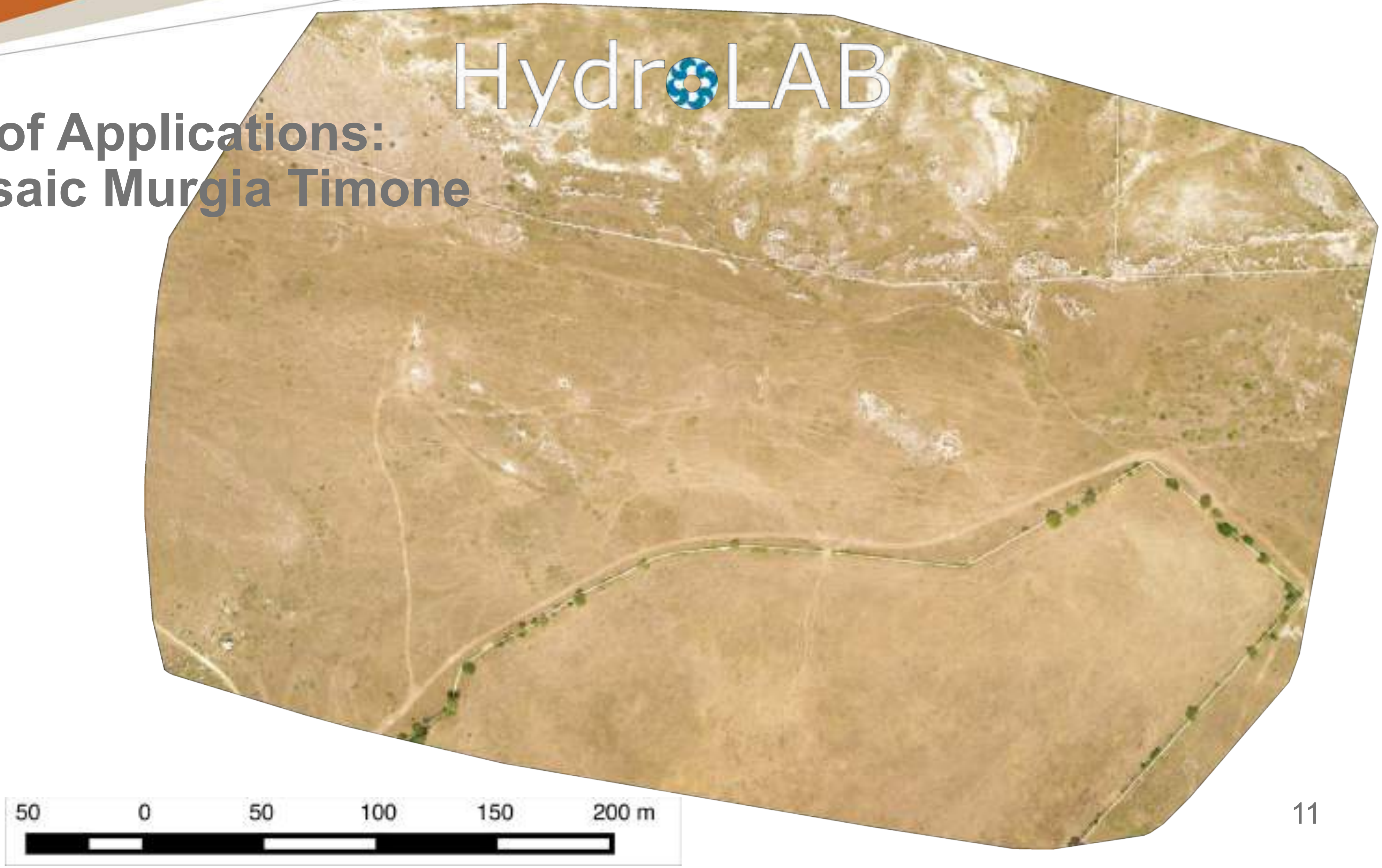

Example of Applications: Orthomosaic Murgia Timone (Matera)

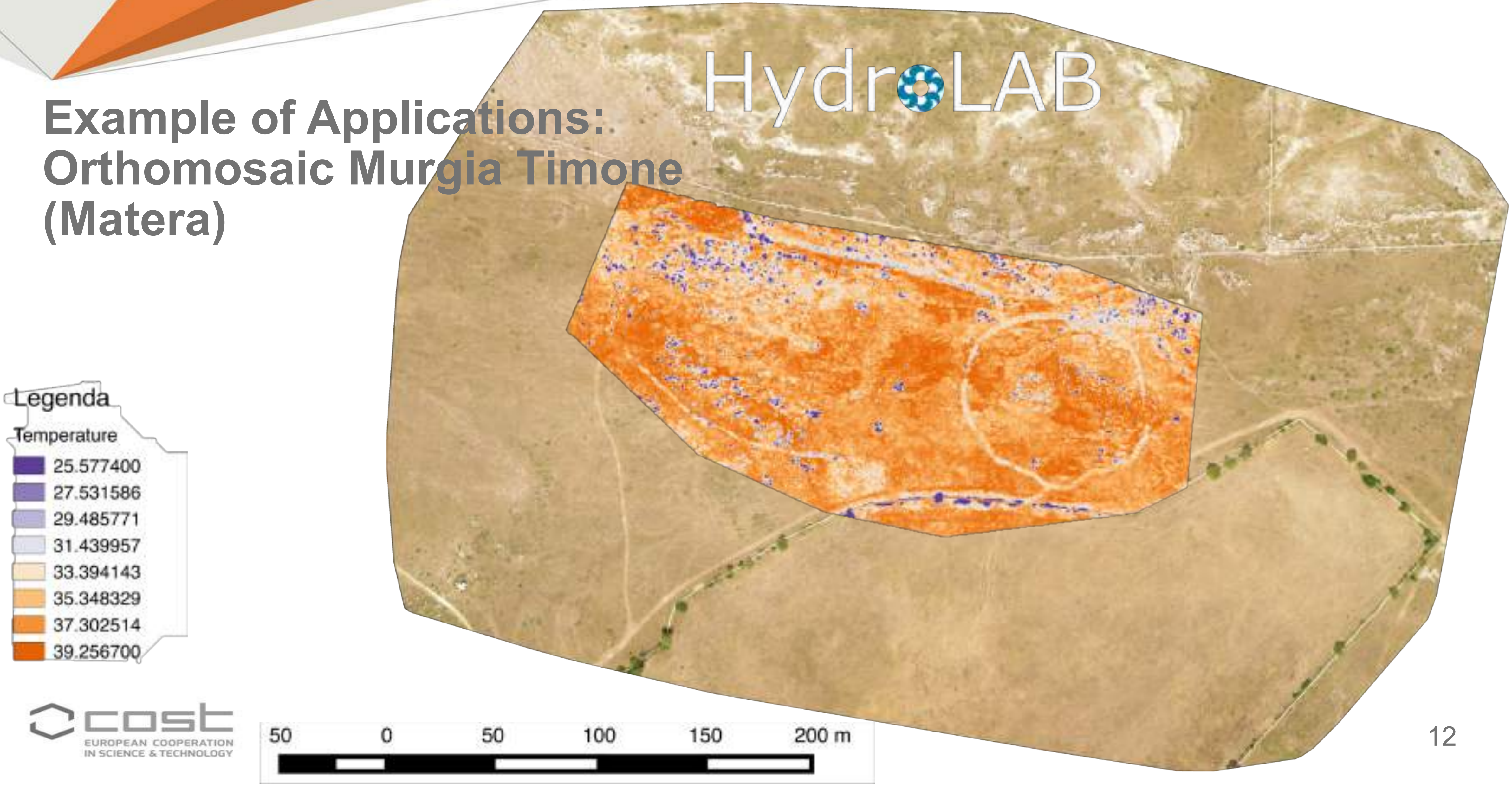

Example of Applications: Orthomosaic Murgia Timone (Matera)

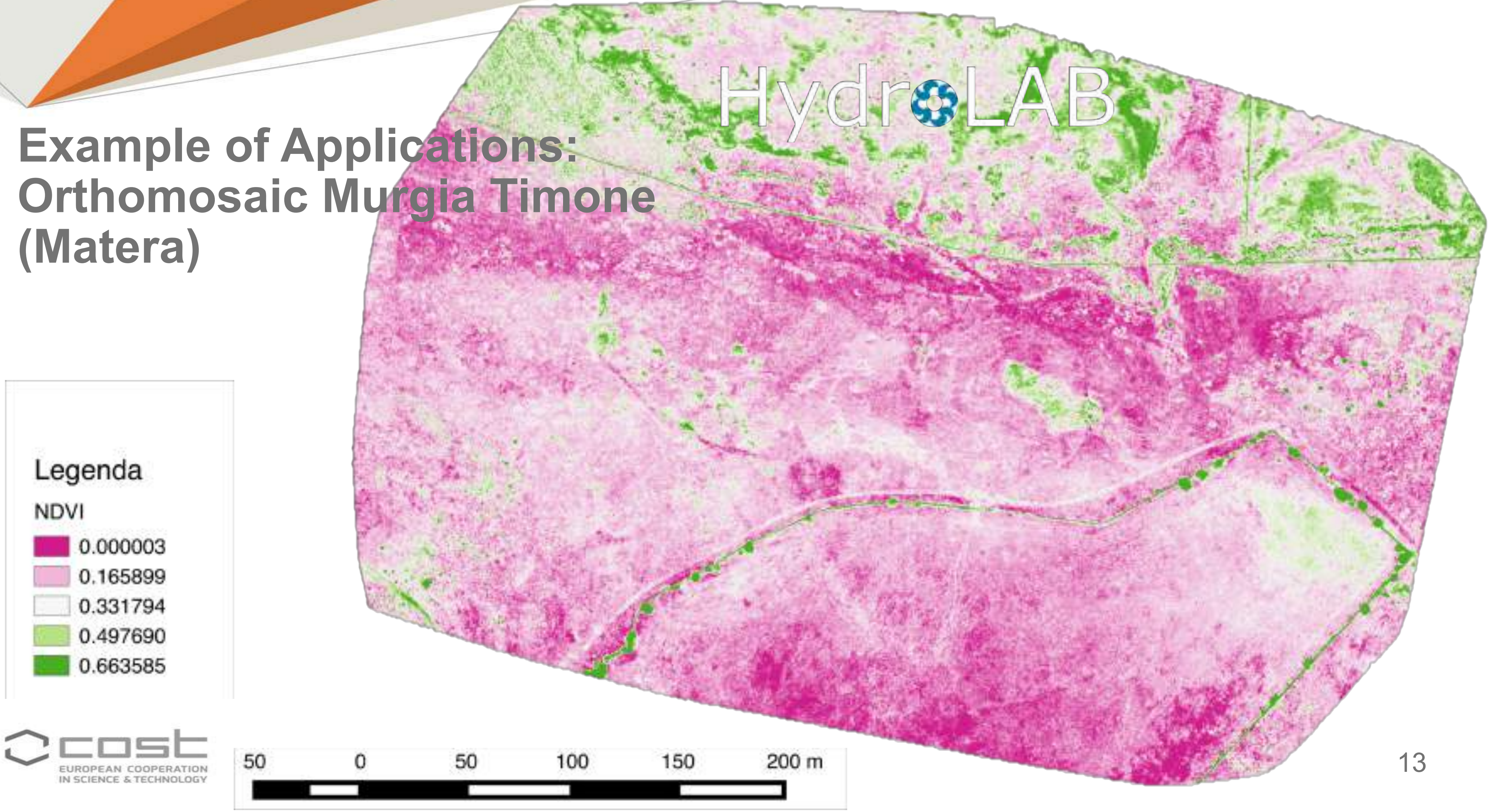

Related Publications

- Manfreda and McCabe (2019). ***Emerging earth observing platforms offer new insights into hydrological processes***, Hydrolink.
- Perks, Hortobágyi, Le Coz, Maddock, Pearce, Tauro, Dal Sasso, Grimaldi, Manfreda (2019) **Towards harmonization of image velocimetry techniques for determining open-channel flow**, Earth system science data (in preparation).
- Manfreda, Dvorak, Mullerova, Herban, Vuono, Arranz Justel, Perks (2019) ***Assessing the Accuracy of Digital Surface Models Derived from Optical Imagery Acquired with Unmanned Aerial Systems***, Drones.
- Manfreda, ***On the derivation of flow rating-curves in data-scarce environments***, Journal of Hydrology, 2018.
- Dal Sasso, Pizarro, Samela, Mita, and Manfreda (2018) ***Exploring the optimal experimental setup for surface flow velocity measurements using PTV***, Environmental Monitoring and Assessment.
- Manfreda, McCabe, Miller, Lucas, Pajuelo Madrigal, Mallinis, Ben-Dor, Helman, Estes, Ciraolo, Müllerová, Tauro, De Lima, De Lima, Frances, Caylor, Kohv, Maltese (2018), ***On the Use of Unmanned Aerial Systems for Environmental Monitoring***, Remote Sensing.
- Baldwin, Manfreda, Keller, and Smithwick, Predicting root zone soil moisture with soil properties and satellite near-surface moisture data at locations across the United States, Journal of Hydrology, 2017.
- Manfreda, Brocca, T. Moramarco, F. Melone, and J. Sheffield, ***A physically based approach for the estimation of root-zone soil moisture from surface measurements***, Hydrology and Earth System Sciences, 18, 1199-1212, 2014.
- Manfreda, Lacava, Onorati, Pergola, Di Leo, Margiotta, and Tramutoli, ***On the use of AMSU-based products for the description of soil water content at basin scale***, Hydrology and Earth System Sciences, 15, 2839-2852, 2011.